AD-777 718

ANNUAL RESEARCH REPORT 1 JULY 1972 - 30 JUNE 1973

Armed Forces Radiobiology Research Institute
Bethesda, Maryland

30 June 1973

Research was conducted according to the principles enunciated in the "Guide for Laboratory Animal Facilities and Care," prepared by the National Academy of Sciences - National Research Council.

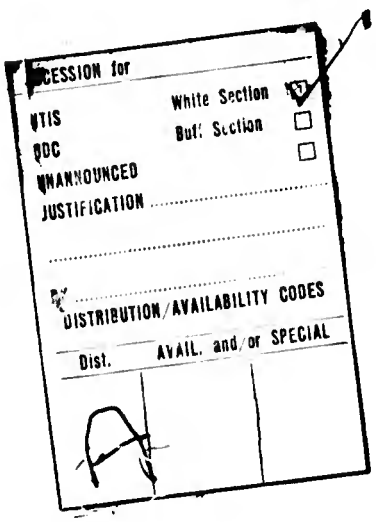

UNCLASSIFIED
Security Classification

DOCUMENT CONTROL DATA - R & D AD 777 718

(Security classification of title, body of abstract and indexing annotation must be entered when the overall report is classified)

1. ORIGINATING ACTIVITY (Corporate author)
Armed Forces Radiobiology Research Institute
Defense Nuclear Agency
Bethesda, Maryland 20014

2a. REPORT SECURITY CLASSIFICATION
UNCLASSIFIED

2b. GROUP
N/A

3. REPORT TITLE
ANNUAL RESEARCH REPORT 1 July 1972 -- 30 June 1973

4. DESCRIPTIVE NOTES (Type of report and inclusive dates)

5. AUTHOR(S) (First name, middle initial, last name)

6. REPORT DATE

7a. TOTAL NO. OF PAGES
123

7b. NO. OF REFS

8a. CONTRACT OR GRANT NO.

b. PROJECT NO.

c.

d.

9a. ORIGINATOR'S REPORT NUMBER(S)
ARR-7

9b. OTHER REPORT NO(S) (Any other numbers that may be assigned this report)

10. DISTRIBUTION STATEMENT
Approved for public release; distribution unlimited

11. SUPPLEMENTARY NOTES

12. SPONSORING MILITARY ACTIVITY
Director
Defense Nuclear Agency
Washington, D. C. 20305

13. ABSTRACT

This report contains a summary of the research projects of the Armed Forces Radiobiology Research Institute for the period 1 July 1972 to 30 June 1973.

DD FORM 1 NOV 65 1473

UNCLASSIFIED
Security Classification

ARR-7

ANNUAL RESEARCH REPORT
1 JULY 1972 — 30 JUNE 1973

ARMED FORCES RADIOBIOLOGY RESEARCH INSTITUTE
DEFENSE NUCLEAR AGENCY
BETHESDA, MARYLAND 20014

ib

FOREWORD

This report describes, in brief summary, the scientific accomplishments of the Armed Forces Radiobiology Research Institute (AFRRI) for the period 1 July 1972 to 30 June 1973.

During this report period, the AFRRI has broadened its research program from one primarily limited to operational problems in radiation biology to one which includes a number of critical biomedical problems of direct interest to the Surgeons General of the Military Departments. The establishment of a Neurobiology Department and the expansion of nuclear medicine activities are reflected in a significant number of technical summaries in this report. In addition, collaborative arrangements have been made with approximately 50 scientific investigators of other medical agencies and activities in the area, and these efforts have resulted in the presentation at national and international scientific meetings and publication in the open literature of a significant number of research reports.

The expansion of the AFRRI research program is continuing, and other aspects will be covered in future reports.

MYRON I. VARON
Captain MC USN
Director

TABLE OF CONTENTS

PATHOPHYSIOLOGICAL STUDIES OF POTENTIALLY TOXIC SUBSTANCES

Principal Investigators: *N. R. Schneider, J. E. Buerkert and S. J. Baum*
Collaborator: *M. E. Andersen, Navy Toxicology Unit*

The objective of this research was to measure and determine the biological pathways of cyclotrimethylenetrinitramine (RDX), as well as its toxic and resultant pathological effects on the various organ systems.

RDX is a primary constituent of Composition C-4, a plastic explosive employed by the military. The primary hazards encountered with RDX are exposure during industrial manufacture and processing, exposure due to environmental contamination and intentional drug abuse. RDX toxicity in man and other mammalian species and its effects on the central nervous, gastrointestinal (including liver), renal and hematological systems have been reported. However, little is known about the metabolic fate of RDX in the mammalian system.

A series of experiments involving toxic levels of RDX were performed to investigate the correlation of plasma concentrations of RDX with seizures and lethality. Rats were administered RDX at a known lethal dosage of 500 mg/kg intraperitoneally. Each animal served as its own control, and serial blood samples were collected until death. Plasma was extracted in benzene for RDX determination and analysis was accomplished by gas chromatography in a modification of the method used by Hoffsommer and Rosen.[1]

All rats exhibited convulsive seizures, but the time of initial seizure onset was variable as well as the number of seizures per animal. The initial seizure did not occur until the interpolated plasma concentration of RDX reached 5.19 ± 0.42 μg/ml (SE). Seizures occurred most frequently when plasma concentrations were in the range of 5-13 μg/ml. The concentrations at death differed to a greater extent, ranging from 6.9 - 27.3 μg/ml. The tissue concentrations and tissue to plasma ratio are summarized in Table I.

The data indicate that absorption of RDX from the peritoneal cavity is variable and incomplete at lethal dosages. Initial signs of RDX toxicity can usually be observed when plasma concentrations approach 3-4 μg/ml, with seizures occurring at 5 μg/ml or above. Lethality can be expected whenever plasma concentrations exceed 8 μg/ml. These levels are well below the solubility limit of RDX in plasma (30 μg/ml), so that a great potential hazard exists if increased absorption of RDX occurs or is enhanced in any way. Tissue concentrations at lethality were found to be higher in the liver and kidney and lower in heart and brain, but all were greater than plasma concentrations alone. Tissue to plasma ratios suggest that RDX may have a tendency to accumulate more in the liver and kidney at toxic dosages.

Table I. Intraperitoneal Lethality Study: Tissue RDX Concentrations and Tissue/Plasma (T/P) Ratios

Rat #	Plasma concentration μg/g	Brain concentration μg/g	Brain T/P ratio	Heart concentration μg/g	Heart T/P ratio	Liver concentration μg/g	Liver T/P ratio	Kidney concentration μg/g	Kidney T/P ratio
1	5.78	N/D	--	N/D	--	N/D	--	N/D	--
2	6.76	N/D	--	N/D	--	N/D	--	N/D	--
3	12.85	26	2.023	19	1.479	25	1.946	40	3.113
4	26.48	41	1.548	35	1.322	46	1.737	68	2.568
5	8.18	22	2.689	19	2.323	21	2.567	44	5.379
6	18.31	32	1.748	26	1.420	72	3.392	65	3.550
7	9.54	37	3.878	27	2.830	44	4.612	53	5.556
8	11.02	33.4	3.031	33.4	3.031	53.6	4.864	77	6.987
9	9.04	18.8	2.080	20.8	2.301	34.1	3.772	74	8.186
10	9.89	26	2.629	20	2.022	38	3.842	33	3.337
	11.79	29.5	2.453	25.0	2.091	41.7	3.342	56.8	4.834
S.E.	± 1.97	± 2.7	± 0.270	± 2.3	± 0.229	± 5.8	± 0.412	± 5.9	± 0.716

* Plasma concentrations in μg/g are obtained by multiplying the concentrations in μg/ml by 0.9737, the factor determined for converting μg/ml to μg/g

In an investigation studying the effects of a lower acute nonlethal dosage of RDX administered intraperitoneally (50 mg/kg), serial plasma and urine samples as well as tissue and feces were collected and assayed. Plasma concentrations rose to 1 μg/ml within 1 hour and then stabilized, whereas the urine concentrations increased and were two to three times the plasma concentrations after plasma levels stabilized. There were no detectable levels of RDX in the feces. The data suggest that the parenterally administered RDX is excreted mainly in the urine and not via the gastrointestinal tract as suggested by Sunderman.[2]

A preliminary histopathological examination was conducted on the tissues of a rat sacrificed 4 hours after administration of 50 mg/kg RDX. The liver exhibited early fatty change and coagulation necrosis in the centrilobular areas adjacent to the central veins. The kidneys revealed severe, acute, diffuse nephrosis with tubular epithelium damage more extensive in the cortex. A complete histopathological study is now underway.

In plasma clearance studies in rats, the RDX was administered intravenously in a solution of dimethylsulfoxide (DMSO) containing 10 mg RDX/ml DMSO. Each rat received 0.125 ml of this solution (equivalent to a dosage of 5.0 - 6.0 mg/kg I.V.). Serial blood samples were taken until 24 hours postinjection, and tissue samples were taken at sacrifice. The mean plasma concentration of 4.4 ± 0.35 μg/ml at 30 seconds decreased to 1.9 ± 0.17 μg/ml in 6 hours. The biological half-life of RDX was computed as 10.8 ± 4.6 hours. No measurable residual RDX was found in the tissues after 24 hours, but tissue concentrations may have been below detectable levels for the method of analysis.

In the oral acute distribution study, fasted rats were given 100 mg RDX/kg body weight in a saline slurry via a gastric tube. Groups of animals were sacrificed at various intervals. Blood, urine and tissues were collected and assayed. None of these animals except those in the 8-hour group showed seizures or other overt signs of toxicity. In the animals sacrificed 8 hours after RDX administration, serial samples of blood were collected from catheters previously placed into the femoral artery. All the animals in the 8-hour group had at least one seizure. The plasma concentrations in this group were higher than expected and often exceeded 5 μg/ml, the threshold of seizures reported in the intraperitoneal uptake study. Plasma, urine and tissue concentrations as well as tissue to plasma ratios are summarized in Table II.

Table II. Oral Acute Distribution Study: Plasma, Urine and Tissue RDX Concentrations ($\bar{x} \pm SE$) and Tissue/Plasma (T/P) Ratios

Time (h)	Plasma concentration μg/g	Urine concentration μg/ml	Brain concentration μg/g	Brain T/P ratio	Heart concentration μg/g	Heart T/P ratio	Liver concentration μg/g	Liver T/P ratio	Kidney concentration μg/g	Kidney T/P ratio
2	1.50 ± 0.26	2.45 ± 0.30	10.36 ± 1.24	8.83 ± 1.69	7.97 ± 1.11	6.87 ± 1.53	4.34 ± 0.90	3.95 ± 0.99	12.86 ± 1.40	10.46 ± 1.38
4	2.09 ± 0.09	5.46 ± 0.96	7.71 ± 0.98	3.70 ± 0.45	6.49 ± 0.96	3.12 ± 0.43	2.16 ± 0.56	1.27 ± 0.37	12.30 ± 1.82	5.93 ± 0.82
6	1.78 ± 0.15	5.02 ± 0.81	7.51 ± 0.57	4.38 ± 0.41	7.13 ± 0.71	4.26 ± 0.54	0.51 ± 0.34	0.43 ± 0.30	13.58 ± 1.37	7.83 ± 0.77
8	5.46 ± 0.47	11.0 ± 0.70	13.79 ± 0.98	2.58 ± 0.22	11.52 ± 0.95	2.17 ± 0.22	9.41 ± 1.19	1.66 ± 0.16	24.27 ± 2.06	4.52 ± 0.41
12	2.55 ± 0.16	5.49 ± 1.03	11.28 ± 1.60	4.63 ± 0.73	11.08 ± 1.82	4.55 ± 0.81	8.51 ± 2.24	3.59 ± 0.96	22.02 ± 2.06	8.81 ± 0.92
18	2.03 ± 0.10	5.58 ± 0.28	6.30 ± 0.20	3.21 ± 0.15	5.58 ± 0.24	2.82 ± 0.19	0.48 ± 0.20	0.28 ± 0.10	12.12 ± 0.83	6.00 ± 0.34
24	3.04 ± 0.48	6.87 ± 0.84	8.91 ± 1.07	3.36 ± 0.44	7.89 ± 0.83	2.91 ± 0.33	2.56 ± 1.15	0.69 ± 0.21	16.85 ± 0.80	6.57 ± 0.82

* Plasma concentrations in μg/g are obtained by multiplying the concentrations in μg/ml by 0.9737, the factor determined for converting μg/ml to μg/g

In a preliminary experiment in the acute distribution study, 1 percent methyl cellulose was proposed as the oral vehicle for RDX. The dosage utilized in this experiment was also 100 mg RDX/kg of body weight. All animals receiving this dosage in methyl cellulose had seizures and died. The time of death ranged from 9 to 49 minutes post-RDX administration. In four of the five animals, plasma concentrations of RDX were below the level expected to produce seizures and lethality. These data are shown in Table III. Thus, the apparent oral lethal dose of RDX in the rat was lowered when methyl cellulose was utilized as the vehicle.

Rat #	Plasma concentration μg/ml
1	3.8
2	3.8
3	9.8
4	2.4
5	3.0

Table III. Oral Administration of RDX Using 1 Percent Methyl Cellulose (100 mg/kg)

These initial experiments indicate that very low plasma concentrations of RDX are responsible for seizures and lethality in rats. With a biological half-life of nearly 11 hours, RDX would be expected to accumulate if repeated administration occurred. The target organs seemingly most affected by RDX toxicity at lethal dosages appear to be the liver and kidney, which had the highest tissue concentrations of RDX at death. At lower dosages, the kidney concentrations of RDX during the first 24 hours after administration were still the most elevated, but liver concentrations were quite variable and at times were lower than plasma concentration.

REFERENCES

1. Hoffsommer, J. C. and Rosen, J. M. Ultramicro analysis of explosives in sea water. White Oak, Maryland, Naval Ordnance Laboratory Report NOLTR-71-151, 1971.

2. Sunderman, F. W. Hazards to the health of individuals working with RDX(B). National Defense Research Committee of the Office of Scientific Research and Development Report OSRD No. 4174, 1944. Arlington, Virginia, Armed Services Technical Information Agency ATI-31099, 1960.

BIOLOGICAL EFFECTS OF ELECTROMAGNETIC PULSES

Principal Investigators: *W. D. Skidmore and S. J. Baum*

The present study tests the hypothesis that pulses of electric and magnetic fields would adversely affect vital ionic and electrochemical processes at the molecular level in biological systems.[1,2] Rodents were exposed to 10^8 pulses from the AFRRI electromagnetic pulse (EMP) simulator which provides five pulses per second with a peak electric field intensity of 447 kV/m, a 5-nsec rise time and 550-nsec 1/e fall time.

When results obtained from EMP exposed animals were compared with those from controls, no changes were observed in the number and production of rat bone marrow cells (Figure 1), the incidence in chromosome aberrations in mitotic bone

These initial experiments indicate that very low plasma concentrations of RDX are responsible for seizures and lethality in rats. With a biological half-life of nearly 11 hours, RDX would be expected to accumulate if repeated administration occurred. The target organs seemingly most affected by RDX toxicity at lethal dosages appear to be the liver and kidney, which had the highest tissue concentrations of RDX at death. At lower dosages, the kidney concentrations of RDX during the first 24 hours after administration were still the most elevated, but liver concentrations were quite variable and at times were lower than plasma concentration.

REFERENCES

1. Hoffsommer, J. C. and Rosen, J. M. Ultramicro analysis of explosives in sea water. White Oak, Maryland, Naval Ordnance Laboratory Report NOLTR-71-151, 1971.

2. Sunderman, F. W. Hazards to the health of individuals working with RDX(B). National Defense Research Committee of the Office of Scientific Research and Development Report OSRD No. 4174, 1944. Arlington, Virginia, Armed Services Technical Information Agency ATI-31099, 1960.

BIOLOGICAL EFFECTS OF ELECTROMAGNETIC PULSES

Principal Investigators: *W. D. Skidmore and S. J. Baum*

The present study tests the hypothesis that pulses of electric and magnetic fields would adversely affect vital ionic and electrochemical processes at the molecular level in biological systems.[1,2] Rodents were exposed to 10^8 pulses from the AFRRI electromagnetic pulse (EMP) simulator which provides five pulses per second with a peak electric field intensity of 447 kV/m, a 5-nsec rise time and 550-nsec 1/e fall time.

When results obtained from EMP exposed animals were compared with those from controls, no changes were observed in the number and production of rat bone marrow cells (Figure 1), the incidence in chromosome aberrations in mitotic bone

marrow cells (Table IV), the concentration of circulating neutrophils (Figure 2), lymphocytes (Figure 3), leukocytes (Figure 4), and erythrocytes (Figure 5). Reticulocytes (Figure 6) appear to have been elevated and platelets (Figure 7) decreased; however, both counts remained within acceptable levels.

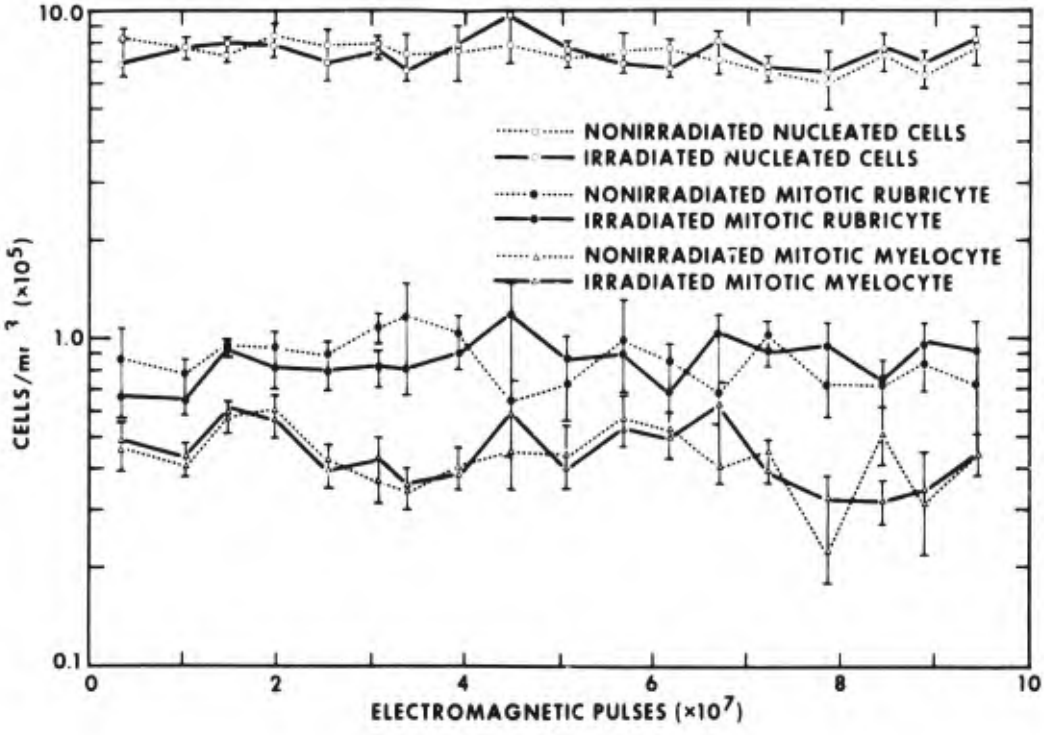

Figure 1. Nucleated cells from the bone marrow of rat femurs during 38 weeks of EMP exposure. Each point shows a mean value with the associated standard error.

Table IV. Chromosome Aberrations in Rats Exposed to 10^8 Electromagnetic Pulses During 38 Weeks

Group	Number of rats	Number of cells	Number of aberrations
Nonirradiated	40	2,000	2
Irradiated	40	2,000	2

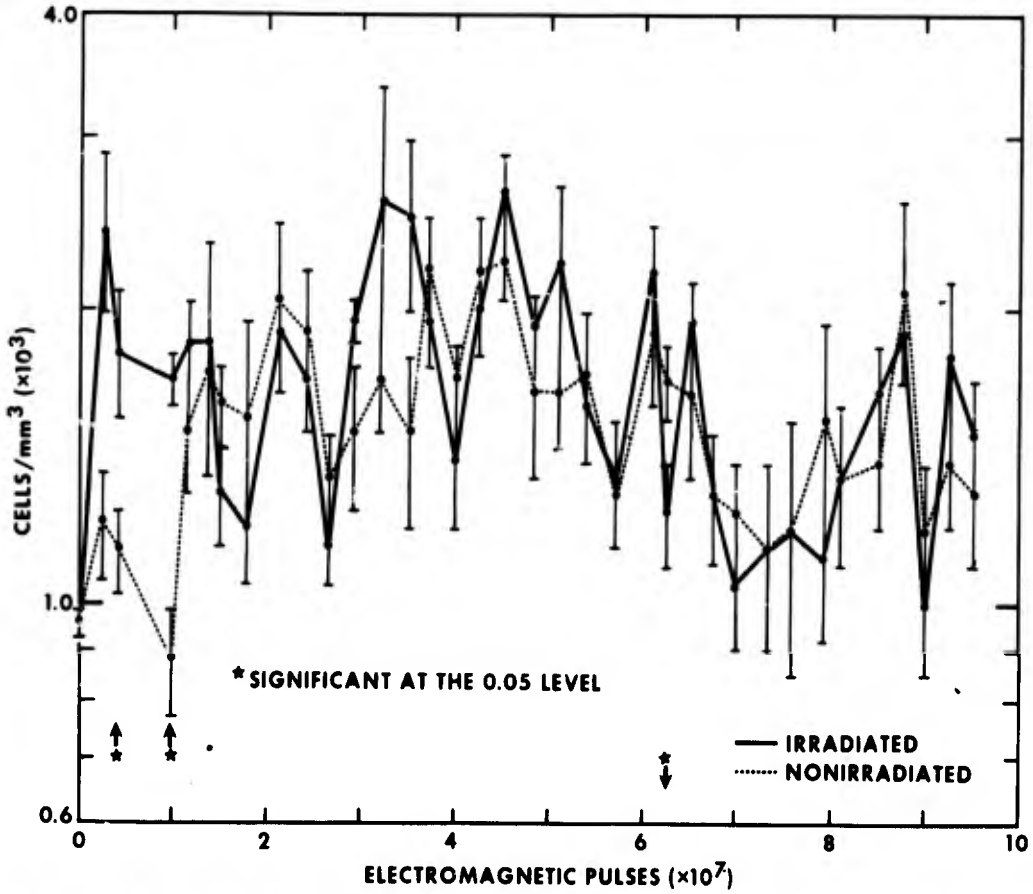

Figure 2. Segmented neutrophils in peripheral blood from rats during 38 weeks of EMP exposure. Each point shows a mean value with the associated standard error.

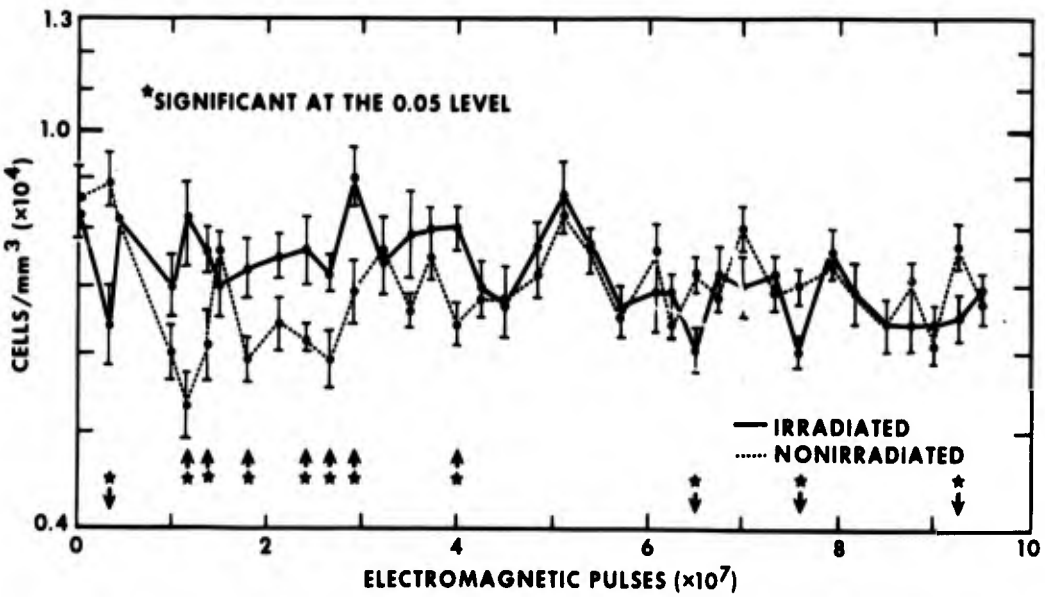

Figure 3. Lymphocytes in peripheral blood from rats during 38 weeks of EMP exposure. Each point shows a mean value with the associated standard error.

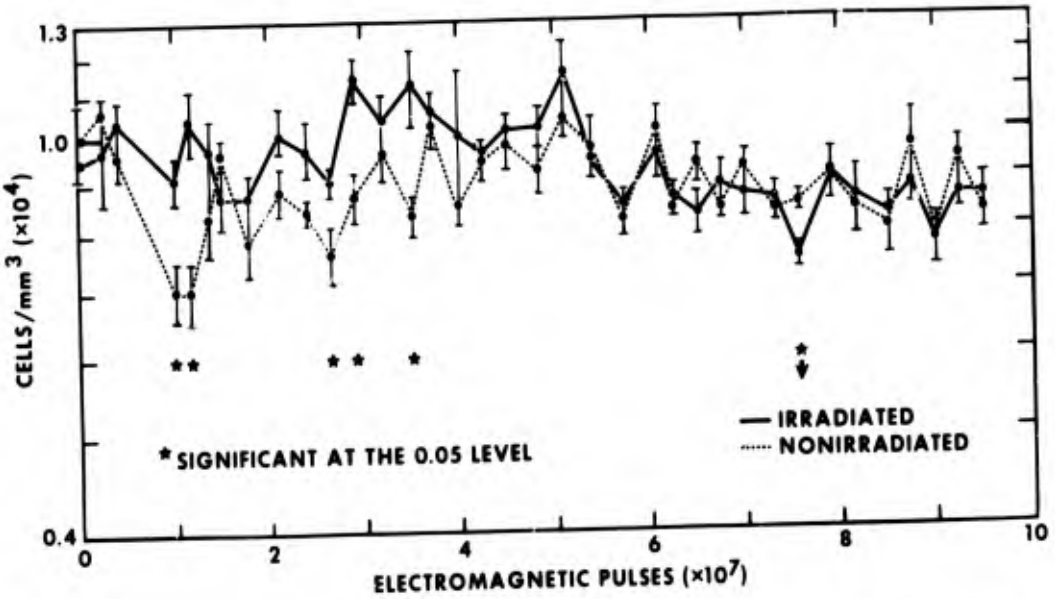

Figure 4. White cells in peripheral blood from rats during 38 weeks of EMP exposure. Each point shows a mean value with the associated standard error.

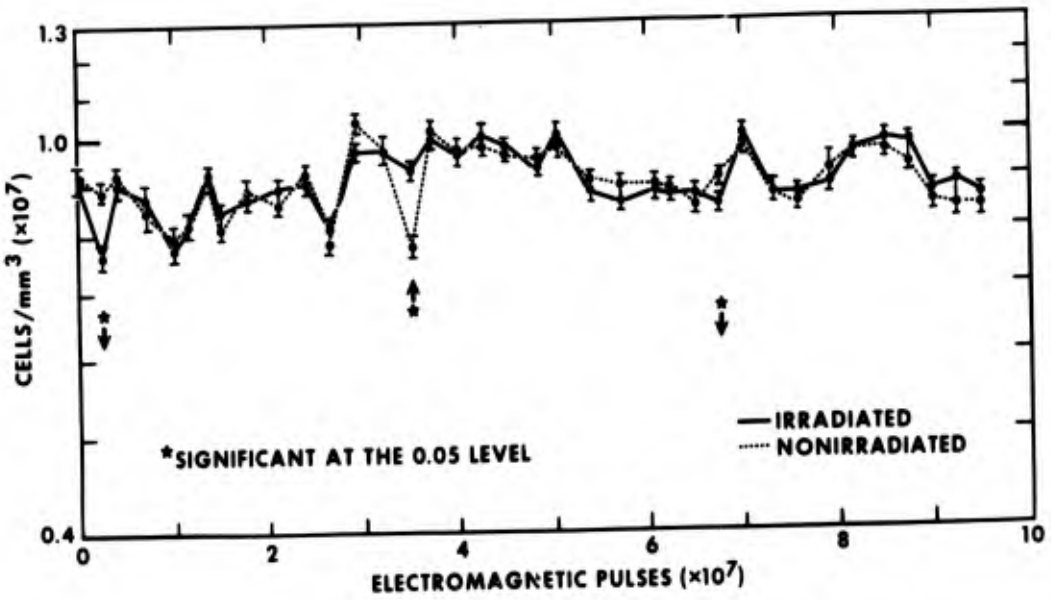

Figure 5. Red cells in peripheral blood from rats during 38 weeks of EMP exposure. Each point shows a mean value with the associated standard error.

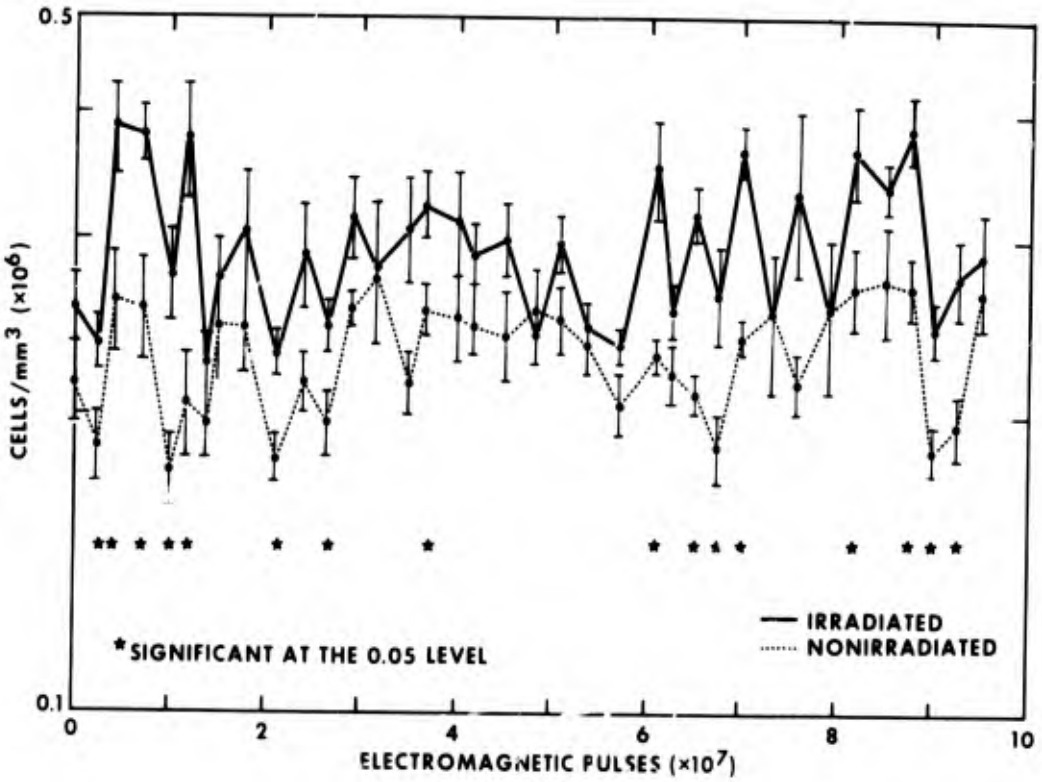

Figure 6. Reticulocytes in peripheral blood from rats during 38 weeks of EMP exposure. Each point shows a mean value with the associated standard error.

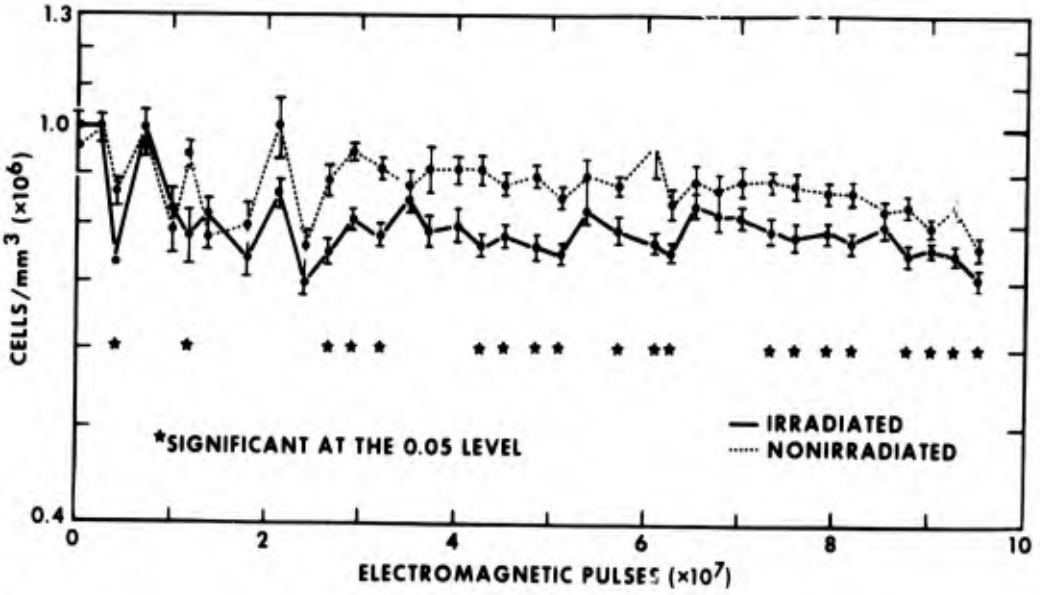

Figure 7. Platelets in peripheral blood from rats during 38 weeks of EMP exposure. Each point shows a mean value with the associated standard error.

No incidence of mammary tumors was observed in the female Sprague-Dawley rats. In leukemia-prone AKR/J male mice, leukemia did not occur earlier in EMP exposed animals, nor was the fraction of leukemic mice greater in this group when compared with the nonirradiated control mice (Table V).

Table V. Incidence of Spontaneous Leukemia in AKR/J Male Mice

	Group	
	Nonirradiated	Irradiated
Electromagnetic pulses (33 wk)	0	8.6×10^7
Surviving fraction	24/50	42/50
Leukemic fraction	11/24	9/42
Thymus weight (mg)	165 ± 39	130 ± 27
Spleen weight (mg)	181 ± 73	115 ± 23
WBC (cells/mm^3)	9500 ± 1000	10,000 ± 900

The present data do not indicate an acute biological hazard to rodents from EMP exposures. The possibility for the development of late effects and malignancies will be determined during the second half of the rodents life-span.

REFERENCES

1. Baum, S. J., Skidmore, W. D. and Ekstrom, M. E. Continuous exposure of rodents to 10^8 pulses of electromagnetic radiation. Bethesda, Maryland, Armed Forces Radiobiology Research Institute Scientific Report SR73-23, 1973 (in press).

2. Skidmore, W. D. and Baum, S. J. Biological effects in rodents exposed to pulsed electromagnetic radiation. Bethesda, Maryland, Armed Forces Radiobiology Research Institute Scientific Report SR73-10, 1973.

RECOVERY AND RESIDUAL INJURY OF THE HEMATOPOIETIC SYSTEM IN IRRADIATED MAMMALS

Principal Investigators: *K. F. McCarthy, W. D. Skidmore and S. J. Baum*

One objective of this study was to increase postirradiation recovery in animals by stimulating granulopoiesis and concomitantly suppressing erythropoiesis.

Actinomycin D (Act D) was first reported to increase granulopoiesis and suppress erythropoiesis in the nonirradiated mouse. These experiments were repeated in this laboratory using the nonirradiated and irradiated rat.

The experimental design was as follows: Twenty Sprague-Dawley rats were divided into four groups. Group 1 was the control, group 2 was irradiated with 200 rads of gamma radiation, group 3 received Act D (.2 mg/kg body weight) every other day, and group 4 was irradiated with 300 rads and received Act D every other day. Act D was given for either 5 or 13 days. Figure 8 shows the granulocyte count, the lymphocyte count and the percent reticulocytes in the peripheral circulation for animals given Act D through day 5. The experiment in which the Act D treatment was carried through day 13 is not shown but is similar to that shown for the day 5 experiment.

The following observations were made: (1) Act D suppresses reticulocyte formation in both the control and irradiated rats, (2) subcutaneous injections of Act D result in a localized inflammation at the site of injection and (3) a granulocytosis is observed in both the control and irradiated rats injected with Act D.

A second objective was to determine the mechanism of transition of the hematopoietic stem cell from the G_0 state to that of active proliferation.

It has been proposed that there are short-range, tissue-specific factors which control the proliferation of hematopoietic stem cells. In the mouse, stem cells reside primarily in the liver and to a smaller extent in the spleen prior to birth. After birth their habitat shifts to the spleen and bone marrow. If the concentration of these short-range factors varies from organ to organ then it might be expected that stem cell populations found in those organs might proliferate at different rates. An effort was therefore made to determine and compare the proliferative rate of stem cell populations found in bone marrow, spleen, circulation, peritoneal cavity, neonatal spleen, neonatal liver and fetal liver. Due to technical difficulties, the proliferative state of the stem cell populations in the circulation and peritoneal cavity could not be determined. However, for the other five organs the following observations were made. (1) Between birth and the 4th day of neonatal life the stem cell population of the neonatal liver decreases tenfold while that of the spleen increases tenfold (Figure 9). (2) The fraction

of the stem cell pool in the S-phase of the cell cycle was determined by killing cells synthesizing DNA with high specific activity tritiated thymidine. As shown in Figure 10 the fraction of stem cells in the S-phase of the cell cycle was 0.4 for both stem cell populations found in 3-day-old liver and spleen. In adult marrow and spleen less than 5 percent of the stem cells were in the S-phase of the cell cycle. (3) The mean cell volumes of the stem cells found in 15-day fetal liver, 3-day-old neonatal spleen and liver, and adult spleen were determined using velocity sedimentation (Figure 11). It was found that stem cells from the 15-day fetal liver, 3-day neonatal spleen and 3-day neonatal liver have a mean cell volume of approximately 530 μm^3, while the stem cells from adult spleen have a mean cell volume of 310 μm^3. The larger cell volume of the neonatal stem cells as compared to the adult stem cells indicates that these cells are in a state of rapid proliferation.

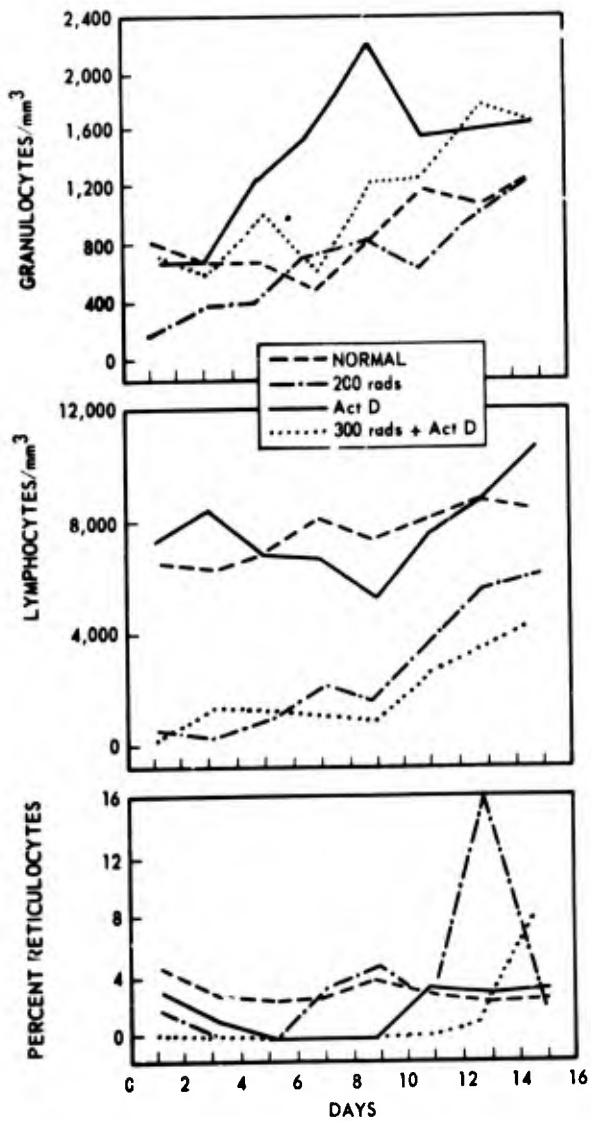

Figure 8.
Changes in blood cells following irradiation and actinomycin D treatment

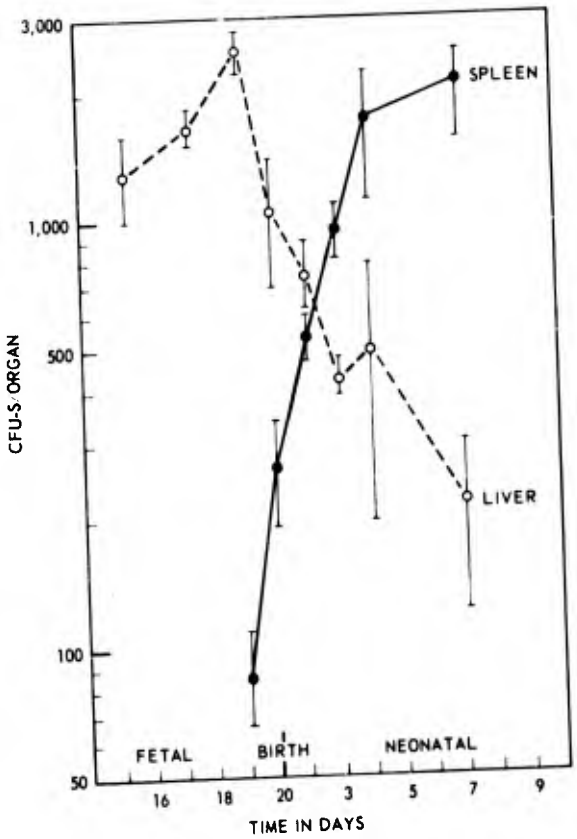

Figure 9.
Changes in CFU-S in the spleen and liver of the mouse at various times before and after birth. The number of CFU-S was not corrected for seeding efficiency.

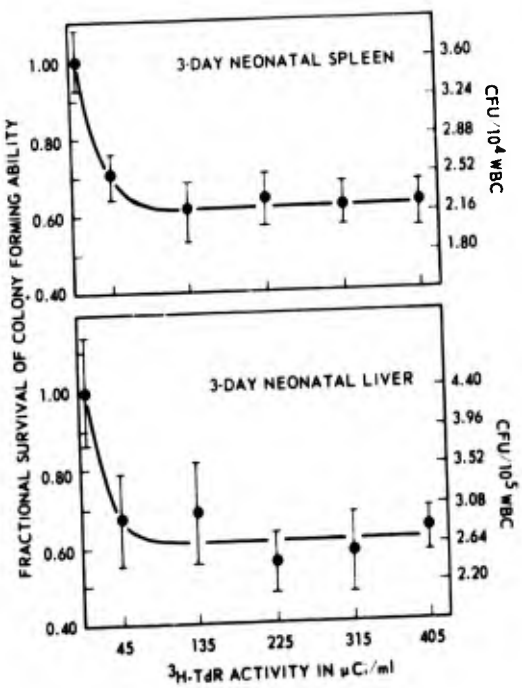

Figure 10.
Effect of 30-minute exposure in vitro to various concentrations of ^{3}H-thymidine on the CFU-S content of 3-day neonatal spleen and liver. Standard errors of the mean colony counts are indicated. The specific activity of the ^{3}H-thymidine was 18 Ci/mmole.

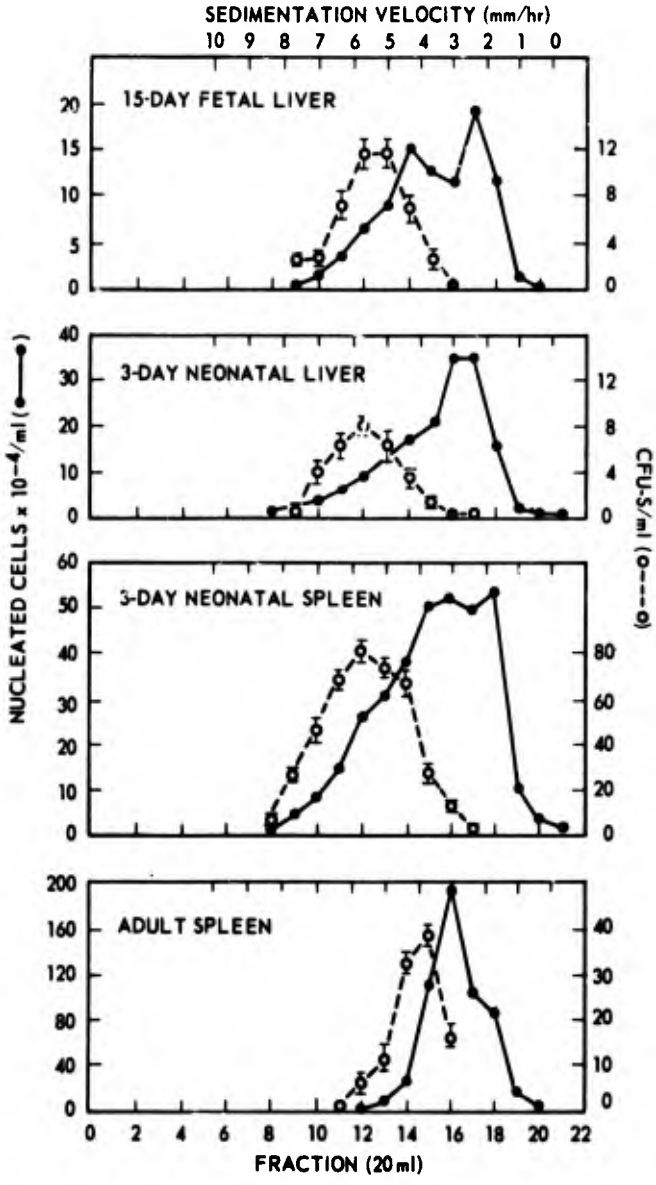

Figure 11. Sedimentation velocity profiles for total nucleated cells and CFU-S from fetal and neonatal liver and neonatal and adult spleen. The CFU-S are uncorrected for seeding efficiency.

The important conclusion to be drawn from these observations is that although the stem population is decreasing exponentially in the 3-day-old neonatal liver and increasing exponentially in the spleen, both stem cell populations appear to be proliferating at

the same rate. Thus it would appear that the proliferative state of stem cell populations found in the neonatal mouse is not controlled by tissue-specific factors, but rather by humoral factors. However, it would appear that tissue-specific factors determine the size of the stem cell pool within an organ by a mechanism independent of the proliferative rate of that stem cell pool.

◆◆◆◆◆◆◆◆◆

CONTROL OF WHITE CELL POPULATION IN THE POSTIRRADIATED ANIMAL

Principal Investigators: *T. J. MacVittie, K. F. McCarthy and S. J. Baum*

The objective of this study was to test the hypothesis that postirradiation production of granulocytes may be improved by accelerating the recovery of their primitive progenitors. It was furthermore assumed that granulopoiesis is under control of both stimulatory and inhibitory agents.

The initial experiments were designed to determine the in vitro noncytotoxic, tissue-specific inhibitory nature of our granulocyte extract.

Cytotoxicity. To test for a cytotoxic effect on sensitive progenitor cells, marrow cell suspensions were preincubated with the fresh granulocyte extract for 1 hour at 37°C. Table VI shows that the viability of the marrow cells as well as the incidence of the progenitor and stem cells assayed, i.e., the in vivo colony forming units (CFU), in vitro colony forming cell (CFC) and in vivo diffusion chamber progenitor cell (DCPC), was not reduced by treatment with chalone in concentrations up to 50 percent of culture medium. The agar colony forming cells were monitored with three sources of colony stimulating factor (CSF) on mouse target cells.

In vitro inhibition. The candidate chalone was then assayed for its capacity to inhibit cellular proliferation in several in vitro tissue-specific assay systems. Table VII shows that the chalone when used at 10 percent of culture volume significantly reduced agar colony formation induced by CSF from three sources to values averaging 50 to 70 percent inhibition of those in control animals. ^{3}H-thymidine (^{3}H-TdR) uptake in rat marrow was also reduced to a maximum inhibition of approximately 32 percent. It is noted that this reduction of ^{3}H-TdR uptake was reached at a chalone concentration of 20 percent and did not significantly diminish ^{3}H incorporation below the 32 percent level while the chalone concentration was increased to 50 percent of culture volume.

Table VI. Effect of Preincubation with Granulocyte Chalone on the Incidence of Progenitor Cells in Mouse Marrow

Chalone* (percent)	Viability (percent)	Assay	Mean number of colonies (± S.D.)			
			A	B	C	
0	88.7	CFC†	61 ± 7	147 ± 6	139 ± 11	NSD‡‡
20	91.8	CFC	59 ± 8	150 ± 9	133 ± 7	
0	88.9	CFU‡	3.2 ± 0.9			
20	88.2	CFU	3.4 ± 1.2	NSD		
30	91.4	CFU	4.1 ± 1.1			
50	86.3	CFU	3.1 ± 0.7			
0	91.3	CFU_R§	7.0 ± 2.0	NSD		
20	88.7	CFU_R	7.1 ± 2.4			
0	83.8	DCPC**	$7.69 \times 10^5 \pm 0.46$	NSD		
50	86.4	DCPC	$7.62 \times 10^5 \pm 0.56$			
0	76.5	$DCPC_R$††	$9.13 \times 10^5 \pm 0.57$	NSD		
50	74.7	$DCPC_R$	$9.09 \times 10^5 \pm 0.71$			

* 0 percent chalone = equivalent amount (v/v) of nonpyrogenic saline
† CFC, in vitro agar colony forming cell assayed with: A. Mouse endotoxin sera, B. L-cell CM, and C. Rat endotoxin sera. Colonies per 10^5 cells.
‡ CFU, in vivo spleen colony forming unit. Colonies per 10^4 marrow cells.
§ CFU_R, regenerating marrow as source of cells
** DCPC, in vivo diffusion chamber progenitor cell. Relative number indicated by mean chamber cellularity at day 4 of harvest.
†† $DCPC_R$, regenerating marrow as source of cells for chamber inoculation
‡‡ No significant difference within groups due to chalone treatment

Table VII. Effect of Granulocyte Chalone on Agar Colony Formation

CSF source	Mean colony number*		Percent inhibition
	Control CSF	CSF + chalone†	
Rat endotoxin serum	123 ± 9	47 ± 6	61.9
Mouse endotoxin serum	63 ± 5	20 ± 5	70.5
Mouse L-cell CM	167 ± 11	94 ± 9	43.7

* Colonies per 10^5 mouse marrow cells (± S.D.) average of five replicate experiments
† Chalone at a concentration of 10 percent (v/v) of culture medium

Tissue specificity. On the other hand, the chalone at a concentration of 20 percent of culture volume did not significantly reduce the lymphocytic response to phytohemagglutinin (PHAp), using both rat and mouse spleen cell suspensions, or the rat marrow cell response to erythropoietin as measured by ^{3}H-TdR and ^{59}Fe uptake, respectively.

In addition, chalone did not significantly affect viability, plating efficiency, or ^{3}H-TdR uptake of mouse L-929 cells in monolayer culture.

These data are interpreted to indicate that a certain degree of noncytotoxicity, tissue specificity and nonspecies specific inhibitory action for granulocytes is associated with the chalone obtained from granulocytic extracts.

In vivo inhibition. The in vivo inhibitory action of the chalone on the growth of normal and regenerating mouse marrow cells in in vivo diffusion chambers was investigated and findings were as described below.

Normal marrow. As may be seen in Figure 12, chalone significantly influenced growth of cells in the chambers when injected intraperitoneally in 1.5 ml aliquots, as early as 5 hours after implantation and thereafter at 20, 24 and 28 hours during the 1st day and at 44 and 48 hours during the 2nd day of culture. Chamber growth in nonregenerating marrow was depressed throughout the period of treatment

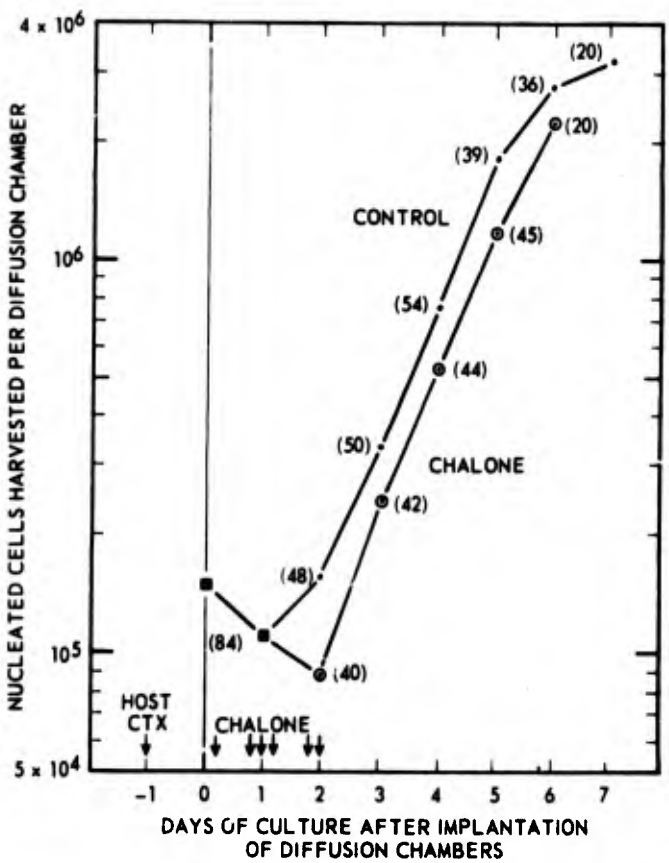

Figure 12. The effect of chalone injections on the growth of cells (granulocytes and macrophages) in diffusion chambers inoculated with 1.5 x 10^5 normal bone marrow cells. Results of five replicate experiments. Number of chambers harvested for each mean value (± SEM) indicated in parentheses.

to values approximately 50 percent of those seen in controls at day 2 of culture. At that time, control treated cultures had already initiated exponential growth. Cessation of chalone injections resulted in a phase of rapid growth and cell recovery to values within 70 percent of controls by the 3rd day. During this recovery or rebound phase, the chalone treated cells increased with a doubling time of 15.4 hours while control cells doubled only every 20.8 hours. Thereafter, days 3 through 5, the growth rates were similar for both groups.

Regenerating bone marrow. Figure 13 indicates a similar pattern of inhibition and recovery with regenerating marrow, although growth was exponential from the onset of culture, through day 4, in both control and chalone treated groups. Growth rates in chalone treated chambers were reduced until day 2 when treatment with the inhibitor substance was terminated. Thereafter, this was characterized with a rebound phase which had a doubling time of approximately 16 hours while the control cells had doubled only every 22 hours over the same time period.

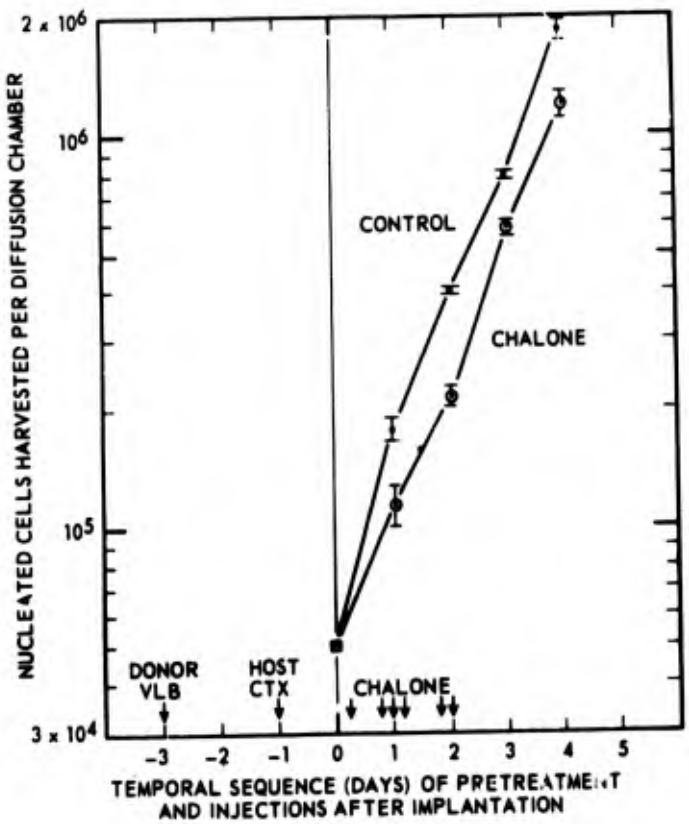

Figure 13. The effect of chalone on the growth of granulocytes and macrophages in diffusion chambers inoculated with 5 x 10^4 regenerating bone marrow cells. Results of a duplicate experiment with a total of 20 chambers for each mean value (± SEM).

Parent progeny. In addition to altering the growth kinetics, chalone as administered to our culture system reduced the linear relationship established within control treated chambers between the size of the marrow inoculum (and therefore progenitor cell content) and the number of granulocyte and macrophage progeny formed by day 4 of culture (Figure 14). Comparison of the linear regression lines which describe the data in Figure 14 showed that while the linearity within marrow groups was similar, the number of progeny formed was significantly reduced in both chalone treated groups of marrow inocula over the cell dose range studied ($p < .001$).

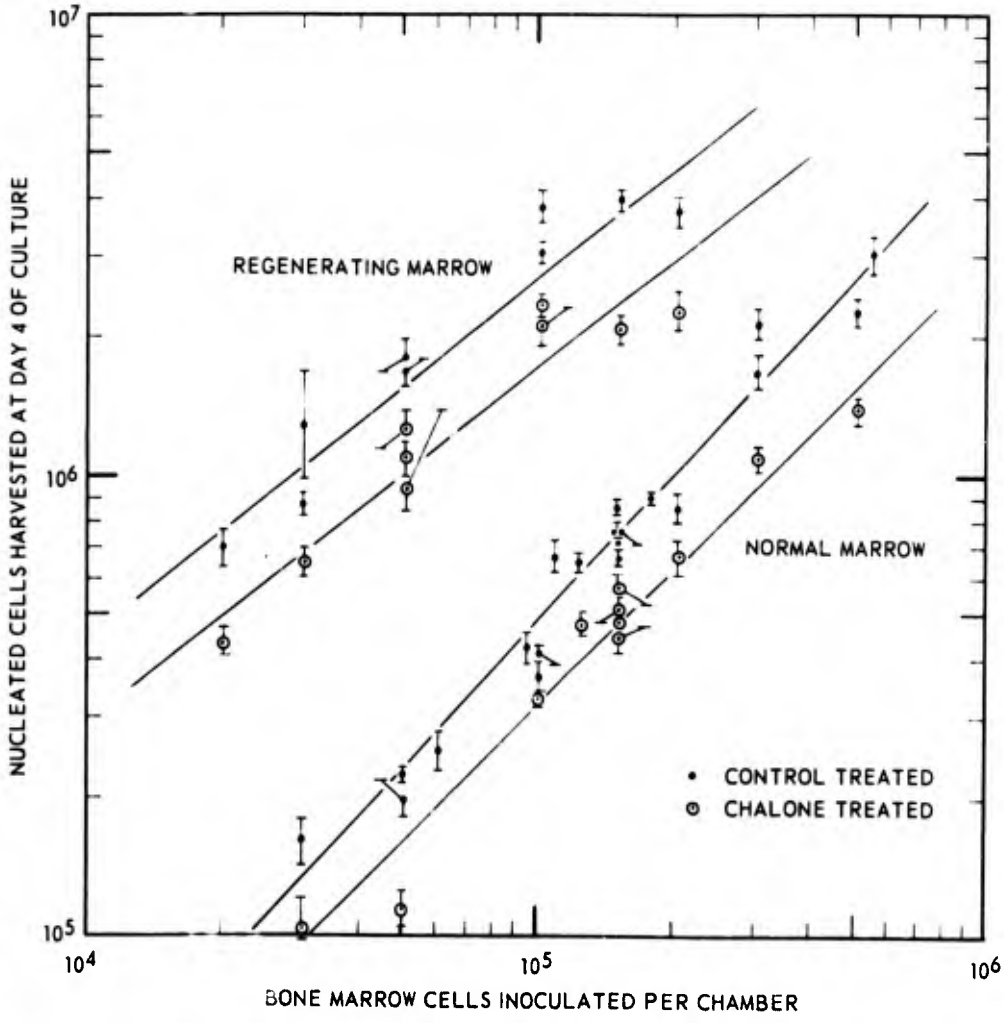

Figure 14. The number of bone marrow cells inoculated, normal and regenerating, versus the mean number of granulocytes plus macrophages harvested at day 4 of culture (± SEM). The regression lines for regenerating marrow are described by the equations $y = (27.099)x^{0.786}$ and $y = (17.299)x^{0.773}$ for control and chalone treated groups respectively (respective correlation coefficients 0.913 and 0.880). Normal marrow relationships are described by $y = (4.703)x^{1.070}$ and $y = (3.123)x^{1.041}$ for control and chalone treated groups respectively (respective correlation coefficients 0.963 and 0.950).

Table VIII shows the reduced number of granulocytic progeny formed both per CFU and per marrow cell inoculated as a result of chalone treatment. Chalone reduced the number of progeny formed on day 4 of culture by approximately 30 percent in both cases.

Table VIII. Effect of Chalone on the Number of Granulocyte Progeny Formed per Stem Cell (CFU) and per Marrow Cell Inoculated

Marrow inoculum	Treatment	Granulocyte progeny* per CFU inoculated	Percent reduction	Granulocyte progeny per marrow cell inoculated
Normal	Control	12.6×10^3	30.0	4.2
	Chalone	8.6×10^3		2.8
Regenerating	Control	35.3×10^3	30.0	25
	Chalone	22.8×10^3		16

* Granulocytes (proliferative plus nonproliferative) harvested at day 4 of culture

In summary, the initial studies dealt with establishing the existence of a granulocytic inhibitor or chalone and the results permit the following conclusions.

The granulocyte extract used in the present studies contains an inhibitor or granulocytic chalone which exerted a tissue-specific, noncytotoxic and nonspecies inhibitory effect on in vitro and in vivo granulopoiesis. The reduction of granulocyte progeny formed in diffusion chambers may be the result of chalone acting during the early phase of culture to reduce the active growth fraction of granulocyte progenitor cells and thereby diminishing the amplification potential inherent in the initial cell inoculum.

◆◆◆◆◆◆◆◆

RESTORATION OF IMMUNE CAPABILITIES IN POSTIRRADIATED ANIMALS

Principal Investigators: *M. P. Fink, C. L. Cloud and K. F. McCarthy*

Prior immunization of a lymphoid cell donor against the histocompatibility antigens of the prospective recipient can diminish the intensity of the graft versus host (GVH) reaction. Both immunologic enhancement and partial tolerance have been proposed as

the mechanism of this immunosuppression. Preliminary evidence obtained in our laboratory favored the enhancement explanation. Hence, a study was undertaken to test the hypothesis that the reduction of GVH activity following donor sensitization is due to active enhancement mediated by blocking antibodies secreted by cells transferred with the graft. [1]

The GVH reactivity of Lewis (L) rat spleen cells was measured using a popliteal lymph node (PLN) assay in Lewis-Brown Norway F_1 hybrid (LBN) recipient rats. Specific sensitization of donors with a single intravenous injection of LBN spleen cells 7-14 days prior to assay resulted in a significant decrease in GVH reactivity. Third-party sensitization of donors with Lewis-Buffalo spleen cells did not alter GVH reactivity. L spleen cells suspended in L anti-LBN serum were equally as reactive in the PLN assay as L spleen cells suspended in normal L serum. An association was observed between the degree of immunosuppression as a function of time after sensitization and the titer of cytotoxic antibody in the donor serum (Figure 15).

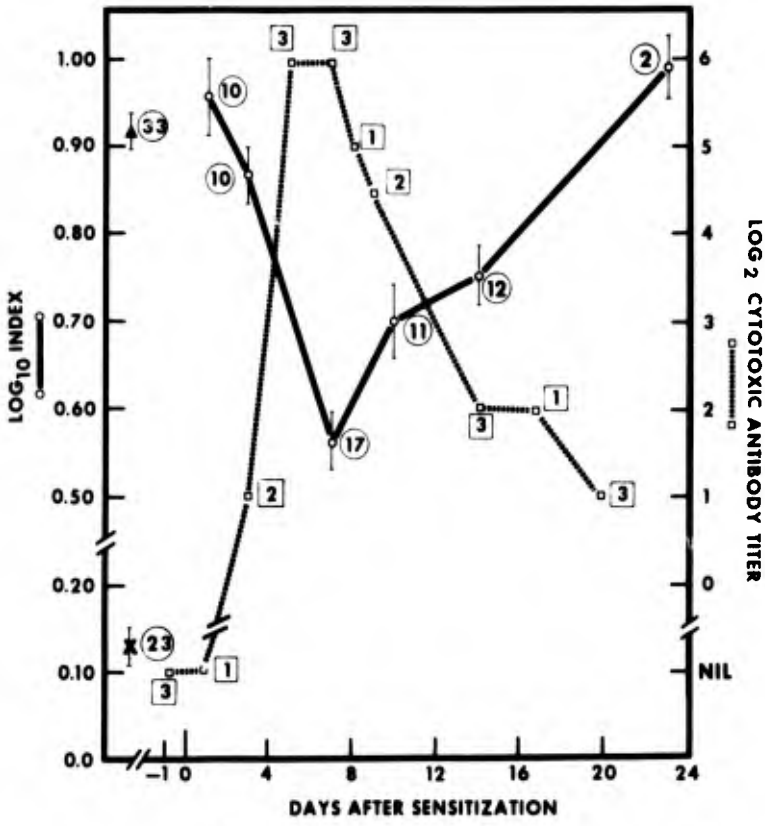

Figure 15. PLN indices (o——o) and donor serum cytotoxic antibody titers (□·····□) as a function of the interval between sensitization and assay. Each small circle represents the geometric mean (± 1 SE) of the indices obtained by measuring the GVH reactivity of cells from the number of donors indicated within the large circle adjacent to each point. Mean PLN indices were also obtained for normal L cells (▲) and LBN cells (x). Each small square represents the geometric mean of antibody titers determined in replicate assays of pooled serum. Serum from two identically sensitized rats was used per assay. The number of replicate assays performed is indicated within the large square adjacent to each small square.

Velocity sedimentation was used to separate spleen cells obtained from specifically sensitized L rats into fractions either enriched or depleted of antibody-forming cells (AFC). The addition of 10^5 or 10^6 sensitized cells from the AFC-enriched fraction to 10^7 normal spleen cells resulted in a significant decrease in GVH reactivity (Figure 16). The addition of 10^6 sensitized cells depleted in AFC did not significantly change the GVH reactivity of 10^7 normal L spleen cells. From these data we concluded that the suppression in GVH reactivity produced by donor sensitization can be accounted for by immunoblocking antibodies secreted with the graft.

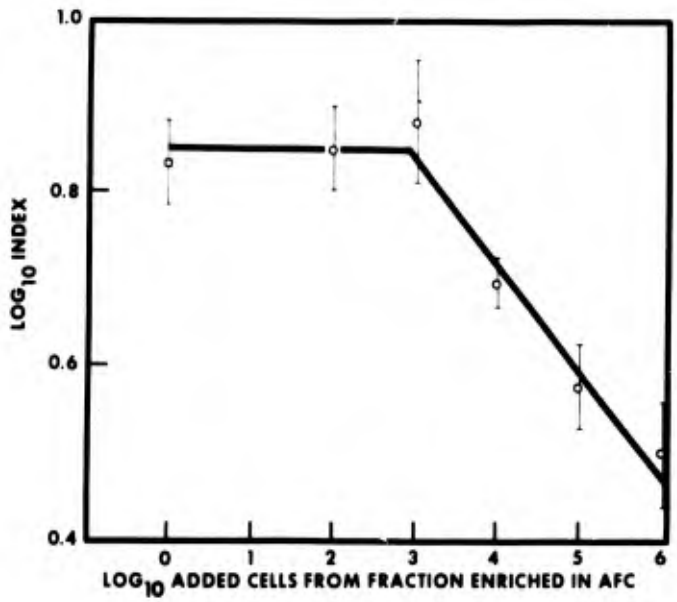

Figure 16. PLN indices obtained by adding various numbers of sensitized spleen cells from the fraction enriched in antibody-forming cells (AFC) to 1×10^7 normal L spleen cells. Each circle represents the geometric mean (± 1 SE) of the indices obtained in two replicate experiments. As a control for each experiment three or four LBN rats were injected with only 1×10^7 normal L spleen cells. The geometric mean (± 1 SE) of the indices thus obtained is represented by a square.

REFERENCE

1. Fink, M. P., Cloud, C. L. and McCarthy, K. F. Local graft versus host reaction suppressed by immunoblocking antibody secreted by antibody-forming cells transferred with the graft. Bethesda, Maryland, Armed Forces Radiobiology Research Institute Scientific Report SR73-22, 1973 (in press).

EFFECTS OF PHYSIOLOGICALLY ACTIVE AGENTS ON THE PERMEABILITY OF THE BLOOD-BRAIN BARRIER IN POSTIRRADIATED ANIMALS

Principal Investigator: *A. A. René*
Technical Assistance: *J. L. Parker*

Radiogenic edema in irradiated nervous tissue is considered to be the most serious complication in human radiotherapy. It therefore becomes important from a therapeutic standpoint to discover agents which have permeability effects on the blood-brain barrier (BBB). A large number of drugs have been found to influence the functional capacity of the BBB. Some of these are known to have membrane stabilizing properties. The objective of this study was to determine if some of these drugs have a stabilizing influence on the BBB after a large dose of whole-body radiation is administered to the animals.

Young healthy adult Sprague-Dawley rats were exposed to doses of 15 krads of mixed gamma-neutron radiation. Drug effects on the permeability of the BBB were studied by injecting intraperitoneally preselected nontoxic doses of specific drugs (Table IX) which have the ability to decrease the permeability of the BBB (i.e., dexamethasone, hydrocortisone, prednisolone and chlorpromazine).

Table IX. Drug Doses

Drugs	Dose/kg body weight
Dexamethasone	0.3 mg
Hydrocortisone	0.4 mg 20 mg/day, 5 days
Prednisolone	0.4 mg
Chlorpromazine	50 mg

Irradiated and control animals were pretreated with the drugs prior to radiation exposure. Permeability studies of the BBB of the central nervous system of control and experimental animals were accomplished with the use of horseradish peroxidase (HRP) and microperoxidase (MP). Control and irradiated animals were injected with HRP or MP, 5 to 30 minutes before sacrifice. The animals either received 0.3 ml of saline alone or saline containing 0.20 to 0.25 mg HRP or MP. At sacrifice the animals were anesthetized and the brain fixed by perfusion with 2.0 percent glutaraldehyde. The medulla specimens were removed, cut into sections 40 μm in thickness and incubated in a special medium. The specimens were then prepared for electron microscopic analysis.

The electron microscopic examination of brain tissue from supralethally irradiated Sprague-Dawley rats pretreated with the drugs showed no conclusive evidence to support the view that these drugs possess special membrane stabilizing properties.

EFFECTS OF RADIATION ON RENAL FUNCTION

Principal Investigator: *J. E. Buerkert*

The objective of this research was to define and characterize postirradiation diuresis, and to determine the significance of this diuresis in the radiation syndrome of acute intestinal death.

Clearance studies were performed in 16 dogs with surgically formed hemibladders to evaluate the intrinsic renal effects of 2000 rads of x rays administered as a single dose to the left kidney. These studies were conducted under conditions of water diuresis in 10 dogs on days 1, 7 and 14 postexposure. Additional studies were performed 21 and 28 days after exposure in eight of these dogs and 56 days later in four. Six dogs were studied under conditions of osmotic diuresis at all of these intervals.

While the glomerular filtration rate (GFR) tended to remain constant until the studies performed on the 56th day, abnormalities in renal tubular function were evident within 24 hours of irradiation. In water diuresis, free water clearance (C_{H_2O}) was significantly greater within a day of exposure averaging 0.88 ± 0.23 ml/min (SE) from the control kidney (CK) and 1.34 ± 0.31 ml/min from the irradiated kidney (IK) ($p < 0.001$). These differences became greater over the intervals studied and were independent of changes in GFR. Fractional excretion of sodium was also greater from the IK within a day of exposure averaging 0.37 ± 0.11 percent from the CK and 0.54 ± 0.18 percent from the IK. Such differences persisted in the same degree throughout the interval of the study. When vasopressin was infused, urine flow (V) fell significantly at all intervals studied postirradiation. However, V was significantly greater 24 hours after radiation exposure averaging 0.36 ± 0.08 and 0.54 ± 0.10 ml/min from the CK and IK respectively ($p < 0.001$). This difference in V correlated well with a marked increase in the excretion of total solute and sodium. By day 14 urine flow from the irradiated kidney was not different from control kidneys. Twenty-eight days following exposure, V from the IK tended to be greater than from the CK. These differences were associated with a significant decline in negative free water clearance ($T^c_{H_2O}$) from the IK (0.30 ± 0.08 ml/min) when compared to the CK (0.52 ± 0.08 ml/min, $p < 0.01$).

The tubular maximum for T^{c}_{H2O} (Tm^{c}_{H2O}) was determined in six dogs which were studied while undergoing a brisk osmotic diuresis and being infused with vasopressin. There was a significant decline in Tm^{c}_{H2O} 21 days after exposure which became more marked by day 28 averaging 1.18 ± 0.10 ml/min from the CK and 0.015 ± 0.13 ml/min ($p < 0.001$) from the IK.

When urine was collected 18-24 hours after complete food and water deprivation and osmolality was determined no differences were seen until day 21. By day 28 osmolality of urine collected from the IK was half that obtained from the CK averaging 930 ± 148 and 1898 ± 259 mosmol/liter respectively.

Thus the earliest effects of radiation are related to the ability of the proximal tubule to reabsorb sodium and are manifested by both an increase in the fractional and absolute excretion of sodium within 24 hours of exposure which continues throughout the interval of the study and by a marked increase in the excretion of C_{H2O} within a day of exposure which becomes greater with time. Approximately 3 weeks postexposure, but before GFR declines, the concentrating segment of the nephron is improved. These studies suggest that renal tubular injury is the major early effect of radiation.

◆◆◆◆◆◆◆◆

EXPERIMENTAL COMMUNICATING HYDROCEPHALUS IN THE PRIMATE: ULTRASTRUCTURAL AND PATHOPHYSIOLOGICAL STUDIES

Principal Investigators: *W. J. Flor, J. S. Stevenson, AFRRI; and A. E. James, Jr., Johns Hopkins Medical Institutions*

Collaborators: *J. H. Flinton, AFRRI; N. Ghaed, Walter Reed Army Medical Center; and B. L. Rish, U. S. Naval Hospital*

Technical Assistance: *J. L. Parker, E. L. Barron, J. K. Warrenfeltz, M. E. Flynn, N. L. Fleming, B. W. Rogers, G. L. Dunson, M. K. Mellor, AFRRI; and C. Digel, Johns Hopkins Medical Institutions*

The objective of this research is to produce a model of communicating hydrocephalus in the primate to study the development of the pathology and pathophysiology of this disease and to investigate countermeasures to the disease processes.

Communicating hydrocephalus most commonly results from inflammation of the leptomeninges as a consequence of infection, hemorrhage or irritation by particulate matter. The leading contributor is subarachnoid hemorrhage, either from head injury,

ruptured aneurysms or intracranial operations. Following instillation of a protein-bound radionuclide into the cerebrospinal fluid (CSF) space to image CSF flow (cisternography), there is in these patients reflux of the isotope into the cerebral ventricles rather than normal passage of isotope over the surfaces of the brain with no ventricular entry. Although patients have chronically normal CSF pressure, a significant number of them show unexplained clinical improvement after cerebral ventriculovenous shunting.

We have developed an experimental model of communicating hydrocephalus in the primate Macaca mulatta by modifying the method of James et al.[2] in the dog. A room temperature curing silicone rubber is implanted via a polyethylene intracatheter in the anterior basal cisterns. The cisterna magna is punctured with a 17-gauge needle and the catheter passed around the brainstem and into the anterior cisterns under fluoroscopic control. One milliliter of Silastic is then infused, and the animal oriented with head dependent until polymerization is complete (20-30 minutes), to avoid occlusion of the foramina of Luschka and Magendie and to optimize the Silastic "seal" at the tentorial notch. This technique is relatively atraumatic to the animal when done properly and it avoids many of the problems attendant to other methods for experimental production of hydrocephalus. At least 70 percent of the implanted animals survive the procedure with no immediate difficulty.

Development of communicating hydrocephalus is monitored by repeated cisternography with 750 μCi of ^{99m}Tc labeled human serum albumin in a volume of less than 0.2 ml introduced at the cisterna magna. We have reported the normal cisternographic patterns in the rhesus monkey[1] as a result of our base-line studies before implantation. Ventricular entry of radiopharmaceutical, characteristic of communicating hydrocephalus, develops in these implanted animals over a chronic time period. Initial entry has been observed in some animals at 1 to 1-1/2 months, and in others as late as 9 months after implantation. Animals with ventricular entry usually demonstrate a qualitative motor deficit.

Histological and ultrastructural studies have begun. Animals are fixed by vascular perfusion with Karnovsky's formaldehyde-glutaraldehyde fixative, postfixed in osmium tetroxide, dehydrated and embedded in Epon 812. Preliminary studies verify the ventricular enlargement detected by cisternography and the patency of the foramina of the fourth ventricle. In general, ventricular expansion occurs at the expense of white matter. The ventricular ependyma becomes flattened and even denuded, especially in the vicinity of the callosal-caudate angle, apparently allowing bulk movement of CSF into brain parenchyma. Perivascular as well as parenchymal edema is observed, with fluid often dissecting along vessels within the basement membrane. Because of the chronic time course of this disease model, secondary changes in neuronal elements and fiber tracts can be studied in these animals as well. Corticospinal tract, motor cortex and cerebellar changes have been observed in the preliminary studies.

In summary, we have produced a model of chronic communicating hydrocephalus in the nonhuman primate. The cisternographic patterns observed in these animals parallel closely those observed in patients with this disease. The chronic time period of our model is much closer to that observed in patients than previous models of hydrocephalus. Because of this chronic time period, presumably we shall be able to investigate those long-term pathologic changes which are responsible for the clinical signs observed in patients with this disease. Additional studies to evaluate the role of altered cerebral blood flow and altered CSF flow and reabsorption in the development of the pathology of communicating hydrocephalus are being formulated. Studies of the early changes will direct efforts to evaluate countermeasures to this disease process.

REFERENCES

1. Flor, W. J., Stevenson, J. S., Ghaed, N. and James, A. E., Jr. Cisternograms in the primate Macaca mulatta. Bethesda, Maryland, Armed Forces Radiobiology Research Institute Scientific Report SR73-21, 1973 (in press).

2. James, A. E., Jr., Strecker, E.-P. and Bush, M. A catheter technique for the production of communicating hydrocephalus. Radiology 106:437-439, 1973.

BONE MARROW CELLULARITY IN MINIATURE SWINE

Principal Investigators: *J. E. West, J. F. Taylor and M. E. Ekstrom*
Technical Assistance: *F. A. Mitchell, J. Witz, P. E. Haynesworth, D. F. Trainor and J. E. Egan*

Miniature swine have been used as valuable laboratory animal models for AFRRI biomedical research in radiobiological investigations and are currently utilized in studies involving radiopharmaceuticals and related nuclear medicine procedures having clinical application in human medicine.

Because miniature swine have several physiological and anatomical parameters similar to man, their use in diverse biomedical research involving ionizing radiation, chemical and drug toxicology, dentistry and surgery is well documented.[1] Despite extensive utilization in research studies affecting the hematopoietic system, no definitive data exist on the marrow myelogram of normal untreated miniature swine. Peripheral blood cell indices in the normal and pathological states have been extensively reported.

To determine the possible role of bone marrow cell renewal systems in the mechanism of radioresistance induced in swine after split-dose gamma irradiation, the development of statistically valid quantitative data on bone marrow cellularity prior to irradiation was mandatory. Purposes of this study were to develop (1) surgical techniques for obtaining repetitive samples of representative bone marrow using local anesthesia and (2) the marrow myelogram for normal young adult (5 to 6 months old) miniature pigs.

The sternum and spinous processes of thoracic and lumbar vertebrae were selected for bone marrow sampling because of the proximity of bone and marrow cavity to the skin surface, the thin cortical bone encompassing the marrow cavity and the several sternebrae and dorsal spinous processes permitting multiple sampling from previously undisturbed marrow tissue. Using aseptic technique and local anesthesia (2-3 ml 2 percent Xylocaine hydrochloride subcutaneously), small volumes (approximately 0.2 ml) of marrow fluid were aspirated from each site, using a sterile 18-gauge, 1-inch Rosenthal needle. Cover slip smears were quickly prepared, air-dried, stained with Wright's-Leishman stain and 1000 nucleated marrow cells differentiated microscopically on stained smears from each aspirate.

Table X shows the comparative data on key bone marrow cell renewal compartments from sternal and vertebral samples. Statistical analyses using the nonparametric Wilcoxon matched pairs sign rank test showed that marrow cellularity from the two sites was not significantly different at the $p = 0.05$ level of significance.

Table X. Comparison of Sternal and Vertebral Marrow Cellularity in Miniature Swine*

Cells*	Differential percent in marrow compartment	
	Sternum	Vertebra
Erythrocytic		
DE	25.95 ± 0.04	26.38 ± 0.03
TE	35.47 ± 0.05	36.85 ± 0.05
Granulocytic		
DG	8.69 ± 0.03	10.62 ± 0.02
TG	45.08 ± 0.05	42.65 ± 0.06
Myeloid: Erythroid ratio	1.31 ± 0.31 : 1.0	1.20 ± 0.35 : 1.0
	2.50 ± 0.54 : 1.0†	2.16 ± 0.50 : 1.0†
Other cells	19.45 ± 0.03	20.50 ± 0.03
Total nucleated cells mm^3	97,800 (60,600 - 139,000)	111,900 (83,100 - 138,400)

* Based upon 29 differential marrow cell counts from sternum and 31 from vertebral spinous processes

* DE=Proliferative erythrocytic cell compartment (rubriblast, prorubricyte, and rubricytes - basophilic and polychromatophilic)
TE=Total nucleated erythrocytic precursor cells - DE plus normochromatic and metarubricytes
DG=Proliferative granulocytic cell compartment (myeloblast, progranulocyte, myelocytes)
TG=Total granulocytic precursor cells. DG plus bands (mature segmenters not included)

† Uncorrected for hemodilution (mature segmenters counted)

Results of this study demonstrated that approximately 70 percent of the total erythrocytic cell renewal compartment consists of immature proliferating stages compared to only 20 percent for the granulocytic cell compartment. These findings provided a valuable reference for quantitating radiation-induced changes which occurred within the radiosensitive proliferating cell stages following split-dose gamma irradiation in these animals.

REFERENCE

1. Bustad, L. K. and McClellan, R. O., editors. Swine in Biomedical Research. Seattle, Washington, Frayn Printing Co., 1966.

◆◆◆◆◆◆◆◆

MECHANISMS OF CEREBRAL EDEMA

Principal Investigator: *L. S. Solomon*

Several recent reports have suggested that 5-hydroxytryptamine (5-HT) produces brain edema; however, each of these works suffers from serious shortcomings[1-4] which make the results questionable.

The objective of this research is to measure the effects of 5-HT on the blood-brain barrier in primates while carefully controlling physiological parameters.

Five-hydroxytryptamine was perfused into rhesus monkeys by the ventriculocisternal route and its concentration in the caudate nucleus and corpus callosum determined. It was shown that a 5-HT concentration gradient was established and ^{14}C 5-HT levels ranged from 1-800 times endogenous levels. No significant increase in blood-brain barrier permeability was noted in the periventricular tissues (Figure 17).

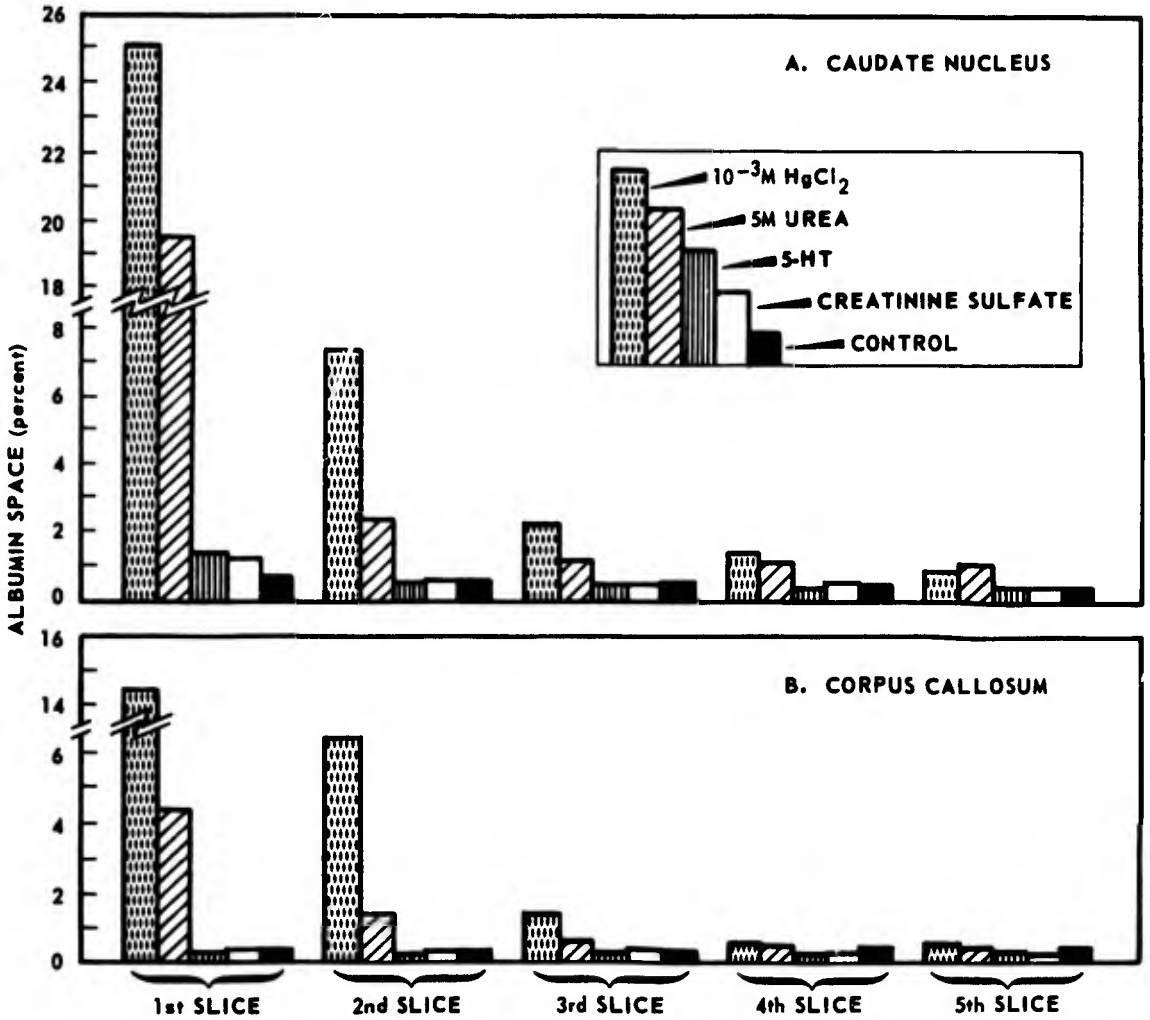

Figure 17. ^{125}I albumin space in successive slices after ventriculocisternal perfusion with various substances

REFERENCES

1. Bulle, P. H. Effects of reserpine and chlorpromazine in prevention of cerebral edema and reversible cell damage. Proc. Soc. Exp. Biol. 94:553-556, 1957.

2. Clasen, R. A., Pandolfi, S., Laing, I., Oelke, D. and Hass, G. M. Reserpine in experimental cerebral edema. Neurology 16:1194-1204, 1966.

3. Gomirato, G. and Zanalda, A. Azione edemizzante "in vitro" comparativa della 5-idrossitriptamina (5-HT) ed istamina sul tessuto nervoso centrale. Archivio per le Scienze Mediche 106:323-325, 1958.

4. Osterholm, J. L., Bell, J., Meyer, R. and Pyenson, J. Experimental effects of free serotonin on the brain and its relation to brain injury. J. Neurosurg. 31: 408-421, 1969.

◆◆◆◆◆◆◆◆◆

EVALUATION OF HEALING OF LONG BONE GRAFTS IN DOGS BY QUANTITATIVE TECHNETIUM-99m PHOSPHATE BONE IMAGING

Principal Investigators: *J. S. Stevenson, AFRRI; R. W. Bright, Naval Medical Research Institute; and F. R. Nelson, U. S. Naval Hospital*

Technical Assistance: *E. L. Barron, W. W. Wolfe, J. K. Warrenfeltz, M. E. Flynn, N. L. Fleming, G. L. Dunson, V. L. McManaman, M. D. Sinclair, AFRRI; and A. Strash, Medical College of Virginia, Richmond*

The objectives of this research[1] were to assess the effect of freeze-drying on the incorporation of autologous and allograft bone substitutes, and to develop surgical reconstructive techniques that will facilitate limb reimplantation and transplantation. In addition, the project was aimed towards evaluating technetium-99m phosphate bone scanning radiopharmaceuticals as a nondestructive, quantitative means of determining the rate of bone regeneration and graft incorporation.

Freeze-dried cancellous autografts and freeze-dried cortical segmental allografts were transplanted into surgically created, 2-cm defects in the distal ulnas of the forelegs of adult mongrel dogs. Fresh autologous bone was inserted as a control graft in one ulna while the experimental bone graft was inserted into the contralateral ulna. The autografts were used to evaluate the effects of freeze-dried autologous bone graft substitutes on the healing process of bone while allografts were transplanted to study the graft materials routinely provided by the U. S. Navy Tissue Bank to military and civilian institutions.

Sequential bone graft imaging was done as follows: 0.5 mCi/kg body weight of technetium-99m phosphate radiopharmaceuticals was given intravenously. Bone images were obtained on a Nuclear-Chicago HP scintillation camera 2-1/2 hours after dosing and photographic records were made on Polaroid and 35-mm film. In addition, the

data were stored on magnetic tape and later analyzed by the Med-II Nuclear Data computer. Bone images were obtained on each dog at 2, 4, 6, 8, 12, 18, and 24 weeks postgrafting and roentgenograms of each leg were obtained at the same time of the imaging procedure.

The bone imaging technique revealed either healing or nonunion of each graft and the scan data were able to depict the fate of the graft 3 to 8 weeks prior to its demonstration by the roentgenograms. When healing occurred, the radioactivity at the graft-host junctional areas progressively migrated together coalescing into one central peak. This provided a dynamic measure for determining the rate of bone healing.

Standard methods of evaluating bone grafts including tetracycline labeling, roentgenograms, tissue biopsy, and biomechanical testing all have their own inherent limitations. The scanning method described avoids these limitations and provides a method of quantitating the rate of bone graft incorporation. This technique can now be objectively applied to identify the most effective bone graft materials and to evaluate tissue graft modifications in order to potentiate the best features of a particular graft material. Early identification of a graft destined to nonunion can now substantially shorten a patient's clinical course by clearly defining the timing of early operative intervention or initiation of appropriate antirejection therapy.

REFERENCE

1. Stevenson, J. S., Bright, R. W., Dunson, G. L., Nelson, F. R., Barron, E. L. and Merriman, M. L. Technetium-99m polyphosphate bone imaging: A quantitative method for assessing bone healing. Bethesda, Maryland, Armed Forces Radiobiology Research Institute Scientific Report SR73-11, 1973 (in press).

EVALUATION OF HEALING OF MANDIBULAR BONE GRAFTS IN DOGS BY QUANTITATIVE TECHNETIUM-99m POLYPHOSPHATE BONE IMAGING

Principal Investigators: *J. F. Kelly, J. D. Cagle, R. W. Bright, Naval Medical Research Institute; and J. S. Stevenson, AFRRI*

Technical Assistance: *G. L. Dunson, E. L. Barron, W. W. Wolfe, M. E. Flynn, J. K. Warrenfeltz and N. L. Fleming*

The objective of this research project is to develop improvements in bone grafting techniques used in oral and maxillofacial reconstruction. In addition, techniques are used to quantitatively evaluate the various allograft, autograft and osseous tissue combinations used to replace severely traumatized or diseased mandibles.

The approach consisted of surgically creating discontinuity defects in the jaws of adult beagle dogs and correcting these defects with various graft substitute systems. Sequential ^{99m}Tc phosphate bone imaging correlated with ^{241}Am bone scan density studies along with routine radiographs were performed to quantitatively assess bone graft incorporation. An equal number of animals are being followed for different time periods after grafting (Figure 18), then sacrificed and the graft site recovered for biochemical and biomechanical testing and evaluation. Studies to date indicate that americium-241 bone density measurements as well as the technetium-99m phosphate bone imaging and roentgenograms will reveal graft incorporation and will determine the rate of bone graft healing. The study also includes patients from the National Naval Medical Center for evaluation of bone incorporation of graft substitutes which have been placed in the mandible for various clinical indications (Figure 19).

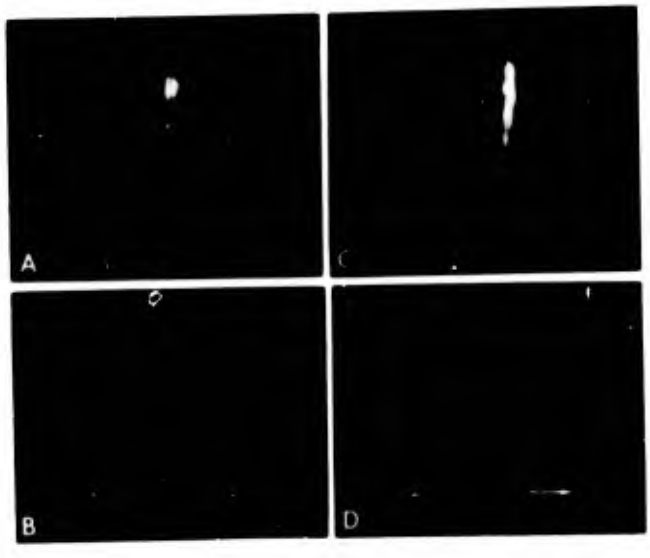

Figure 18. Computer display of bone scan (A) with accompanying histogram (B) of a bone mandibular graft 1 day after surgery. The negative defect represents the nonviable bone graft substitute. Six weeks postsurgery the bone scan (C) with accompanying histogram (D) reveals excellent viability of the bone graft substitute consistent with healing.

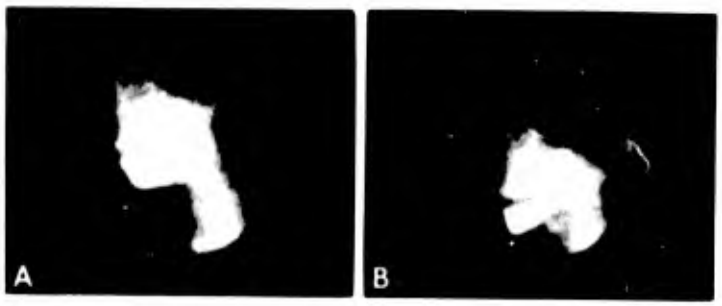

Figure 19. Bone scan (A) of left mandible 1 day after surgery in a patient who had a malignant bone tumor removed and the defect replaced by an appropriate bone graft substitute. The bone scan 6 weeks after surgery (B) reveals the graft (represented by the negative defect on scan A) has healed and has excellent viability.

◆◆◆◆◆◆◆◆

EVALUATION OF TECHNETIUM-99m RADIOPHARMACEUTICALS FOR BONE MARROW SCANNING

Principal Investigator: *G. L. Dunson*
Collaborators: *S. M. Pinsky, R. B. Grove and M. C. Johnson, Walter Reed General Hospital*

The objective of this study was to evaluate several chemical compounds and methods of compounding ^{99m}Tc colloids for use as bone marrow scanning agents.

Studies indicated that ^{99m}Tc sulfur colloid made by a hydrogen sulfide gas method gave smaller particle size than ^{99m}Tc sulfur colloid prepared using thiosulfate. The term ^{99m}Tc minicolloid was introduced in order to make this distinction. It was also learned that the smaller particle size gave better bone marrow localization and better migration through successive lymph nodes. Therefore, a second study was initiated on the use of ^{99m}Tc sulfur colloid for radionuclide lymphography. Results from the study are reported separately.

Other chemical forms of ^{99m}Tc are under investigation for bone marrow imaging. The most promising agent to date is ^{99m}Tc phytate. This radiopharmaceutical and other radionuclides being evaluated for nuclear lymphography will be tried for bone marrow imaging quality as well.

◆◆◆◆◆◆◆◆

NUCLEAR LYMPHOGRAPHY

Principal Investigator: *G. L. Dunson*
Collaborators: *J. H. Thrall, Walter Reed General Hospital; and J. S. Stevenson, AFRRI*

The objective of this study was to develop a clinically useful gamma scanning technique for nuclear lymphography, using ^{99m}Tc radiopharmaceuticals.[1] Technetium-99m minicolloid, a radiopharmaceutical developed for bone marrow imaging, was shown to be more effective than other ^{99m}Tc colloids or ^{198}Au for radionuclide lymphography. This radiopharmaceutical was also demonstrated to have significant advantages over radiographic lymphography. A method was developed for radionuclide lymphography using ^{99m}Tc minicolloid and scintillation camera imaging 90 minutes after subcutaneous interdigital administration and intermittent exercise.

Patient use of the radiopharmaceutical was initiated at Walter Reed General Hospital (WRGH) and a collaborative study involving lymphatic system evaluation of monkeys was started with the Walter Reed Army Institute of Research (WRAIR).

Studies are continuing in three areas: comparison of ^{99m}Tc minicolloid with other chemical species of ^{99m}Tc; comparison of ^{99m}Tc with other radionuclide species, especially ^{67}Ga, ^{111}In and ^{169}Yb; and the application of procedures developed to the evaluation of lymphatic system diseases in collaborative investigations with WRGH and WRAIR.

REFERENCE

1. Dunson, G. L., Thrall, J. H., Stevenson, J. S. and Pinsky, S. M. Technetium-99m minicolloid for radionuclide lymphography. Bethesda, Maryland, Armed Forces Radiobiology Research Institute Scientific Report SR73-12, 1973 (in press).

◆◆◆◆◆◆◆◆

PREPARATION AND COMPARISON OF TECHNETIUM-99m DIPHOSPHONATE, POLYPHOSPHATE AND PYROPHOSPHATE BONE IMAGING RADIOPHARMACEUTICALS

Principal Investigators: *G. L. Dunson and C. M. Cole*
Collaborators: *J. S. Stevenson, AFRRI; and F. Hosain, Johns Hopkins Medical Institutions*

This study was undertaken after it was determined that ^{99m}Tc polyphosphate was not satisfactory for use in quantification studies or long-term bone healing studies because of inconsistent image quality.

A method was developed[1] for preparing the diphosphonate and pyrophosphate pharmaceuticals in compounding kits using starting materials that were synthesized as needed. These kits can be prepared in 10-vial to 1000-vial lots for subsequent use as needed. The three radiopharmaceuticals were compared for safety, effectiveness, pharmaceutical quality, image reproducibility and toxicity. ^{99m}Tc diphosphonate was determined to be the better agent of the three and is currently used in animal and patient studies.

REFERENCE

1. Dunson, G. L., Stevenson, J. S., Cole, C. M., Barron, E. L., Mellor, M. K. and Hosain, F. Preparation and comparison of technetium-99m diphosphonate, polyphosphate and pyrophosphate nuclear bone imaging radiopharmaceuticals. Bethesda, Maryland, Armed Forces Radiobiology Research Institute Technical Note TN73-7, 1973 (in press).

QUANTITATIVE RADIOISOTOPE ANGIOGRAPHY USING CATHETERIZATION TECHNIQUES

Principal Investigators: *V. L. McManaman and J. S. Stevenson*
Technical Assistance: *E. L. Barron, N. L. Fleming, M. E. Flynn and J. K. Warrenfeltz*

The objective of this study was to evaluate the dynamic blood circulation through the various regions of the heart on a quantitative statistical basis by imaging intravenously injected radiopharmaceuticals using the scintillation camera and the Med-II computer system. Data from these dynamic cardiac function studies will be compared to those obtained after radiopharmaceutical administration through a cardiac catheter. Results of this study comparing the two techniques are expected to reveal important information on the relative accuracy of the intravenous route of radiopharmaceutical administration used in clinical medicine practice.

Efforts to find suitable ways to analyze cardiac blood flow data from experimental animals continue. Histograms of the activity distribution as a function of time throughout various regions of the heart may now be generated. However, efforts are continuing to find some technique for obtaining reproducibility of the data. Several procedures for analyzing the data require the use of a more powerful computer than the Med-II system. Efforts are therefore underway to make the magnetic tape from the Med-II system compatible with the IBM 360 computer at the National Institutes of Health (NIH). It is expected that complete compatibility should be achieved within the near future.

Videotapes from approximately 12 cardiac flow studies at the Walter Reed General Hospital have been brought to AFRRI for analysis. Preliminary evaluations on these are presently underway; however, additional evaluation requires a more powerful computer. Analyses will be completed when the magnetic tape of the Med-II computer is made compatible with the IBM computer at NIH.

TECHNETIUM-99m METHOTREXATE STUDIES

Principal Investigators: *P. T. Kirchner, U. S. Naval Hospital; and J. S. Stevenson, AFRRI*

Collaborators: *R. H. Adams, L. L. Heck, J. W. Duley, U. S. Naval Hospital; D. B. Short and G. L. Dunson, AFRRI*

The objective of this study was to determine the metabolic fate including distribution of intravenously administered technetium-99m methotrexate in dogs and rodents and to determine the metabolic fate of intrathecally administered technetium-99m methotrexate in monkeys.

Intrathecal methotrexate is a major therapeutic modality in the treatment and prevention of leukemia involving the central nervous system (CNS). Methotrexate is also an important agent in the treatment of systemic leukemia. Available data on the metabolism of intravenously administered methotrexate are based on studies with tritium labeled methotrexate. The fate of intrathecally administered methotrexate has not been adequately studied. Recent studies of the kinetics of small molecules injected intrathecally revealed that in many instances only a small percent of the injected radiopharmaceutical reaches the cerebral cisterns. Quantitative studies with a gamma emitting label on methotrexate may allow accurate assessment of the distribution of this agent in the CNS.

The approach used in this study was to first label methotrexate with technetium-99m. The fate of the intravenously administered methotrexate was then studied in rodents and dogs. Measurements included blood clearance, plasma protein binding, urinary excretion, and qualitative whole-body distribution as a function of time as disclosed by sequential gamma camera images. Whole-body distribution has been studied in four groups of rats (five animals in each group) at 30 minutes, 1 hour, 6 hours and 24 hours after injection and serially monitoring blood cell counts. Initial studies are inconclusive at this time.

The fate of intrathecally administered technetium-99m methotrexate was evaluated in monkeys and in dogs using a quantitation technique by serial gamma camera images and sequential sampling of the cerebral blood and spinal fluid after administration of the radiopharmaceutical. Serial blood and urine samples were also monitored. Preliminary data revealed that the migration of the technetium-99m methotrexate appears to stop at the foramen magnum with very little movement into the cerebral area. Further studies are underway to substantiate this initial impression.

◆◆◆◆◆◆◆◆◆

QUANTITATION OF CEREBRAL BLOOD CIRCULATION

Principal Investigators: *V. L. McManaman and J. S. Stevenson*
Collaborator: *M. D. Sinclair*

The main objective of this study was to increase the diagnostic value of dynamic cerebral carotid and regional cerebral blood circulation using radionuclide angiography and the scintillation camera and computer systems.

Raw data from ^{133}Xe dynamic studies on experimental animals are recorded by the scintillation camera and stored by an intermediary video tape recording system. The data are then transferred to the Med-II computer via videotape for analysis.

Programs were written for the Med-II system as well as the AFRRI SDS 920 computer system for faster processing. Mathematical models are being fitted to the raw data to determine various parameters, i.e., cerebral blood flow, compartmental cerebral blood flow, and blood flows within and the weights of the white and gray brain matter.

Processing of experimental data will be conducted on a continuing basis. In addition, since the primary research program demands reliable and prompt data processing, a complete backup software package is currently being developed for the IBM 360 computer system at the National Institutes of Health.

QUANTITATION OF TOMOGRAPHIC DATA

Principal Investigators: *V. L. McManaman, J. S. Stevenson and M. D. Sinclair*
Technical Assistance: *E. L. Barron, N. L. Fleming, J. K. Warrenfeltz and M. E. Flynn*

The objectives of this study are (1) to establish the limits of detectability and optimum operating parameters for the Tomocamera (scintillation camera and Tomocamera accessory), (2) to develop procedures for quantitating tomographic data utilizing the Med-II computer system, and (3) to compare quantitative data derived with the tomographic system with the qualitative data provided by the standard Polaroid film.

The operating characteristics of the scintillation Tomocamera using experimental phantoms were evaluated. The limits of detectability of a tumor located at various depths within the Alderson head phantom were established for the Tomocamera. These data have been compared with those from the high resolution collimator, the pinhole collimator, and the rectilinear scanner. For surface type tumors, the rectilinear scanner appears superior to the other three which are about equally effective. The rectilinear scanner was able to detect deep-seated tumors which none of the other three components could detect. Line spread functions and modulation transfer functions will be calculated for these two specific conditions, as well as for others, to determine if this is indeed expected behavior. A table for quickly determining planes of focus for a scintillation Tomocamera was prepared.[1] Other studies to further evaluate the parameters of the Tomocamera will continue.

Considerable support was provided to the Orthopedic Service of the U. S. Naval Hospital and the Dental Research Department of the Naval Medical Research Institute for evaluating potential bone diseases and bone grafts in patients using the Tomocamera. Clinically relevant data are being obtained which otherwise would have been unattainable without the Tomocamera. These are presently being compiled and evaluated.

The scintillation camera console and videotape units were modified so that tomographic data may be recorded onto videotape for playback at a later time. The primary advantage is the alteration of control settings during playback which will give views of additional planes of focus which were not recorded on the original raw data so that minimum patient time is required for a complete evaluation of the study.

REFERENCE

1. Sinclair, M. D. and McManaman, V. L. A table for quickly determining planes of focus for a scintillation Tomocamera. Bethesda, Maryland, Armed Forces Radiobiology Research Institute Technical Note TN73-19, 1973 (in press).

◆◆◆◆◆◆◆◆◆

THE DETECTION OF PULSED MICROWAVE BY THE MONKEY (MACACA MULATTA)

Principal Investigators: *R. W. Young, G. R. Middleton and C. R. Curran*
Collaborator: *E. D. Finch, Naval Medical Research Institute*
Technical Assistance: *J. R. Harrison*

Recent reports indicate that microwave elicits an auditory sensation in some observers.[1] Despite recent studies by Guy et al.[2] which attempt to define the neural substratum of this auditory sensation for the cat, the mechanism and its parameters remain in dispute or undefined for primates. The purpose of this study was to develop a behavioral model for testing the monkey which would produce definitive data concerning the detectability of microwave radiation.

Various parameters have been reported to affect the perception of the acoustical clicks associated with pulsed microwave exposure.[2] The most often cited parameters are the frequency and peak power of the microwave radiations. Based largely on the work by Guy et al.,[2] the microwave energy used in this study was delivered at 2450 megahertz, pulsed at 10 hertz with a 45-microsecond pulse width. The peak power was 4.5 W/cm^2, with an average power density of 2 mW/cm^2.

The subjects were tested in a soundproof isolation chamber, using a conditioned fear response (CFR) paradigm with a free operant avoidance base line. Under these testing conditions, the presentation of any detectable discriminative stimulus (S^D) will

produce a clear increase in response rate. The microwave radiation was used as the S^D for this study. Since testing was accomplished in a room devoid of other auditory stimulation, a response rate increase in the presence of microwave stimulation (S^D) was operationally defined as evidence of detection.

The results of the study are presented in Figures 20 and 21. These figures represent typical response rate increases observed in the presence of microwave stimulation of the two subjects tested in this study. There is a clear increase in response during the microwave-on epoch. This representative response pattern was repeated for each subject for 50 trials. Systematic response rate increase excursions were not observed for any microwave-off epochs, including control periods in which the microwave generator was turned on but its output fed to a dummy load rather than to the horn over the monkey's head. These data are taken as evidence for the detection of microwave by the monkeys tested.

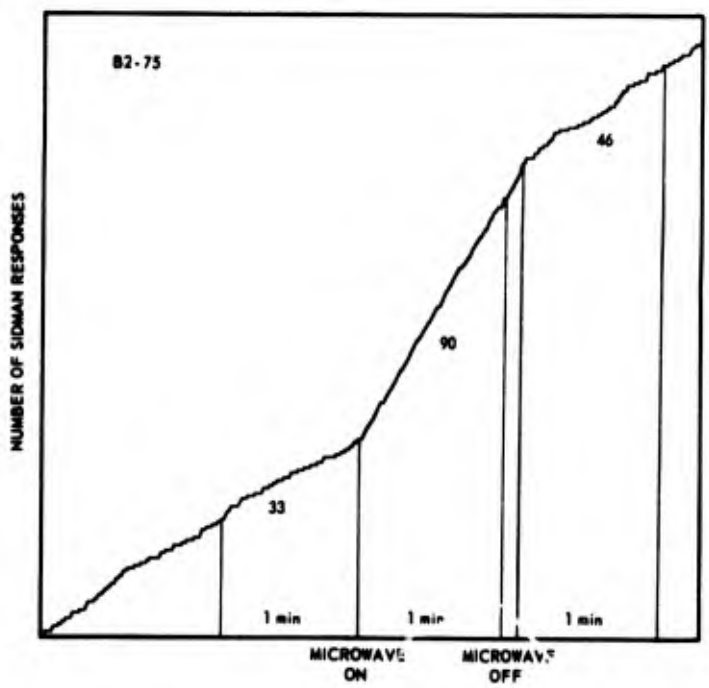

Figure 20. Response rate changes during microwave exposure

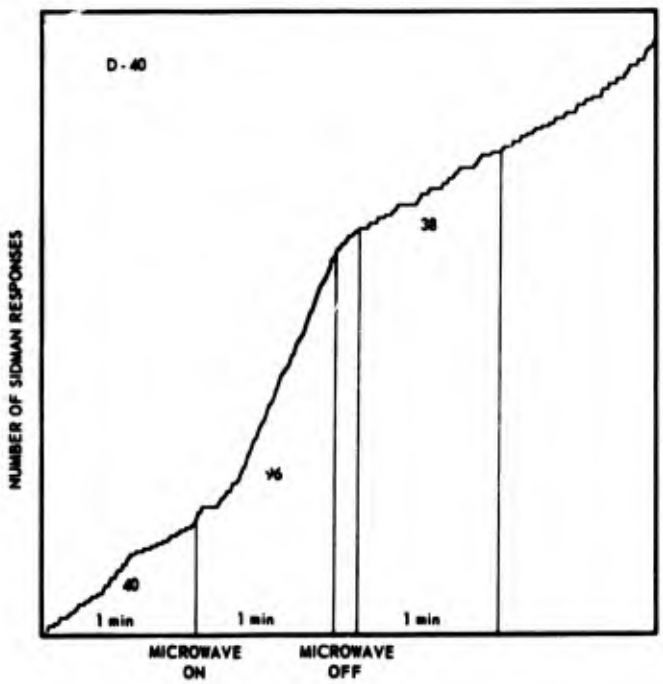

Figure 21. Response rate changes during microwave exposure

REFERENCES

1. Frey, A. H. Biological function as influenced by low-power modulated RF energy. IEEE Trans. Microwave Theory and Techniques 19(2):153-164, 1971.

2. Guy, A. W., Taylor, E. M., Ashleman, B. and Lin, J. C. Microwave interaction with the auditory systems of humans and cats. In: Digest of Technical Papers, IEEE G-MTT International Microwave Symposium, June 4-6, 1973, Boulder, Colorado, University of Colorado, pp. 321-323. New York, N. Y., The Institute of Electrical and Electronics Engineers, Inc., IEEE Cat. No. 73 CHO 736-9 MTT, 1973.

THE INCIDENCE OF BEHAVIORAL INCAPACITATION IN THE MONKEY (MACACA MULATTA) AS A FUNCTION OF PULSED WHOLE-BODY GAMMA-NEUTRON RADIATION DOSE

Principal Investigators: *R. W. Young and G. R. Middleton*
Technical Assistance: *J. R. Harrison, P. Mannon and G. G. Kessell*

The purpose of this study was to define the effective dose (ED) of pulsed mixed gamma-neutron radiation which would produce 10, 30, 50 and 70 percent incidence of behavioral incapacitation in the monkey.

One hundred and twenty monkeys, trained to a shock-avoidance visual discrimination task, were irradiated with single whole-body doses of pulsed gamma-neutron radiation from the AFRRI-TRIGA reactor (n/g = .4). Twenty subjects were irradiated at each of six doses: 800, 1200, 1800, 2700, 3800 or 5300 rads (midhead dose). The incidence of early (i.e., within 30 minutes of irradiation) behavioral incapacitation at each dose level is presented in Figure 22.

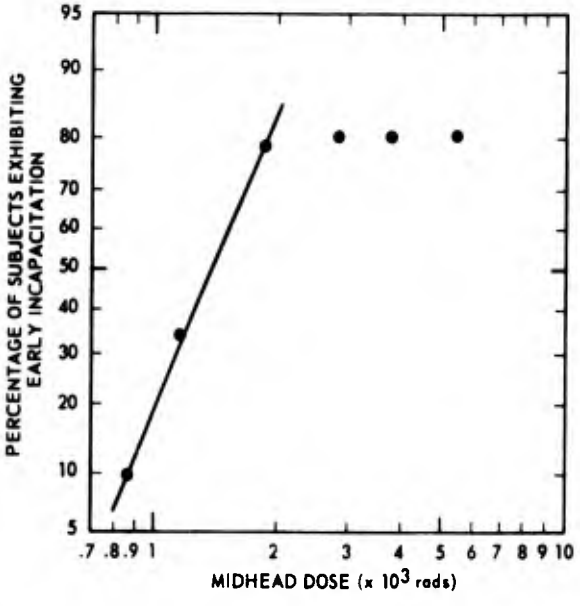

Figure 22. Percent early behavioral incapacitation as a function of dose

As can be seen, there is a distinct discontinuity in the dose-response relationship above 1800 rads. For doses below that point the number of early incapacitations increases as a function of the log of the dose. Below 1800 rads, the relationship between the percentage of the sample exhibiting incapacitation and dose is perfectly described by the model for probit analysis. Increasing the dose, however, from 1800 to

5300 rads produced essentially no change in the number of early incapacitations. Thus, the range of doses from 800 rads to 1800 rads encompasses the effective doses for producing from 10 to 80 percent early behavioral incapacitation in the monkey.

Two types of early incapacitation were observed: permanent and transient. At doses below 1800 rads most early incapacitations were transient; whereas, for doses above that point the number of early permanent incapacitations increased with dose. The data in Figure 22 reflect both types of early incapacitation.

The survival times observed in this study were inversely related to the log of the dose in a manner which corresponds closely to the distribution reported for the incidence of early behavioral incapacitation (Figure 22).

The discontinuity observed in the dose-response relationship for both survival time and the incidence of early behavioral incapacitation is taken to suggest a fundamental difference in effect for doses above and below that inflection point.

◆◆◆◆◆◆◆◆

THE PERFORMANCE OF UNRESTRAINED MONKEYS (MACACA MULATTA) FOLLOWING EXPOSURE TO 2000 RADS OF IONIZING RADIATION

Principal Investigator: *C. R. Curran*
Technical Assistance: *C. G. Franz, W. R. Wiegel, L. Clark and R. L. Brubaker*

The objective of this study is to determine the effects of exposure to a supralethal dose of radiation on the ability of primates (Macaca mulatta) to perform a physical activity task.

Fourteen primates were assigned to three treatment groups: (1) Seven animals were trained to operate an activity wheel and conditioned over a 10-week period to the point where they could maintain a 10-minute run/5-minute rest cycle for 6 hours. (2) Five animals were trained to perform a visual discrimination task using backlit pressplates positioned on one wall of the physical activity wheel apparatus. The position of the wheel was held stationary and the animals were not exercised. Operation of the pressplates by the primates required little movement. (3) Two animals were trained to perform both the visual discrimination and physical activity tasks in the activity wheel. Final training of these animals lasted 8 weeks.

With the exception of one animal, all animals were given a base-line test which approximated postirradiation conditions (Figure 23). One week later the animals were transported to Exposure Room No. 1 of the AFRRI-TRIGA reactor and after a behavioral pretest were exposed to a single pulsed 2000-rad dose of gamma-neutron radiation (n/g = .4). Two of the animals in group 1 were eliminated because subsequent analysis of their pretest performance revealed a deviation from base-line levels of more than 10 percent (previously determined criterion of acceptable performance). Testing began 5 seconds after exposure and lasted for 6 hours for all animals except the animal noted above. In addition, two of the group 1 animals were tested for 2 hours daily until death.

Figure 23 presents the mean group performance levels for groups 1 and 2 as well as the individual performance graphs for the two animals in group 3. The group of

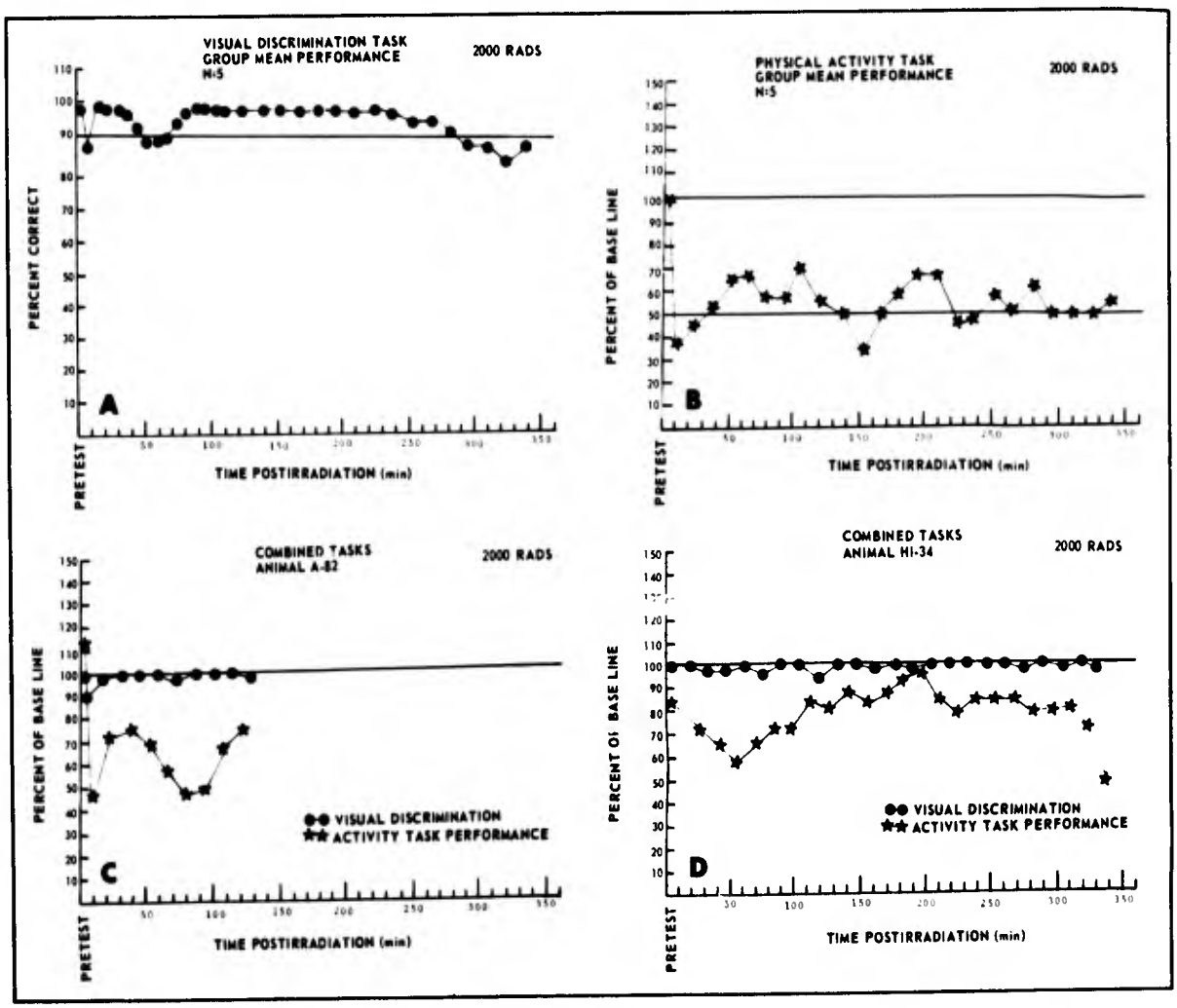

Figure 23. Postirradiation performance of animals trained to the visual discrimination, physical activity and combined tasks

animals performing the visual discrimination task (Figure 23A) exhibited a minor performance decrement within the first 15 minutes postirradiation and a secondary decrement 60 minutes postirradiation. One animal in this group was incapacitated for 3.5 minutes beginning 6 minutes postirradiation but was back to base-line performance levels by 20 minutes postirradiation. The group data then show a gradual decline beginning 4 hours postirradiation. In contrast to the relatively minor disruption of performance observed in the group performing the discrimination task, the group of physical activity animals (Figure 23B) exhibits a significant decrease in performance capability postirradiation. Every animal in this group exhibited at least one period of transient incapacitation during the first 2 hours after exposure. In addition, group performance never exceeds 70 percent of base-line performance during the recovery period (30-120 minutes postirradiation). Data from two of the physical activity animals also indicated that the performance level reached during the recovery period on the 1st day postirradiation is maintained until a few hours before death (7 days postirradiation). The postirradiation performance of the two animals required to perform both tasks (Figure 23C and 23D) (group 3) indicates that animals required to perform a cognitive task and a physical activity task will generate performance levels on both tasks similar to those produced by animals required to perform only one of the tasks. It would thus appear that tasks requiring physical activity or exertion postirradiation are more severely affected than are cognitive tasks requiring little movement and that, following exposure to 2000 rads, recovery of physical activity performance never approaches base-line levels before death.

TEMPORAL CHANGE IN RADIOSENSITIVITY OF MINIATURE SWINE AS EVALUATED BY THE SPLIT-DOSE TECHNIQUE

Principal Investigator: *J. F. Taylor*
Collaborators: *J. L. Terry, M. E. Ekstrom, J. E. West and T. J. MacVittie*
Technical Assistance: *J. E. Egan, P. E. Haynesworth and G. D. Lee*

Earlier studies using the split-dose technique with domestic swine revealed that these animals overrecovered from the effects of a sublethal dose of whole-body radiation. In most species studied by the split-dose technique, exposure to a conditioning dose of radiation which is two-thirds of the normal $LD_{50/30}$ will not result in mortality, but will definitely injure the animal. Doses of this magnitude (two-thirds of the normal $LD_{50/30}$) are at levels where a low but finite level of mortality might be expected, however is rarely seen. Recovery may be complete, or partial if permanent

damage has been done. The split-dose technique is based on the premise that if immediately after the conditioning dose the animals were given another radiation dose equal to the difference between the $LD_{50/30}$ and the conditioning dose, that 50 percent of the animals would succumb, and there would be no recovery at time zero.

A redetermined $LD_{50/30}$ can be calculated at various times (days or weeks) after the conditioning dose. This $LD_{50/30}$ measures the radiosensitivity of the animals after the prior irradiation and indicates the degree of recovery which has occurred.

Recovery from the sublethal conditioning dose can be calculated according to the following equation:

$$\text{percent recovery} = \frac{D_2 - (D_1 - D_c)}{D_c} \times 100$$

where D_2 is the split dose or redetermined $LD_{50/30}$, D_1 is the normal $LD_{50/30}$ and D_c is the conditioning dose.

All exposures for large animal split-dose studies have been with high energy photon radiations and high dose rates. Figure 24 depicts responses seen in ^{60}Co gamma irradiated miniature swine of this study and of other species exposed with 1 MVp x radiation.

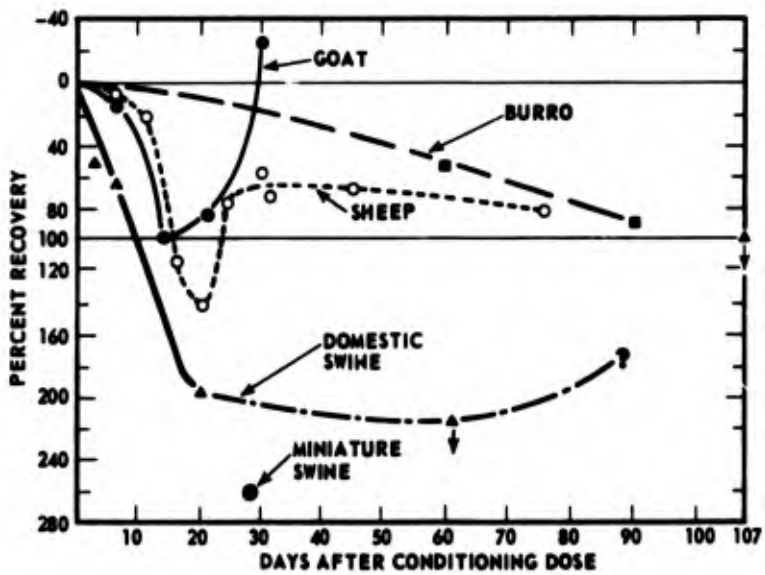

Figure 24. Interspecies comparison of recovery patterns after sublethal conditioning doses as evaluated by the split-dose technique

In this study on miniature swine, the normal $LD_{50/30}$ was determined to be 237 rads. The redetermined $LD_{50/30}$ dose, delivered 28 days after the 150-rad conditioning dose, was 477 rads, significantly greater than the normal single dose $LD_{50/30}$

of 237 rads. In terms of recovery, not only was there no evidence of residual injury from the initial 150 rads, but also additional radiation above the normal $LD_{50/30}$ dose was necessary to produce 50 percent lethality. This is interpreted as overrecovery or acquired radioresistance and is arithmetically stated as 260 percent recovery. These miniature swine data are compared with earlier large animals studies in Figure 24.[1]

As these studies involved dose levels within the range producing deaths in the bone marrow syndrome, overrecovery has been thought to be a reflection of changes in hematopoietic kinetics. Quantitative and qualititative analyses of bone marrow samples taken from several miniature swine during the split-dose study have not revealed significant cellular kinetic changes that could account for the underlying mechanism(s) responsible for the overrecovery phenomenon.

Further studies of bone marrow cell kinetics coupled with detailed serum biochemical analyses will hopefully shed additional light on the physiological changes which are responsible for the marked radioresistance seen in swine in association with their recovery from prior sublethal irradiation.

REFERENCE

1. Taylor, J. F., Still, E. T., Page, N. P., Leong, G. F. and Ainsworth, E. J. Acute lethality and recovery of goats after 1 MVp X-irradiation. Radiation Res. 45:110-126, 1971.

◆◆◆◆◆◆◆◆

RADIATION EFFECTS ON VISUAL ACUITY

Principal Investigator: *C. R. Curran*
Technical Assistance: *C. G. Franz*

The objective of this study is to determine the immediate postirradiation effects of 2500 rads of 43 MeV electrons on the visual acuity of primates (Macaca mulatta).

To date, two animals have been irradiated with 2500 rads of 43 MeV electrons from the AFRRI linear accelerator. The animals were so positioned that the electron beam entered at the site of the lateral canthus of the right eye and passed mesad striking the medial surfaces of both eyes and exiting from the area adjacent to the lateral canthus of the left eye.

The first animal irradiated was a naive male that was held for 10 days postirradiation. Light microscopic histological analysis indicated that there was edema of the ciliary body and iris of the eyes but no edema of the retinal tissue. In addition, the retina appeared free of degeneration with all layers intact.

The second primate was trained to perform a Landolt "C" ring visual acuity test which uses a modification of the Blough technique for threshold determination. This animal was then exposed to 2500 rads while performing at threshold levels and tested for 1 hour after irradiation. At no time during postirradiation testing did the animal's visual acuity deviate from preirradiation threshold levels (i.e., 20/15 vision). In addition, this animal's visual acuity was tested periodically for 10 days postirradiation. During this time, visual acuity remained at preirradiation levels.

RADIATION EFFECTS ON BEHAVIOR AND THE EEG OF THE MONKEY (MACACA MULATTA)

Principal Investigator: *W. L. McFarland*
Collaborator: *S. G. Levin*
Technical Assistance: *E. E. Sereno and J. F. Lee*

The objective of this study is to identify brain bioelectric responses of the monkey to radiation and to correlate these responses with behavioral alterations.

In one phase of the study, three monkeys fitted with EEG recording electrodes at deep brain sites and cortex were irradiated (whole body) in the LINAC with 2500 rads. Over a period from 2 to 15 minutes after the pulse, high amplitude slow wave activity appeared prominently in leads from parieto-occipital cortex, septal area, and caudate nucleus. Minimal alterations were seen in the electrical activity of the hippocampus, mesencephalic reticular formation, or thalamus (Figure 25). However, in one monkey, sporadic bursts of spiking activity seen in the hippocampus before irradiation changed to a constant spiking pattern after irradiation.

Another way to test the functional integrity of the brain after irradiation is to apply known sensory inputs, in this case flashing a strobe light in the monkey's eyes, and recording the visual evoked response from the lateral geniculate body and other sites. The responses decreased in amplitude after 2500 rads of whole-body irradiation from the LINAC and then partially recovered by 40 minutes after irradiation. Figure 26 illustrates the changes seen in the original EEG traces. Slow wave activity

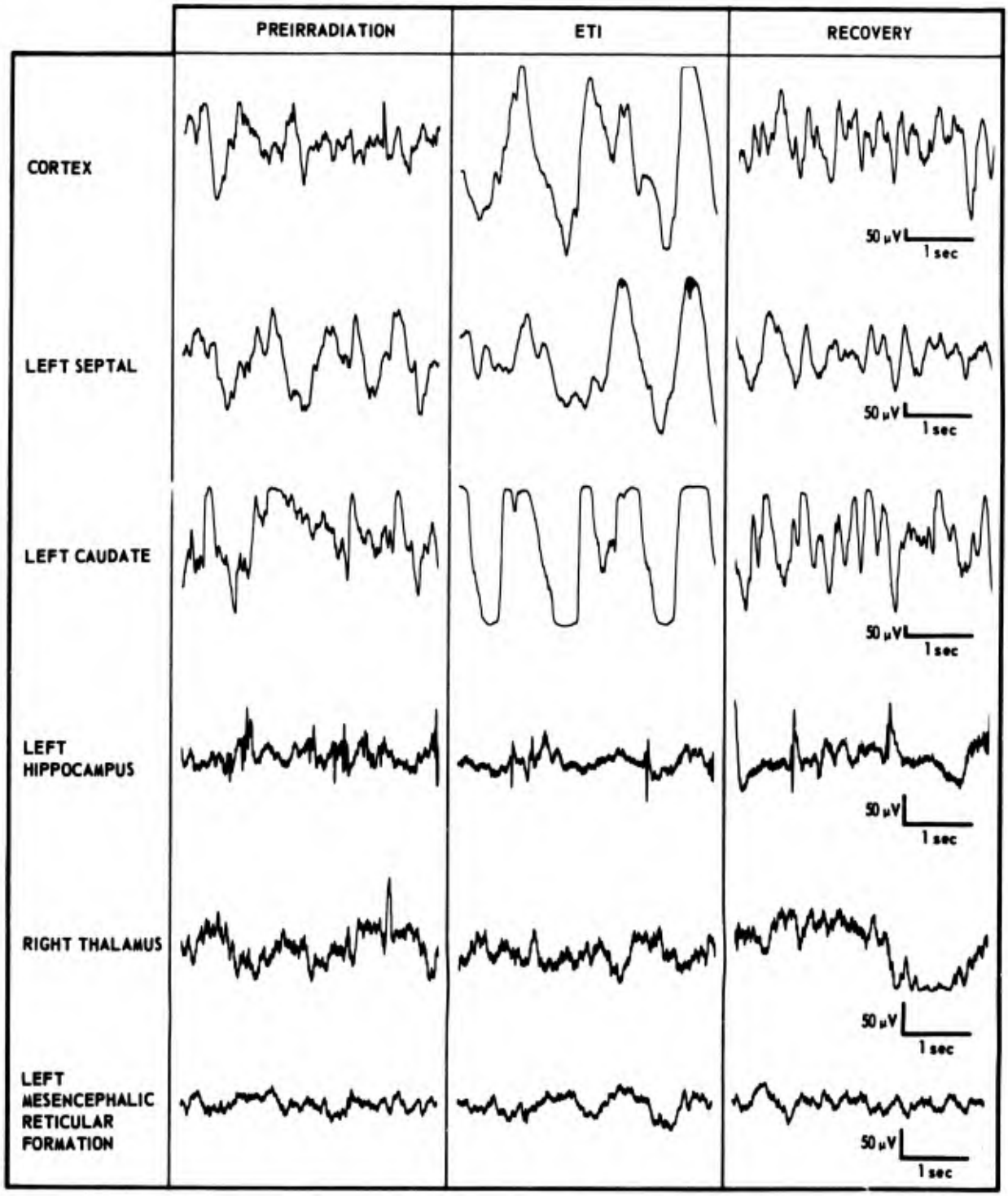

Figure 25. EEG recordings preirradiation, during ETI and recovery

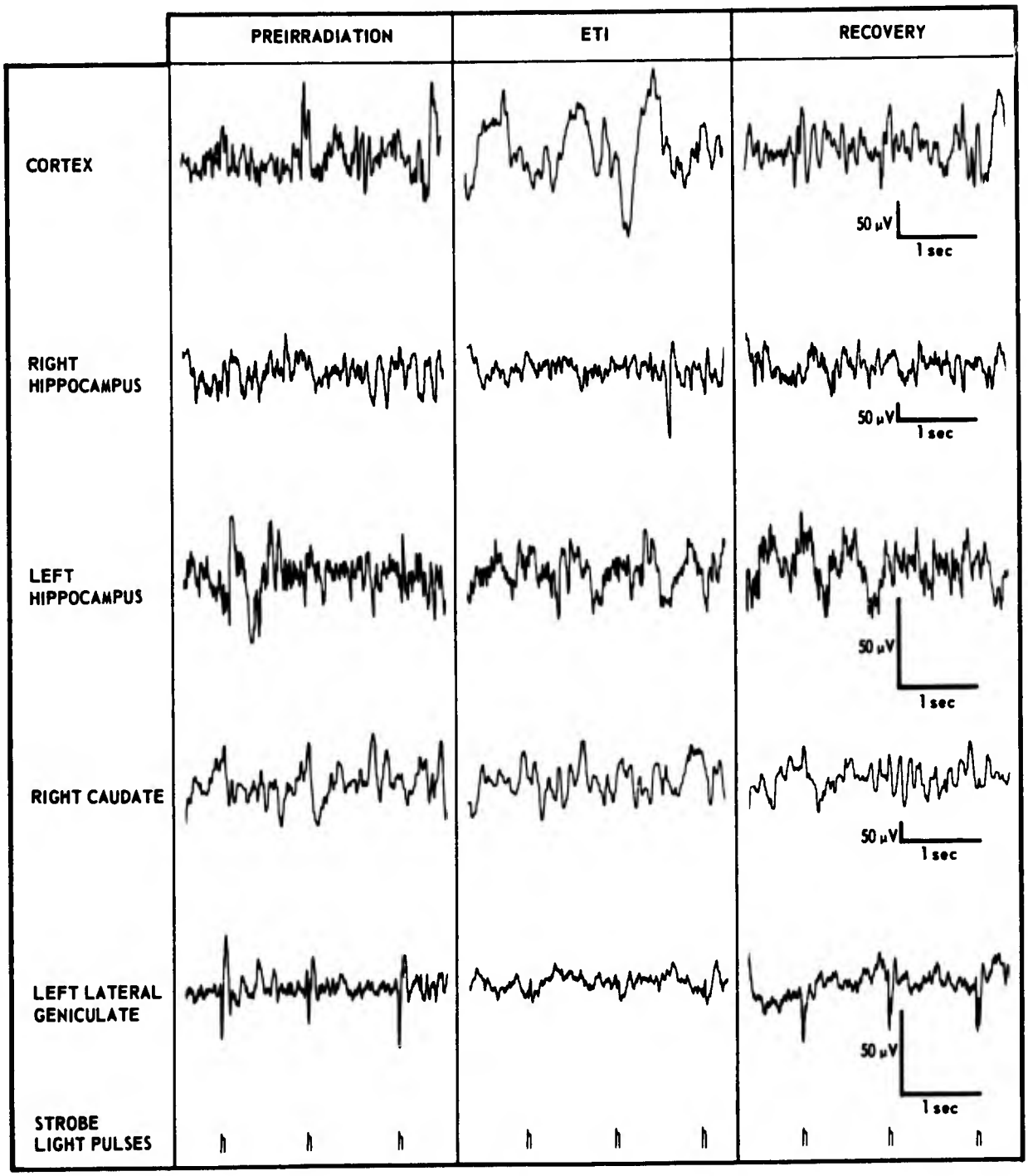

Figure 26. EEG recordings preirradiation, during ETI and recovery

in the cortex and caudate nucleus appeared prior to the change in evoked activity and recovered prior to the recovery of the evoked response. These results suggest that (1) electrical activity of the brain is not uniformly affected by LINAC electron beam irradiation, and (2) a structure (e.g., lateral geniculate body) can be functionally impaired without the appearance of abnormal slow wave activity. A second method of testing brain functional integrity after radiation has utilized electrical stimulation of the hypothalamus to increase systemic blood pressure. During the initial sharp drop in pressure after 2500 rads irradiation with the TRIGA reactor, a pressure increase can still be obtained with stimulation, although of a diminished magnitude (stimulation current intensities are identical before and after irradiation). This would suggest that the functional capacity of this part of the cardiovascular regulation system is still relatively intact after irradiation.

RELATIONSHIPS OF BRAIN BIOELECTRIC ACTIVITY TO SKELETAL MUSCULAR ACTIVITY AND RADIATION

Principal Investigator: *W. L. McFarland*
Collaborator: *H. Teitelbaum, University of Maryland*
Technical Assistance: *W. N. Fry*

This study has the combined purpose of determining the relationships between hippocampal bioelectric activity (especially that in the theta band, 6 to 8 Hz) and movement and of determining some of the neuroanatomic bases and pharmacologic properties of the theta rhythm.

Previous work in this laboratory,[1] showing that hippocampal bioelectric activity can be markedly altered by training rats to run, has been extended by demonstrating a relationship between hippocampal theta waves of rats and forced running on a treadmill device. The latter experiment shows that (1) theta waves are related to locomotion per se, (2) the amplitude of the movement-induced theta pattern is proportional

to the speed of movement, and (3) movement-induced theta waves are not simply the result of increased proprioceptive feedback, since the theta waves often persist after the cessation of movement.

In another experiment to determine the relationship of hippocampal theta to locomotion, theta activity was varied rather than behavior. High frequency (80 Hz) electrical stimulation of the medial septal nucleus blocks theta in the hippocampus and low frequency (8 Hz) stimulation is reported to induce hippocampal theta. In rats trained to run for water, it was found that 80 Hz stimulation of the medial septal nucleus blocked running and 8 Hz stimulation had no effect.

In a study designed to assess the effects of radiation on hippocampal theta and locomotion, rats were trained to run for water or forced to run on a treadmill, then exposed to 10,000 rads whole-body radiation from the LINAC. In the 48-hour observation period after irradiation, the rats would generally neither run to obtain water nor spontaneously move on the treadmill. They would drink if given water and would move on the treadmill if forced to do so. Cortical activity in the rats trained to run for water decreased in amplitude on the day after irradiation and on the following day returned to slightly above base-line amplitude levels. Theta activity was seen in the cortex before irradiation, was absent on day 1 postirradiation, and returned on day 2 postirradiation when the rats occasionally moved. Hippocampal activity showed a slight increase in amplitude the day after irradiation and a larger increase by the 2nd day. Theta waves were prominent in the hippocampus whenever the rats did move on the day after irradiation and also on the 2nd day, although higher frequency activity was appearing by then. The bioelectric activity of the rats running on the treadmill showed essentially the same changes, although one rat showed hippocampal activity at about 4-5 Hz when running after irradiation as compared to 6-7 Hz before irradiation.

REFERENCE

1. Teitelbaum, H. and McFarland, W. L. Power spectral shifts in hippocampal EEG associated with conditioned locomotion in the rat. Physiol. Behav. 7:545-549, 1971.

EFFECT OF 2500 RADS MIXED GAMMA-NEUTRON RADIATION ON CEREBRAL TEMPERATURE OF THE MONKEY (MACACA MULATTA)

Principal Investigators: *W. L. McFarland and J. A. Willis*
Technical Assistance: *J. F. Lee and J. L. Rouch*

The purpose of this study was to determine whether or not temperature changes are uniform in the brain after reactor irradiation and the relationship of these changes to body core temperature changes.

Brain temperature was monitored by means of thermistors implanted in the thalamus and on occipital and motor cortices.[1] Body core temperature was measured by means of a thermistor in a cannula placed in the arch of the aorta. The monkeys were trained to do a simple behavioral task to keep them in a constantly alert state during the temperature measurements. Before irradiation, normal temperature gradients were seen, core temperature was less than that of the thalamus, and the brain surface was cooler than the thalamus. After irradiation, these temperature gradients were maintained, although there was generally an initial drop in temperature at all sites, after the radiation pulse, followed by a gradual rise above base-line levels (Figure 27). Brain temperature appeared to follow core temperature in a relatively uniform manner, i.e., there were no significant regional brain differences in temperature response to radiation.

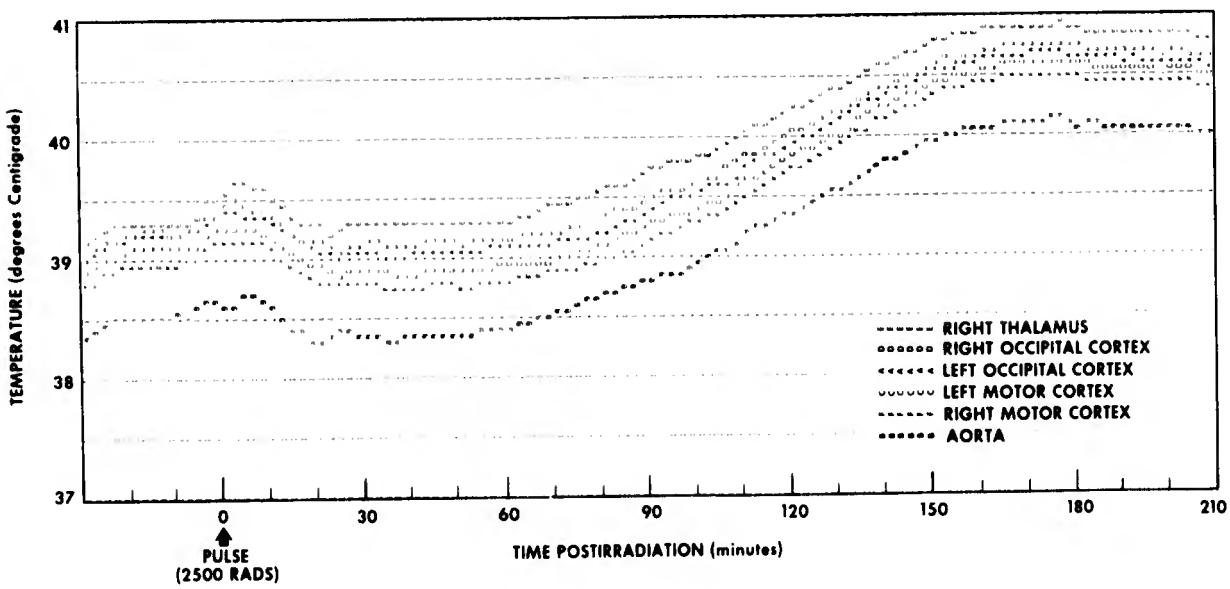

Figure 27. Radiation effects on brain temperature

REFERENCE

1. Willis, J. A. and McFarland, W. L. A computer based physiological temperature measurement system. Bethesda, Maryland, Armed Forces Radiobiology Research Institute Technical Note TN73-12, 1973 (in press).

BEHAVIORAL TOXICOLOGY

Principal Investigators: *R. W. Young and C. R. Curran*
Collaborators: *M. J. Cowan, Navy Toxicology Unit; and G. R. Middleton, AFRRI*
Technical Assistance: *B. A. Dennison, C. G. Franz, R. L. Brubaker, P. Mannon and G. G. Kessell*

Many current systems have as an integral part, or produce as a by-product, substances of possible toxicity to personnel. Further, there is a growing awareness that human performance may be significantly degraded by extremely low levels of some contaminants. These facts, coupled with data which indicate that significant behavioral effects may appear at subclinical exposure levels, have led to the initiation of a study to assess the effects of possible toxic compounds on performance, using trained rhesus monkeys as a model for testing. The purpose of this study was to test the effect on performance of acute venous injection of tetrahydrothiophene 1,1-dioxide (sulfolane-w).

Sulfolane is currently being evaluated for general use as a CO_2 scavenger for self-contained atmospheres. While this compound has potential as a CO_2 scrubber, it has been found to produce clinical toxicity in dogs and squirrel monkeys. The current study was designed to detect any subclinical changes in behavioral performance due to acute injection of the compound. Since, however, any real toxic hazard would be from inhalation rather than injection, the study reported here was conducted only to establish the blood concentrations necessary to produce behavioral toxicity.

A multiple schedule behavioral paradigm was employed to obtain the performance measures for this study. Two rhesus monkeys were trained and stabilized on a discrete avoidance visual discrimination, free operant avoidance schedule. Each animal was tested on successive days to obtain base-line and injection data. Injections were given at 1-hour intervals with doses calculated to produce successive levels of 100, 215, 470 and 1000 μg/ml of total body water in the subject. Between injections, the compound was infused at a rate calculated to maintain the desired blood level. Blood samples were taken before and after injections to verify the sulfolane levels delivered to the animal. Performance was monitored continuously except for periods of injection and blood sampling.

The results indicate no detectable change in the performance of the discrete avoidance visual discrimination task. However, a highly significant dose related depression in both number of responses and response distribution was observed in free operant avoidance. The free operant avoidance data for one subject are presented in Figure 28.

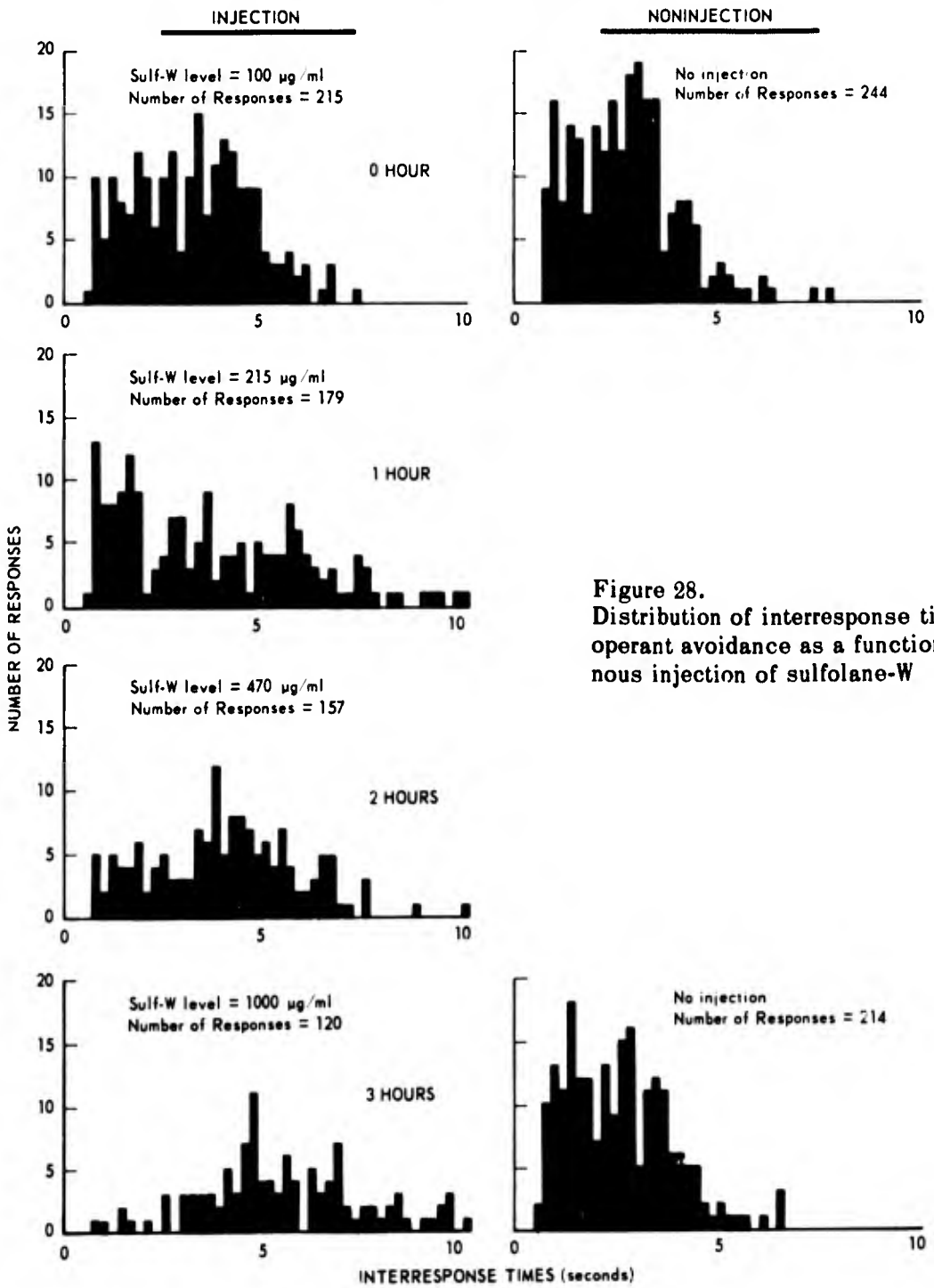

Figure 28.
Distribution of interresponse times on free operant avoidance as a function of intravenous injection of sulfolane-W

Successive dose levels produced successive decreases in performance of this task, so that after the final blood level was achieved the response rate was half the normal level for the subject. This result is interpreted as significant for two reasons: (1) the type of response pattern observed here is very similar to that observed for other compounds known to have depressant effects on behavior and (2) these behavioral effects were observed at dose levels which were insufficient to produce previously observed clinical signs of toxicity, such as vomiting and convulsions. The blood levels established in this study have been used as the basis for dose levels in a study of the effects of chronic inhalation of sulfolane.

EFFECT OF HISTAMINE ANTAGONISTS ON HISTAMINE-INDUCED HYPOTENSION

Principal Investigators: *T. A. Strike and T. F. Doyle*

Recently Black et al.[1] introduced burimamide, a drug capable of suppressing histamine effects insensitive to typical antihistamines. These antihistamine resistant effects have been attributed to the action of histamine on pharmacological receptors defined as H_2 receptors. Receptors whose histamine responses are sensitive to typical antihistamines are classified as H_1 receptors. These investigators have shown that the vasodepressor responses of exogenous histamine in the anesthetized cat are only partially antagonized by mepyramine (typical antihistamine) but could be completely blocked when burimamide was superimposed. The cardiovascular effects of histamine are consistent with the involvement of both H_1 and H_2 receptors in the response.

In our studies, mean arterial pressure values were determined following increasing doses of histamine given intravenously to unanesthetized monkeys. Sufficient time was allowed between each successive dose of histamine for the mean arterial pressure to return to the preinjection value. Chlorpheniramine was then infused into the monkey and the histamine dose-respone curve repeated. Burimamide was superimposed and the sequence repeated.

The effect of histamine receptor antagonists on the vasodepressor response of histamine is shown in Figure 29. After chlorpheniramine, a 50-fold increase of histamine is needed to elicit a 20 percent decrease in blood pressure and a 100-fold increase is needed to elicit a 30 percent decrease. Addition of burimamide appears no more effective than chlorpheniramine alone. If, indeed, burimamide is an H_2 receptor antagonist,

then chlorpheniramine appears capable of antagonizing both H_1 and H_2 receptors and may explain the beneficent cardiovascular effect observed in chlorpheniramine-treated monkeys following supralethal doses of ionizing radiation.[2]

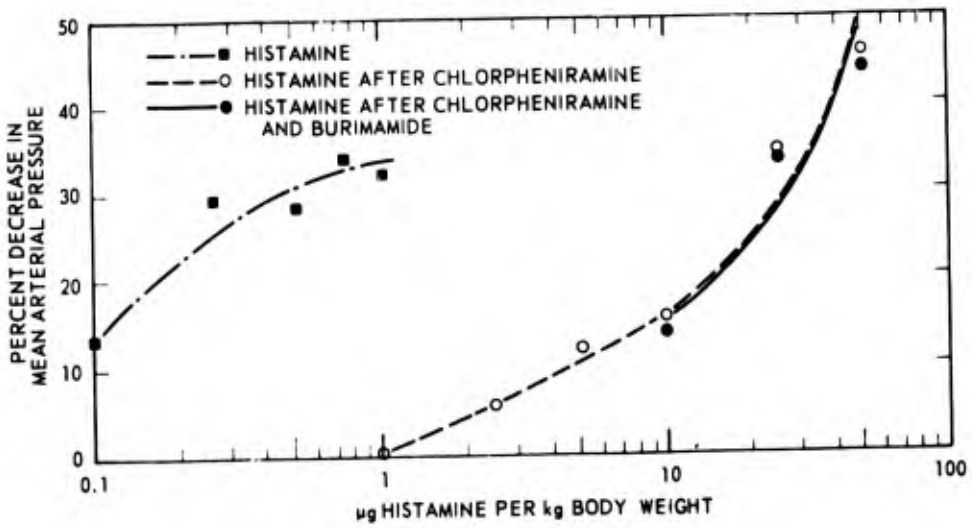

Figure 29. Effect of histamine antagonists on histamine-induced vasodilation in the monkey

REFERENCES

1. Black, J.W., Duncan, W.A.M., Durant, C. J., Ganellin, C. R. and Parsons, E. M. Definition and antagonism of histamine H_2-receptors. Nature 236:385-390, 1972.

2. Doyle, T. F., Curran, C. R. and Turns, J. E. Chlorpheniramine as a prophylaxis to radiation-induced performance decrement in the monkey. Bethesda, Maryland, Armed Forces Radiobiology Research Institute Scientific Report SR73-9, 1973.

PROTEIN-BOUND CARBOHYDRATES AS BIOCHEMICAL CRITERIA IN DIAGNOSIS AND PROGNOSIS OF MALIGNANT NEOPLASIA

Principal Investigator: *A. S. Evans*
Collaborator: *M. F. Dolan, U. S. Naval Hospital*
Technical Assistance: *F. A. Quinn, M. H. Gobbett and G. E. Routzahn*

The present study was designed to investigate the glycoprotein profile of patients with, or suspected of having, malignant neoplasia. These profiles were compared at progressive stages of diagnostic work-ups and treatment regimens and related to the individual's response to therapy to define the utility of such a test battery (1) as an objective diagnostic aid for presurgical estimation of tumor activity, and (2) as a prognostic tool to aid the physician in in-hospital management and outpatient follow-up.

During this period, 727 serum specimens were examined. Three hundred and seventy-one of these samples were from patients in (or outpatients of) the U. S. Naval Hospital, Bethesda, Maryland; 178 from the cancer therapy group, National Institutes of Health (NIH) Clinical Center, Bethesda, Maryland; 177 from AFRRI personnel; and 1 from the Frederick Memorial Hospital, Frederick, Maryland. In addition to the above human patients, sera from 30 cats, some with ^{89}Sr-induced osteosarcomas, were received from the Environmental Protection Agency.

The test battery consisted of total protein, total serum globulins, protein-bound neutral hexoses, hexosamines, sialic acid, and fucose. From these analytical data, a number of additional parameters were derived: ratios of the various carbohydrates to the total protein (mg CHO/dg protein), carbohydrate to globulin ratios (mg CHO/dg globulin), and mole-fraction ratios of the various carbohydrates. The glycoprotein profile consisted of the graphical representation of these analytical and derived data.

Results from the glycoprotein profiles indicate excellent correlation for presurgical differentiation of localized from metastatic tumors and for detection of seeding of occult metastases 2-4 months before the lesions were demonstrable by presently accepted clinical or laboratory procedures.

To illustrate, 178 samples were obtained on 82 individuals being followed by the cancer therapy group, NIH. These patients were 33 Ewing's sarcomas, 15 bronchogenic carcinomas, 14 squamous cell carcinomas, head and neck, 17 breast tumors, and 3 with no clinical disease. Interpretation of the profiles derived from the first samples obtained on each of the 65 patients on whom histories have been received agreed with clinical assessment in only 87.7 percent (57 of 65) of the cases. However, clinical follow-up 1 and 2 months later of the eight patients on whom there was disagreement indicated that they had or were seeding metastatic lesions. In other patients, including several cases who have shown no clinical evidence of recurrent disease for up to 9 years, follow-up profiles indicate that therapeutic control is deteriorating or that recurrent lesions are forming. These patients are being followed intensively by the NIH group.

Similar results were obtained on patients of the U. S. Naval Hospital. More of these cases, however, were sampled before any definitive treatment had been undertaken. A typical profile series is given in Figures 30-32. This patient, a 49-year-old caucasian male, was sampled 16 days presurgery and had a profile compatible with the (later) surgical diagnosis of a localized squamous cell carcinoma of the esophagus (Figure 30). Two hundred seventy-eight days after resection of the circumscribed, noninvasive tumor, the pattern (Figure 31) altered to one indicating a recurrent or metastatic lesion. At this time, no clinical or other evidence suggested the presence of tumor burden. Eighty-one days later (on the patient's next 3-month check-up), 359 days postoperative (Figure 32), this patient's profile indicated active, metastatic disease, but clinical examination still did not demonstrate a tumor. Twenty-seven days after this last profile (3 months and 27 days after the profile illustrated in Figure 31), the patient presented with malignant cervical lymph node involvement. Similar changes have been seen in intestinal and lung tumors, the latter, however, only given 2 to 2-1/2 months' warning.

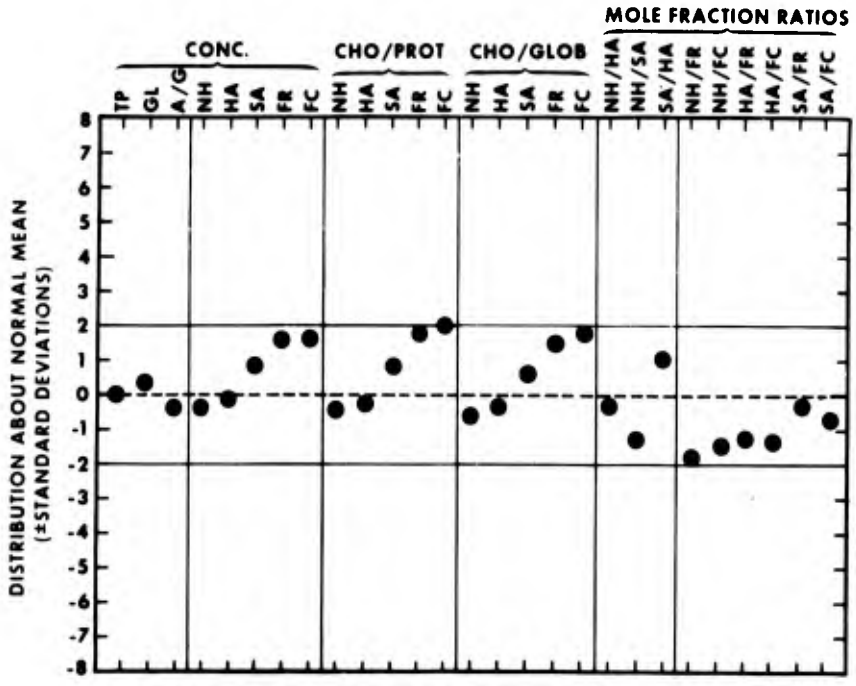

Figure 30. Localized squamous cell carcinoma of the esophagus 16 days preoperative

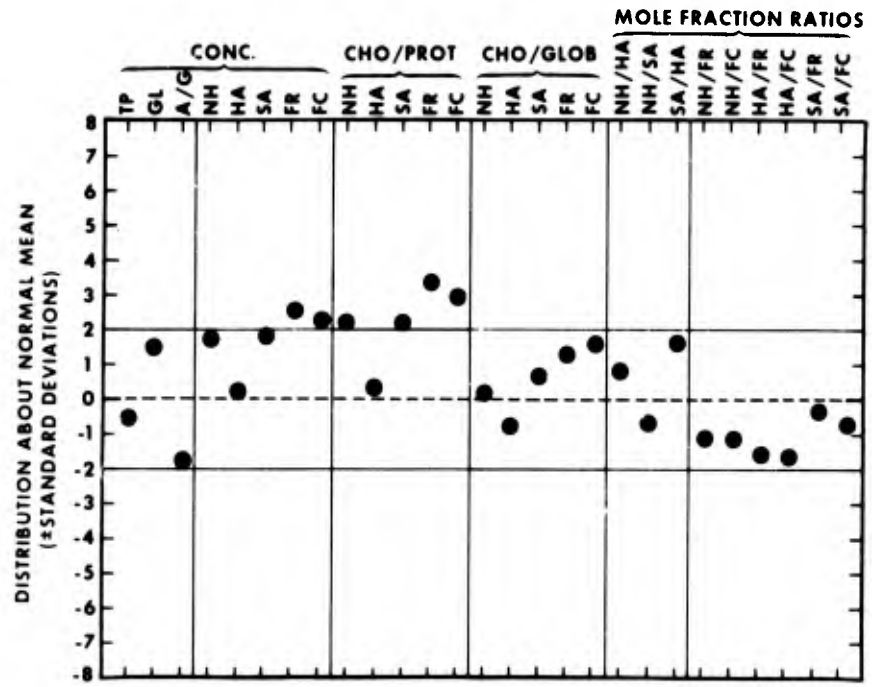

Figure 31. Follow-up on carcinoma esophagus 278 days postoperative. No evidence of disease.

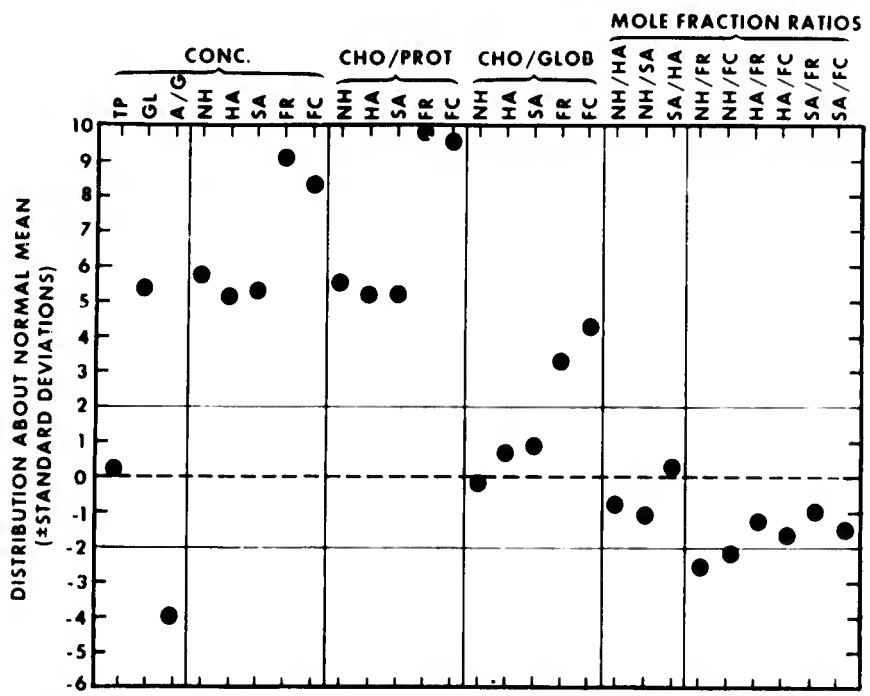

Figure 32. Follow-up on carcinoma esophagus 359 days postoperative. No evidence of disease.

Immunoassay of 16 protein species (albumin and 15 glycoproteins) has been completed on 16 serum samples from five individuals with different tumor types and varied responses to therapy.

Preliminary results from these assays indicate, as one would expect, that the acute phase reactants: α_1-acid glycoprotein, α_1-antitrypsin, and haptoglobin vary directly with the severity of the patient's general condition. However, the consistent depression of the Gc-globulin, transferrin, and hemopexin, together with a uniform elevation of β_1 E-globulin (C'4) suggests that these assays may be of value in adding specificity to the profile battery to aid differential diagnosis.

Calculation and summing of the various carbohydrates bound to the glycoproteins assayed indicate good correlation with the chemical analytic data except in the hexosamines. The presently used technique appears to be underestimating the actual concentrations. It appears also, as was suspected, that the raw fucose values as obtained by the Dische-Shettles CyR3 reaction are being overcorrected for the influence of the neutral hexoses. Both of these procedures are being reexamined.

Blood serum samples were obtained every 2 weeks for 3 months from 20 AFRRI personnel, 10 males and 10 females, to test for individual variation in the glycoprotein profile. The patterns maintained remarkable stability in both sexes for the entire period, indicating that changes seen in pathological specimens are not related to cyclic variation but are responses to the disease state.

The cat appears to be a less than ideal animal model for following the progress of osteogenic malignancies with our present procedures. Certain of the values obtained indicated that the methodology applicable to analysis of human sera is not valid when directly applied to the cat.

◆◆◆◆◆◆◆◆◆

CORRELATES OF MARROW INJURY AND RADIATION SENSITIVITY

Principal Investigator: *M. E. Ekstrom*
Collaborators: *A. S. Evans, J. E. West and J. F. Taylor*
Technical Assistance: *G. D. Lee*

The objective of this project was to further evaluate the possible relationship between preirradiation levels of plasma protein-bound carbohydrates (PBC), measured as neutral hexoses (mannose and galactose), and the relative sensitivity or resistance of animals (C_3H mice) to doses of ionizing radiation producing hematopoietic death.

Previous work by Evans et al.[1,2] indicated that the preirradiation PBC value may be useful in predicting relative radiosensitivity.

Data obtained from 300 young adult healthy male C_3H mice in this study suggested the following: (1) Successive PBC values obtained preirradiation from individual mice do not correlate to the degree required in an effective clinical test. The lack of desired consistency or repeatability may be partly due to measurement error but is probably affected more by the physiologic state of the animal at the time of testing; blood samples were taken at both 3- and 7-day intervals. (2) The correlation between preirradiation PBC value and time to death was not significant. (3) In addition to not significantly aiding in the prediction of time to death, the preirradiation PBC values have not proven adequate as predictors of survival or death after exposures to lethal levels of ionizing radiation. (4) It was concluded that, in the inbred strain of animals tested, the PBC is not a sensitive indicator of radiation sensitivity. In a less genetically homogenous species or strain of animals, it may be useful as a crude indicator but this may be true for any number of measurable physiologic parameters.

Table XI shows data obtained by exposing one group of 104 C_3H male mice, 20 weeks of age, to a calculated $LD_{50/30}$ dose of 875 rads whole-body ^{60}Co gamma irradiation at 40 rads/minute. The results illustrate that the preirradiation PBC values did not serve as good indicators of relative radiation sensitivity.

Table XI. Distribution of Survivor and Nonsurvivor Mice on Either Side of the Median PBC Value for All 104 C_3H Mice Tested. Also Shown is the Time to Death for Mice with Values Below and Above the Median PBC. Note that the Mean ($\bar{x}$) PBC of All Nonsurvivors is Essentially the Same as That for the Survivors. The Mice were Exposed to 875 Rads ^{60}Co Gamma Radiation at 40 Rads/Minute.

PBC (mg/100 ml of serum)	Nonsurvivors	Time to death	Survivors
	$\bar{x}$ PBC of all nonsurvivors = 150.0		$\bar{x}$ PBC of all survivors = 149.2
Range of PBC's below median (122.5 - 147.1)	28 deaths 104 mice tested $\bar{x}$ PBC of dead mice = 137.5	10.6 days	23 survivors 104 mice tested $\bar{x}$ PBC of surviving mice = 140.1
Median PBC = 147.1 (all mice)			
Range of PBC's above median (147.1 - 182.2)	32 deaths 104 mice tested $\bar{x}$ PBC of dead mice = 161.6	10.7 days	21 survivors 104 mice tested $\bar{x}$ PBC of surviving mice = 160.7

Note: $\bar{x}$ PBC of all 104 mice was 149.8 mg/100 ml of serum with a standard deviation of 13.8

REFERENCES

1. Evans, A. S. Effect of ionizing radiations on distribution of plasma protein-bound neutral hexoses in mice and dogs. Radiation Res. 43:152-160, 1970.

2. Evans, A. S., Quinn, F. A., Brown, J. A. and Strike, T. A. Effect of ionizing radiation on total protein-bound neutral hexoses in the plasma of mice. Radiation Res. 36:128-137, 1968.

GAMMA-AMINOBUTYRIC ACID METABOLISM IN RATS FOLLOWING MICROWAVE EXPOSURE

Principal Investigators: *G. H. Zeman, R. L. Chaput, AFRRI; and Z. R. Glaser, Naval Medical Research Institute*

Technical Assistance: *T. K. Dalton*

Animals exposed to microwave radiation even at relatively low power levels have been reported to show a variety of neurologic manifestations, including marked neurochemical alterations. The inhibitory neurotransmitter gamma-aminobutyric acid (GABA) and the enzyme which synthesizes GABA, L-glutamic acid decarboxylase (GAD), play an important role in regulation of neuronal activity in the brain. In view of the current controversy concerning biological effects of microwave exposure, and the sparsity of information on precise mechanisms involved, the possible role of altered GABA metabolism after microwave exposure was investigated. The results of these studies (Tables XII and XIII) indicate that neither whole brain GABA concentrations nor GAD activity were influenced by microwave irradiation in the rat.[1] Therefore, it seems unlikely that alterations in the metabolism of this amino acid neurotransmitter are involved in reported responses of the nervous system to microwave radiation.

Table XII. Whole Brain GABA Concentrations and GAD Activity in Rats Chronically Exposed to 2.86 GHz Microwave Radiation. Data Represent the Mean Value ± SEM for the Number of Animals Indicated in Parentheses.

Duration of exposure	GABA (μmole/g)			GAD activity (μmole/g per h)		
	Unstressed controls	Sham controls	Exposed	Unstressed controls	Sham controls	Exposed
8 hours/day						
3 days	2.09 ± .08 (11)	2.17 ± .08 (8)	2.18 ± .08 (8)	10.7 ± 0.5 (8)	8.9 ± 0.7 (4)	9.3 ± 0.9 (4)
5 days		2.08 ± .10 (8)	2.12 ± .08 (8)		11.7 ± 0.3 (4)	11.6 ± 0.4 (4)
4 hours/day						
4 weeks	2.27 ± .04 (7)	2.30 ± .11 (7)	2.32 ± .08 (7)	12.4 ± 0.8 (6)	10.5 ± 0.6 (7)	10.2 ± 0.7 (5)
8 weeks		2.42 ± .11 (7)	2.40 ± .14 (8)		12.9 ± 0.7 (7)	11.1 ± 0.4 (6)

Table XIII. Whole Brain GABA Concentrations and GAD Activity in Rats Acutely Exposed to 2.86 GHz Microwave Radiation. Data Represent the Mean Value ± SEM for the Number of Animals Indicated in Parentheses.

Treatment	GABA (μmole/g)	GAD (μmole/g per h)
Unstressed controls	2.27 ± 0.04 (7)	12.4 ± 0.8 (6)
Sham controls	2.31 ± 0.11 (4)	13.3 ± 1.2 (3)
40 mW/cm^2 for 20 min	2.28 ± 0.07 (4)	12.1 ± 0.6 (4)
80 mW/cm^2 for 5 min	2.28 ± 0.07 (8)	

REFERENCE

1. Zeman, G. H., Chaput, R. L., Glaser, Z. R. and Gershman, L. C. Gamma-aminobutyric acid metabolism in rats following microwave exposure. Bethesda, Maryland, Armed Forces Radiobiology Research Institute Technical Note TN73-5, 1973 (in press).

ALTERED GAMMA-AMINOBUTYRIC ACID METABOLISM AFTER INCAPACITATING DOSES OF IONIZING RADIATION

Principal Investigators: *G. H. Zeman and R. L. Chaput*
Technical Assistance: *T. K. Dalton*

Animals receiving rapidly delivered doses of ionizing radiation in excess of approximately 5000 rads show convulsions and behavioral dysfunction. In miniature swine these signs begin within seconds after irradiation and terminate minutes later,[1] while rats do not show signs of convulsions until 2 to 4 hours postirradiation (unpublished results). Preliminary results indicated that the metabolism of the inhibitory neurotransmitter gamma-aminobutyric acid (GABA) was significantly altered in the rat within minutes after radiation.[2] Since this amino acid has been implicated in a variety of convulsive disorders, we investigated its metabolism in the miniature swine during the first minutes after radiation. The results shown in Tables XIV and XV indicate that radiation does induce alterations in levels of GABA and L-glutamic acid decarboxylase (GAD), the enzyme which synthesizes GABA activity, in regions of miniature swine brain.[3] Further investigations are being conducted to determine if these metabolic alterations are of physiological significance in postirradiation responses.

Table XIV. GABA Levels in Miniature Swine Brain 4 Minutes After a 10,000-Rad Dose of Radiation

Brain region	GABA level (μmole/g ± S.E.)		Percent of control
	control (N=8)	irradiated (N=8)	
Hypothalamus	3.39 ± .27	3.85 ± .10	113
Midbrain	3.05 ± .18	2.83 ± .15	93
Caudate nucleus	2.86 ± .15	2.89 ± .15	101
Thalamus	2.38 ± .16	2.04 ± .11*	86
Hippocampus	1.77 ± .10	1.66 ± .14	94
Cortex	1.70 ± .06	1.54 ± .08	91
Cerebellum	1.46 ± .04	1.41 ± .06	97
Medulla	1.22 ± .15	1.05 ± .13	86

* Significantly different from controls ($p < 0.05$)

Table XV. GAD Activity in Miniature Swine Brain 4 Minutes After a 10,000-Rad Dose of Radiation

Brain region	GAD (μmole/h/g protein)		Percent of control
	control (N=8)	irradiated (N=8)	
Hypothalamus	417 ± 29	434 ± 41	104
Midbrain	434 ± 19	374 ± 13*	86
Caudate nucleus	300 ± 18	306 ± 23	102
Thalamus	237 ± 8	315 ± 29*	133
Hippocampus	200 ± 16	229 ± 32	114
Cortex	213 ± 7	244 ± 19	115
Cerebellum	242 ± 14	279 ± 27	115
Medulla	191 ± 23	194 ± 15	102

* Significantly different from controls ($p < 0.05$)

REFERENCES

1. Chaput, R. L. and Berardo, P. A. Increased brain radioresistance after supralethal irradiation. Bethesda, Maryland, Armed Forces Radiobiology Research Institute Scientific Report SR73-7, 1973.

2. Chaput, R. L. and Zeman, G. H. Altered gamma-aminobutyric acid metabolism early in the postirradiation response of the rat. Bethesda, Maryland, Armed Forces Radiobiology Research Institute Scientific Report SR73-16, 1973 (in press).

3. Chaput, R. L., Zeman, G. H. and Strike, T. A. Gamma-aminobutyric acid and its role in the radiation induced central nervous system syndrome. Fed. Proc. 32: 348 (Abstract 739), 1973.

METABOLISM OF EXOGENOUS 1-^{14}C-L-FUCOSE IN THE SHAM AND GAMMA IRRADIATED RAT

Principal Investigator: *P. Z. Sobocinski*
Technical Assistance: *W. J. Canterbury and K. M. Hartley*

The methylpentose L-fucose (6-deoxy-L-galactose) is one of several sugar constituents of various glycoproteins and mucopolysaccharides. Serum levels of protein-bound L-fucose have been reported to increase in human diabetes and cancer. The pathophysiologic significance of these findings is not clear at the present time. Knowledge concerning the metabolism of this methylpentose in normal and disease states, however, assumes a new importance in obtaining an explanation of disease-induced alterations in serum fucose levels.

In mammals the degradation of L-fucose, as far as is known, proceeds as follows: L-fucose → L-fucono-1, 5-lactone → L-fuconate → 2-keto-3-deoxy-L-fuconate (KDF). The fate of KDF is unknown. Evidence obtained in this study[3] suggests the existence of a metabolic pathway in the rat through which KDF is metabolized to α-ketoglutarate. Further oxidation of α-ketoglutarate yields CO_2 which under certain experimental conditions is utilized for the production of blood glucose and hepatic glycogen.

The activity of the hepatic enzyme initiating the degradation of L-fucose to L-fucono-1, 5-lactone, L-fucose dehydrogenase, appears to influence the extent of incorporation of ^{14}C from 1-^{14}C-L-fucose into blood glucose and glucosyl residues of hepatic glycogen.

Ionizing radiation and starvation were used to enhance hepatic gluconeogenesis and glycogenesis.[2] Sham irradiation was used to assess the effect of a lethal exposure to ionizing radiation on L-fucose metabolism during the early postirradiation period.

Twelve male Sprague-Dawley rats were selected at random for exposure to ^{60}Co gamma radiation (single whole-body exposure to a midline tissue dose of 850 rads at 20 rads/minute). Twelve control animals were sham irradiated. Food but not water was withheld during the 24-hour period before and after irradiation procedures.

Each animal received an initial 0.3-ml intraperitoneal injection of a normal saline solution containing 12.6 μCi/ml 1-^{14}C-L-fucose immediately after irradiation. A second similar injection was administered 6 hours after irradiation. Animals were sacrificed by decapitation 24 hours after irradiation.

The data presented in Table XVI indicate that, under the experimental conditions employed in this study, ^{14}C from exogenously administered 1-^{14}C-L-fucose is incorporated into blood glucose and hepatic glucose of glycogen in sham and gamma irradiated

rats with an enhanced total hepatic glycogen ^{14}C-incorporation in the latter. Data in Table XVI also show the postirradiation hyperglycemia and glycogen accumulation which are well documented.[2]

Table XVI. Concentrations and Radioactivities of Glucose Residues in Serum and Hepatic Glycogen After Administration of 1-^{14}C-L-Fucose to Sham and Gamma Irradiated Rats

Treatment*	Serum glucose		Hepatic glycogen		
	Concentration†	Specific activity‡	Concentration§	Specific activity**	Total activity††
Sham irradiation (6)	93.5 ± 7.5	257	11.8 ± 2.7	63 ± 33	5,820 ± 1117
850 rads (6)	127.7 ± 11.9‡‡	204	17.8 ± 4.1‡‡	67 ± 50	10,715 ± 7245

* Number of animals is shown in parentheses
† Concentration expressed as mg/dl, mean ± S.D.
‡ Specific activity expressed as dpm/mg, mean of pooled serum of four animals
§ Concentration expressed as mg glucose/g liver wet weight, mean ± S.D.
** Specific activity expressed as dpm/mg, mean ± S.D.
†† Total radioactivity expressed as dpm/liver, mean ± S.D.
‡‡ Significant, $P < 0.05$, one-tailed test

Results obtained from experiments performed to measure the activity of hepatic L-fucose dehydrogenase are shown in Table XVII. A significant difference exists between enzymic activities expressed on a mg protein basis, when values for sham and gamma irradiated rats are compared.

Table XVII. L-Fucose Dehydrogenase (FDH) Activity in Livers of Sham and Gamma Irradiated Rats

Treatment*	FDH activity† ‡ (units/mg protein)
Sham irradiation (6)	0.013 ± 0.001
850 rads (6)	0.017 ± 0.003§

* Number of animals is shown in parentheses
† Units employed are μmoles NADPH formed/minute
‡ Values are expressed as the mean ± S.D.
§ Significant, $P < 0.05$

In our experiments, 1-^{14}C-L-fucose could be expected to yield 1-^{14}C-pyruvate or 1-^{14}C-α-ketoglutarate. Both compounds upon oxidation would yield $^{14}CO_2$ available for incorporation into glucose and hepatic glycogen. In addition, 1-^{14}C-pyruvate could

be directly converted to glucose. However, Rust et al.[1] reported that the ^{14}C-pyruvate from 2-^{14}C-alanine is readily incorporated into hepatic glycogen in the x irradiated rat whereas the incorporation of $^{14}CO_2$ from $NaH^{14}CO_2$ into glycogen proceeds to a limited extent, i.e., less than 1 percent of the tracer dose. Since the amount of ^{14}C-labeling of glycogen found in our experiments is of a similar order of magnitude as that observed by Rust et al.[1] for $^{14}CO_2$, it is not unreasonable to suggest that α-ketoglutarate is an intermediate degradation product of exogenous L-fucose in the rat and that the source of ^{14}C in blood glucose and hepatic glycogen is $^{14}CO_2$, the product of ^{14}C-α-ketoglutarate oxidation rather than ^{14}C-pyruvate oxidation. Furthermore, results obtained in this study indicate that the extent of ^{14}C-incorporation into glycosyl residues is due in part to the activity of L-fucose dehydrogenase.

REFERENCES

1. Rust, J. H., LeRoy, G. V., Spratt, J. L., Ho, G. B. and Roth, L. J. Effect of radiation on intermediary metabolism of the rat. Radiation Res. 20:703-725, 1963.

2. Sobocinski, P. Z. and Altman, K. I. Hepatic gluconeogenesis and glycogenesis in the starved, x-irradiated rat. Radiation Res. 49:390-404, 1972.

3. Sobocinski, P. Z., Canterbury, W. J. and Hartley, K. M. Metabolism of exogenous 1-^{14}C-L-fucose in the sham and gamma irradiated rat. Bethesda, Maryland, Armed Forces Radiobiology Research Institute Scientific Report SR73-14, 1973 (in press).

◆◆◆◆◆◆◆◆◆

AUTOMATED SIMULTANEOUS DETERMINATION OF SERUM TOTAL PROTEIN AND GLOBULIN

Principal Investigator: *F. Z. Sobocinski*
Technical Assistance: *W. J. Canterbury and K. M. Hartley*

Present methods available for the automated determination of serum globulins employ the glyoxylic acid or p-dimethylamino-benzaldehyde reactions for tryptophan. A potential source of error in the determination of serum globulin levels by colorimetric procedures in patients with neoplastic disease is the variations encountered in the free- and bound-tryptophan content of these sera.

This study was undertaken to develop an automated simultaneous procedure for the determination of serum total protein and globulin in which the globulin assay was independent of tryptophan content of serum.[1] In the proposed simultaneous procedure, total protein is determined by the biuret reaction while the globulin is determined by the reaction of globulin with copper in the presence of sulfuric and acetic acids to form colored metalloprotein complexes.

The simultaneous procedure using the AutoAnalyzer (Technicon Corporation, Tarrytown, New York) aspirates serum at a rate of 60 per hour. The serum sample is subsequently separated by a stream splitter into two separate flow manifolds, total protein and globulin. The amount of colored products formed in both reactions is measured at 550 nm. The concentration of each serum constituent is determined from a calibration curve prepared from known human control serum.

Linearity is obtained within the concentration range of 0.0 to 10.1 g/dl total protein and 0.0 to 3.9 g/dl globulin.

Results of replicate analyses performed on a commercial control serum indicate that the standard deviation for the total protein determination is ± 0.10 g/dl and for the globulin determination, ± 0.05 g/dl.

Results of a correlation study between globulin and total protein values in human sera obtained by manual and automated procedures produced a correlation coefficient (r) of 0.874 for globulin and 0.975 for total protein determinations.

The automated globulin method can be readily adapted for the automated analysis of fibrinogen since values for fibrinogen are the differences between globulin assays of plasma and serum.

REFERENCE

1. Sobocinski, P. Z., Canterbury, W. J. and Hartley, K. M. Automated simultaneous determination of serum total protein and globulin. Bethesda, Maryland, Armed Forces Radiobiology Research Institute Technical Note TN73-11, 1973 (in press).

DEVELOPMENT OF A HYPOTHROMBOGENIC BLOOD OXYGENATOR MEMBRANE

Principal Investigator: *P. K. Weathersby*
Collaborators: *T. Kolobow, E. W. Stool and F. Hayano, National Institutes of Health*

Compatibility between blood and synthetic materials remains a major obstacle to the extensive use of artificial internal organs. The reduction of material thrombogenesis in membrane oxygenators is the purpose of this study. We feel that a surface of pure polydimethylsiloxane (PDMS) will be less harmful to blood proteins and platelets than the multicomponent commercial silicone rubber membranes now being used. Progress has been made on several facets of this problem.

Physical variables. The PDMS gum obtained has been sufficiently analyzed to establish its chemical purity. The feasibility of using ionizing radiation in an inert atmosphere to cross-link and graft PDMS onto existing membranes and shunts has been demonstrated, and no appreciable chemical or nuclear (e.g., activation) changes occur.

In applying the mechanically weak PDMS surface to a stronger substrate, a solution coating technique has been used. PDMS is dissolved in a strong solvent (hexane or toluene) and the solution is exposed to the blood contacting faces of membranes, tubes, etc. The rubber substrate swells up to 300 percent and soluble components leach out with apparent diffusion coefficients on the order of 5×10^{-7} cm^2/sec. PDMS diffuses to the surface and adsorbs as a rather discrete coating. The influences of time, concentration and geometry have been studied, prompted by the possible existence of a minimum coating to assure the blood compatibility.

This technique has not yet proved successful in coating an assembled membrane oxygenator. The strong solvents swell the membranes and probably block passage of the PDMS-hexane solution through the small blood channels of the device.

In vitro tests. The in vitro tests of PDMS coatings indicate a marked thromboresistance. Lee-White clotting times of fresh human blood are over 45 minutes. Minimizing the blood-air contact prolongs clotting of the PDMS coated tubing to the range of 90 minutes. A "threshold" effect in the coating has been documented in the latter test. The data spread in these tests does not allow evaluation of process variables.

Ex vivo evaluation. This extracorporeal testing utilizes the "Mini Lung" -- a device that exposes fresh animal blood to small membrane envelopes under a pressure drop related to flow rate, filling and discharge pressures, viscosity and geometry.[1] Monitoring this perfusion pressure allows detection of adhering elements since the pressure is very sensitive to changes in channel clearance.

Numerous tests of coated and uncoated Mini Lungs have been performed with sheep undergoing venovenous bypass. The exact clotting state of the animal depends upon a large number of factors (not all of them known), and this state affects the behavior of blood with a given Mini Lung envelope. When the extremes of entire circuit clotting and heavy anticoagulation are avoided, perfusion pressure-time curves of sequentially run envelopes describe the relative thrombogenicity of the membrane surfaces being tested.

In several sheep, the improvements imparted by coating were striking. Control envelopes showed a pressure rise within 5 minutes and blood coagulation over the entire membrane surface by 15 minutes; PDMS coated envelopes maintained a steady perfusion pressure for over 2 hours and were free of visible thrombi. In one animal the effect was seen with PDMS coatings calculated to be about 5 μm thick, while a 2-μm coating behaved like the controls.

Other experiments using different animals showed very little differences between the two groups of envelopes. This sporadic behavior is being addressed presently by modifying the test circuit and expanding the list of hematologic variables being monitored.

REFERENCE

1. Kolobow, T., Zapol, W. and Marcus, J. Development of a disposable membrane lung for organ perfusion. In: Organ Perfusion and Preservation, Norman, J. C., Folkman, J., Hardison, W. G., Rudolf, L. E. and Veith, F. J., editors. New York, N. Y., Appleton-Century-Crofts, 1968.

EXPERIMENTAL POSTIRRADIATION MYELOPATHY

Principal Investigators: *J. M. Fein, AFRRI; and G. Di Chiro, National Institutes of Health*
Technical Assistance: *L. J. Parkhurst*

Postirradiation myelitis continues to be a significant problem in the treatment of spinal and paraspinal tumors. Neuropathologic studies have emphasized the importance of direct neural injury while other studies have concluded that parenchymal

damage is secondary to vascular injury. Di Chiro[1] has described occlusion of radicular spinal cord arteries 9 months after irradiation with cobalt-60. The changes seen in sequential angiograms suggest that parenchymal dysfunction may be secondary to arterial injury. The purpose of this study is to utilize experimental models of post-irradiation myelitis to differentiate myelopathy caused by vascular injury from direct parenchymal dysfunction.

After undergoing base-line neurologic and angiographic evaluation, rhesus monkeys were brought to the AFRRI. A portal extending from the spinous process of T-10 to the lower lumbar region was outlined. Pulsed doses of radiation utilizing the linear accelerator were then delivered every other day. The dosage delivered varied between different groups of monkeys from 4000 to 10,000 rads. A dosimetry curve was calculated as in Figure 33 to deliver maximal dosage to the thoracolumbar spinal cord. These monkeys are being observed clinically and at the first indication of neurologic deterioration will be reexamined radiographically.

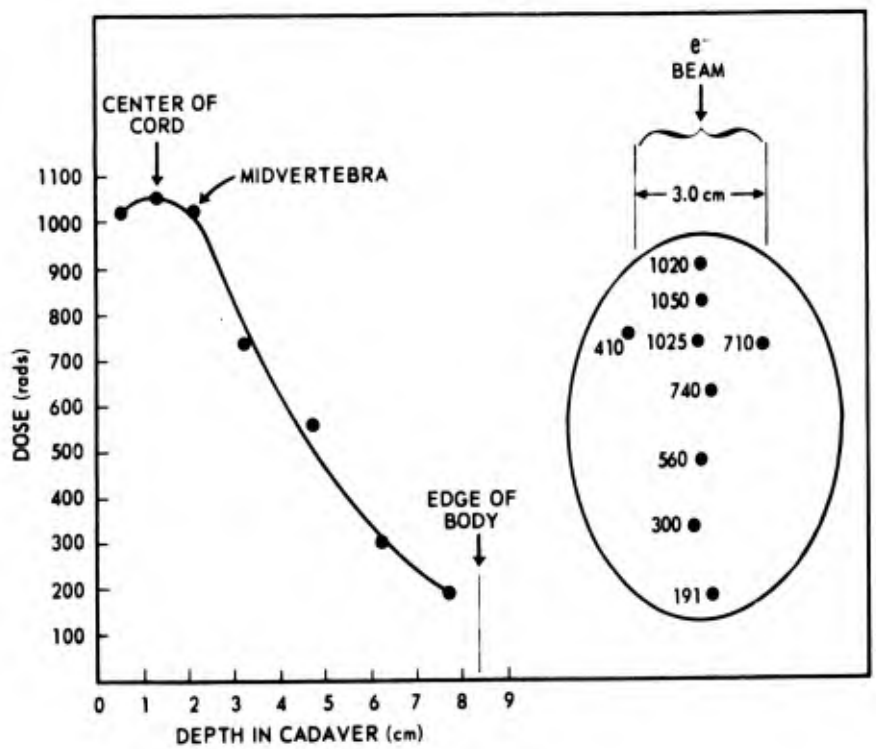

Figure 33. Monkey cadaver body profile at plane of TLD's (T1, T2 interspace)

The latency period between completion of radiation and the development of neurologic dysfunction is generally between 6 and 9 months. At the present time, that latency is just being achieved. No animals to date have demonstrated clear evidence of neurologic dysfunction.

REFERENCE

1. Di Chiro, G. Recent successes and failures in radiographic and radioisotopic angiography of the spinal cord. Brit. J. Radiol. 45:553-560, 1972.

◆◆◆◆◆◆◆◆◆

HEMODYNAMIC EVALUATION OF SUPERFICIAL TEMPORAL CORTICAL ARTERY MICROANASTOMOSIS IN THE DOG

Principal Investigators: *J. M. Fein, AFRRI; and G. F. Molinari, National Institutes of Health*
Technical Assistance: *L. J. Parkhurst*

Microvascular techniques have allowed construction of collateral channels to intracerebral vessels less than 1 mm in diameter to augment the blood supply of the ischemic brain. Superficial temporal cortical microanastomosis has been utilized in 114 clinical cases of focal cerebrovascular disease.[1] As the indications for these procedures become established, there is need for objective hemodynamic data describing the function of these new collaterals. Small anatomic continuity of the graft has not consistently been associated with neurologic improvement. The purpose of this study is to determine the effect of superficial temporal cortical microanastomosis on cerebral blood flow and its autoregulation in the dog.

Thirteen adult foxhounds underwent hemicraniectomy and regional cerebral blood flow studies utilizing the washout of xenon-133 at control steady-state conditions, after occlusion of the middle cerebral stem and after superficial temporal to cortical microanastomosis. Studies were performed under steady-state conditions and during periods of altered blood pressure.

Normoxic normocapnic control animals demonstrated resting mean regional cerebral blood flow values between 30.5 to 36.5 cc per 100 gm/minute. Constancy of blood flow was maintained in all control animals despite a change in mean blood pressure of up to 70 mm Hg. A small degree of hysteresis or lag between blood pressure and blood flow was noted between mean blood pressures of 60 to 140 mm Hg. After middle cerebral stem occlusion, there was a significant reduction in mean regional cerebral blood flow values, especially noted over the temporal regions (Table XVIII), and an intolerance to changes in perfusion pressure (Figure 34). After microanastomosis to temporal cortical branches in five animals, there was an augmentation of regional ($p < .05, < .01, < .025$) cerebral blood flow, and autoregulatory responses showed wide hysteresis loops (Figure 34). Grafting to parietal cortical arteries demonstrated no augmentation of cerebral blood flow. The increase in blood flow noted

after temporal artery grafting was not related to the size of the recipient vessels but rather was in contiguity to those regions demonstrating the severest degree of ischemia. The wide hysteresis curve described after temporal artery anastomosis may bespeak an unstable pressure sensing and volume adjusting mechanism secondary to the surgical trauma sustained by the periadventitial sympathetic innervation.

Table XVIII. Augmentation of Mean Regional Cerebral Blood Flow in the Adult Foxhound After Middle Cerebral Stem Occlusion

	Frontal	Temporal	Parietal
Control (n = 13)	λ H/A* 36.5 ± 6.2	31.1 ± 4.7	30.5 ± 6.6
Occlusion† (n = 13)	λ H/A 21.0 ± 8.5‡	11.1 ± 5.7‡	25.2 ± 9.5
Post-TAA† (n = 7)	λ H/A 28.98 ± 6.7§	15.32 ± 4.1**	34.78 ± 4.1§
Post-PAA† (n = 3)	λ H/A 20.5 ± 9.1	12.7 ± 7.7	23.4 ± 11.0

* λ H/A = stochastic values for blood flow
† Occlusion = values after clip occlusion of middle cerebral artery at level of lenticulostriate arteries; post-TAA and post-PAA = values after microanastomosis to temporal cortical and parietal cortical arteries respectively.
‡ Significant to the .001 level
§ Significant to the .05 level
**Significant to the .01 level

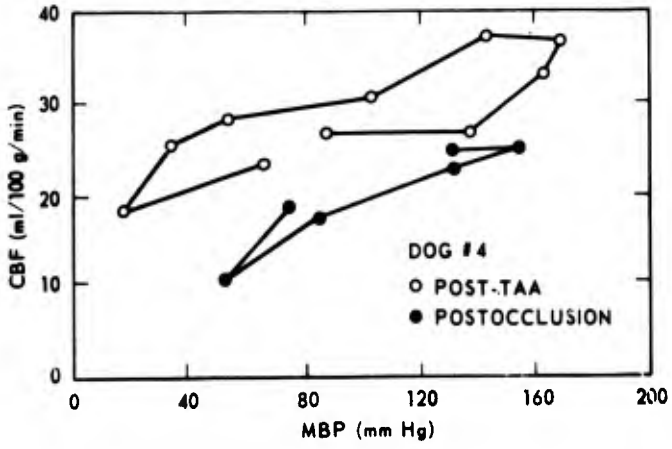

Figure 34.
Mean hemispheric blood flow 10 minutes - 3 hours postocclusion and 2 days after temporal artery graft (normoxia normocapnia)

REFERENCE

1. First International Symposium on Microneurosurgical Anastomoses for Cerebral Ischemia. Loma Linda, California, Loma Linda University Medical Center, June 14-15, 1973.

MYONECROSIS OF SUBARACHNOID ARTERIES IN CEREBRAL VASOSPASM

Principal Investigators: *J. M. Fein, W. J. Flor, S. L. Cohan and J. Kabal*
Technical Assistance: *L. J. Parkhurst*

Current concepts of cerebral vasospasm are consistent with the hypothesis that there is a tonic contractile mechanism under sympathetic influence that can be evoked by arterial rupture clinically and a multitude of agents experimentally. Previous studies on autoregulation of blood flow in rhesus monkeys after experimentally induced subarachnoid hemorrhage suggested a loss of vasoreactivity to hypotensive stimuli after 18 hours of vasospasm.[1] The purpose of this study was to identify and describe ultrastructural changes in cerebral vessels which would account for a loss of elasticity after prolonged vasospasm.

Rhesus monkeys underwent cerebral angiography followed by either puncture of the intracranial internal carotid artery or intracisternal injection of 3 cc of fresh arterial blood. Carotid angiography was repeated over 2 - 12 days to document the presence of vasospasm (Figure 35). The brains were then perfused with a mixture of Macewen's saline followed by Karnovsky's formaldehyde-glutaraldehyde fixative. The cerebral arteries were then dissected free of the brain parenchyma and washed in buffered 10 percent sucrose. Blocks were then postfixed and embedded in Epon 812. Areas for ultrastructural study were selected and thin sections were then examined in a Siemens Elmiskop 1A electron microscope.

Specimens from the group in which spasm persisted for less than 1 day demonstrated early electron lucent changes in the muscle cells within 8 hours. Condensed lysosomes and degenerating mitochondria were present and lipid figures were observed among the pinocytotic vesicles beneath the sarcolemmal membrane. In specimens from animals with prolonged spasm lasting 2 to 7 days, there was rounding of the endothelial cell nuclei and cytoplasm with cell processes assuming a flattened configuration along the elastica as well as a permanent loss of tight connections between cells. Smooth muscle cells were more electron dense than normal and those nearest the adventitia contained many intracytoplasmic vacuoles of various sizes and content. Smooth muscle cells adjacent to the crest of the elastica contained degenerating organelles and lipid figures. In some sections frankly pyknotic muscle cells were encountered. After 1 week of vasospasm the endothelial cells assumed a more normal spindle shaped configuration with return of tight intracellular junctions. The internal elastic lamina remained electron dense but smooth muscle cells still contained large vacuoles as previously described. Throughout the media there were muscle cell remnants of increased electron density with a loss of complex internal structures suggesting a loss of vasoelasticity in prolonged spasm.

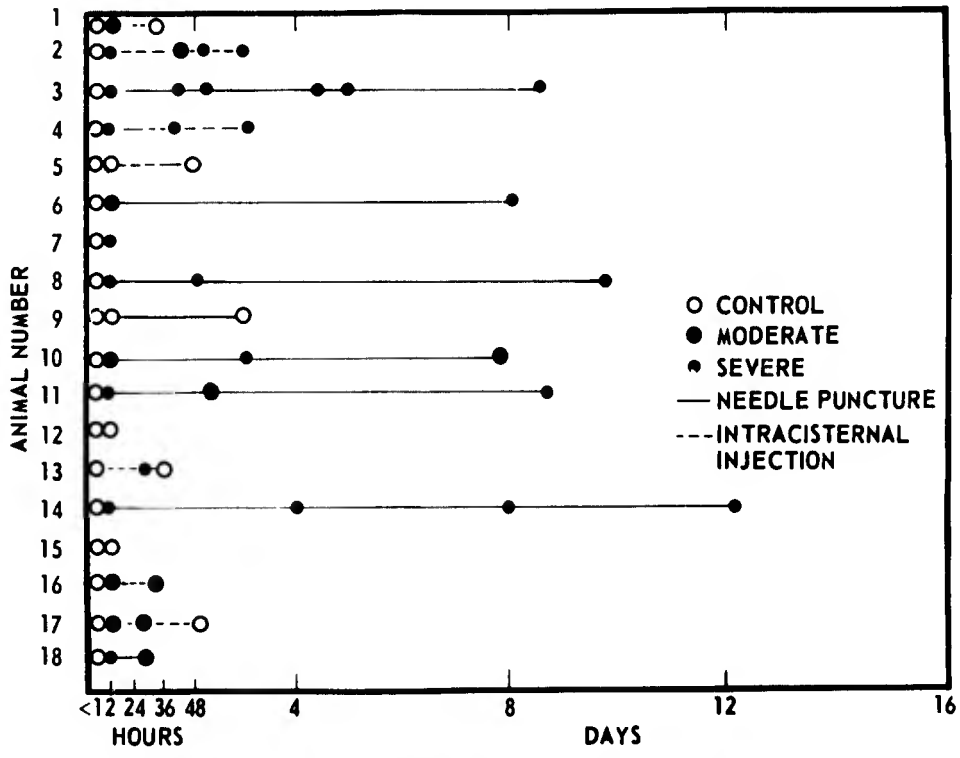

Figure 35. Duration and severity of vasospasm

REFERENCE

1. Fein, J. M. and Boulous, R. Local cerebral blood flow in middle cerebral artery vasospasm. J. Neurosurgery 39:337-347, 1973 (in press).

CIRCADIAN RHYTHM AND OPIATE EFFECTS ON BRAIN CATECHOLAMINE AND INDOLEAMINE METABOLISM

Principal Investigators: *G. N. Catravas, V. A. Kieffer and Q. H. Shelton*

It is known that the sleep-wake pattern of drug addicts is altered so that they become nocturnal. Circadian rhythmic fluctuations in the levels of brain serotonin and acetylcholine have been reported to occur and it was suggested that these neurotransmitters may be involved in the sleep-wake mechanism. The objective of this study is

to investigate the changes which occur in the levels of the brain biogenic amines, their amino acid precursors and enzymes associated with their metabolism over a 24-hour period and also the effects of opiates on the interval.

Experiments have been completed using rat whole brain homogenates for the determination of norepinephrine and serotonin as well as their respective precursors, tyrosine and tryptophan, during three intervals, 0800, 2000 and 0800 hours, in a 24-hour time scale. A combined extraction procedure was developed by our laboratory which permits the determination of all four metabolites in the same tissue sample. Results are shown in Figures 36-39. Significant changes (decrease) in the levels of total and free tyrosine and (somewhat less pronounced) norepinephrine were observed in the whole brain of rats sacrificed at 2000 hours. Tryptophan and serotonin did not demonstrate any significant differences. To determine whether the food diet had any effect on the levels of the metabolites under study, a series of experiments were conducted in which the rats were deprived of food for 24 hours prior to sacrifice. No significant changes were observed when compared with the animals fed ad libitum (Figures 36-38).

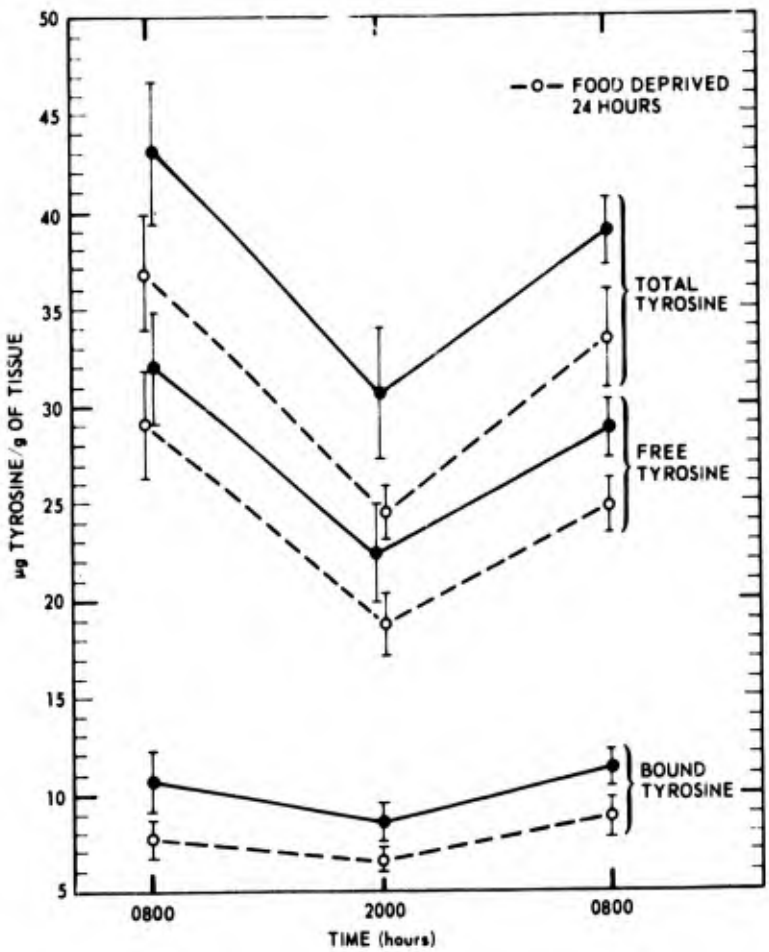

Figure 36. Changes in the levels of rat brain tyrosine during circadian rhythm

Experiments have been initiated to determine the changes in the levels of these four metabolites during the circadian rhythm in discrete brain areas (hypothalamus, thalamus, midbrain and hippocampus).

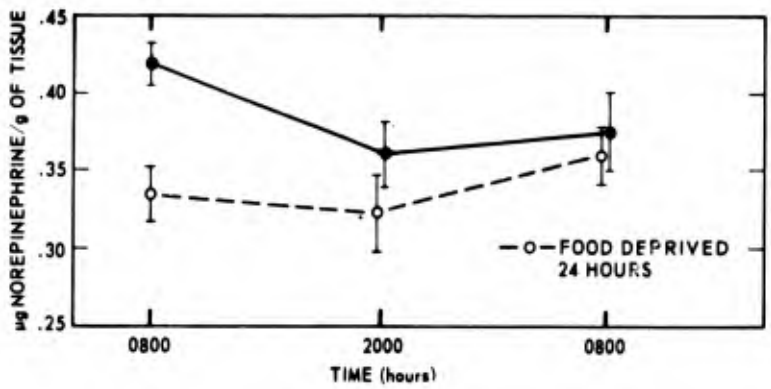

Figure 37. Changes in the levels of rat brain norepinephrine during circadian rhythm

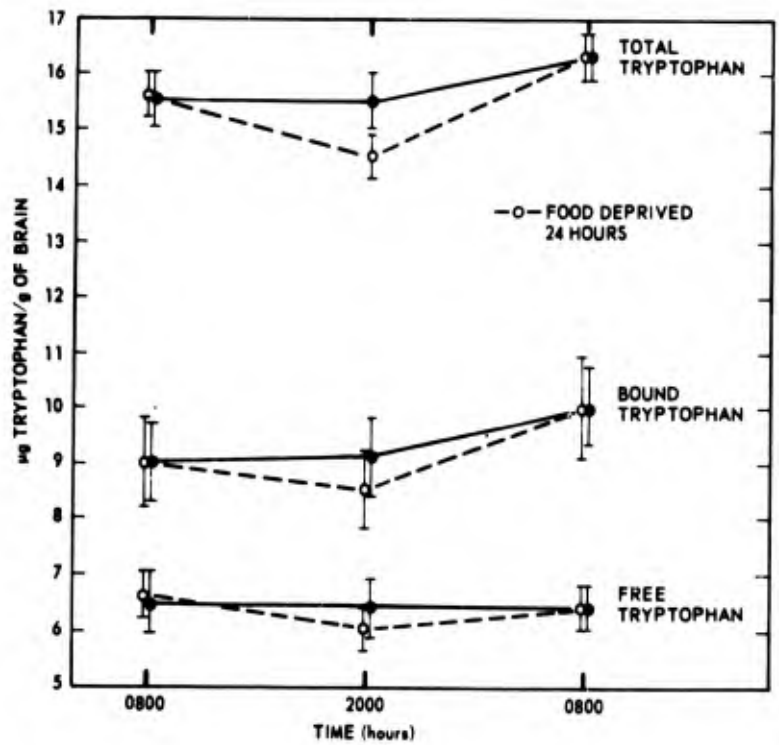

Figure 38. Changes in the levels of rat brain tryptophan during circadian rhythm

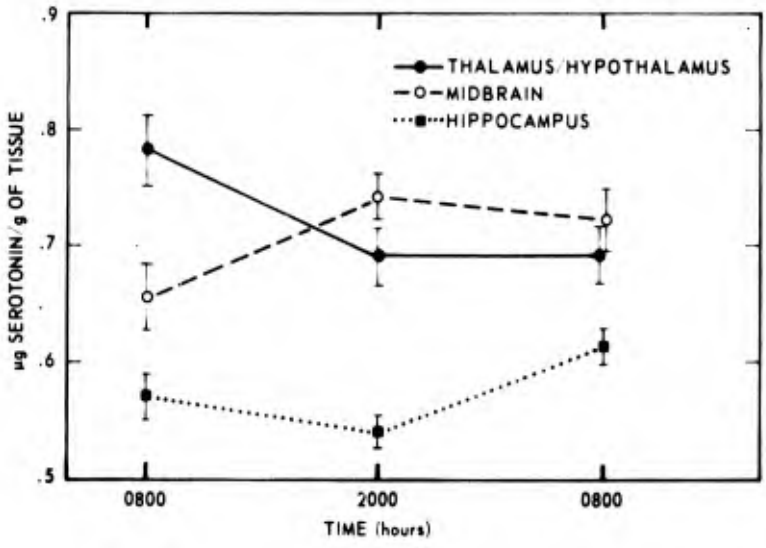

Figure 39. Changes in the levels of rat brain serotonin during circadian rhythm

◆◆◆◆◆◆◆◆◆

MECHANISM OF MORPHINE ANTAGONISM OF RESERPINE-INDUCED DEPLETION OF BRAIN CATECHOLAMINES

Principal Investigator: *J. C. Blosser*

A characteristic of the development of tolerance to morphine by rats is an increased resistance to the catecholamine depleting effects of reserpine in the brain. Reserpine blocks the uptake and storage of biogenic amines into synaptic vesicles. The inhibition appears to be initially reversible by high concentrations of catecholamines but later becomes irreversible. The object of this study is to attempt to characterize the mechanism by which morphine might cause an antagonism of reserpine's action. To this end, studies have focused on the effects of morphine in the absence or presence of reserpine on the in vitro uptake of norepinephrine by rat brain synaptic vesicles.

Synaptic vesicles isolated from rats made tolerant to morphine by two daily doses of morphine (30 mg/kg) for 1 week exhibited uptake rates of ^{3}H-d,l-norepinephrine which were essentially indistinguishable from those of control preparations. Likewise, acute treatment (60 mg/kg) with morphine did not alter uptake rates. When morphine

was added in vitro to synaptic vesicles from control animals, essentially no effect was seen on uptake with concentrations up to 100 μM. However, naloxone, an antagonist of morphine analgesia, did inhibit norepinephrine uptake by 35 percent at 10 μM morphine; when added together to the vesicle preparation, transport was reduced to 30 percent of control rates. Reserpine added in vitro to vesicles from control and morphine tolerant animals inhibited uptake in both preparations to essentially the same extent (Table XIX). Likewise, active transport of norepinephrine by vesicle preparations from control and experimental rats was equally susceptible to reserpine administered in vivo (5 mg/kg) 2 hours prior to sacrifice (Table XX). The data suggest that the increased resistance of morphine tolerant animals to the amine depleting effects of reserpine is not a result of an alteration in the synaptic vesicle transport mechanism.

Table XIX. Effect of Reserpine In Vitro on ^{3}H-d, 1-Norepinephrine Uptake by Synaptic Vesicles

Reserpine (μM)	Percent of control	Percent morphine tolerant
10^{-6}	9	7
10^{-7}	19	16
10^{-8}	41	47

Table XX. Effect of Reserpine In Vivo on ^{3}H-d, 1-Norepinephrine Uptake by Synaptic Vesicles

	Percent of control ± S.E.
Control	100
Control + reserpine	10.2 ± 3.3
Morphine tolerant + reserpine	15.3 ± 2.6

THE EFFECT OF MORPHINE ON TYROSINE HYDROXYLASE ACTIVITY

Principal Investigators: *S. L. Cohan, J. R. Abbott and G. N. Catravas*
Technical Assistance: *O. Z. Williams*

Tyrosine hydroxylase (TH) catalyzes the conversion of tyrosine to dihydroxyphenylalanine (dopa) and is the rate limiting enzyme in the synthesis of catecholamines. It has been reported that a single injection of morphine causes an increase in the rate of turnover of catecholamines in the mouse central nervous system and that with repeated injections the turnover rate returns to normal. Presumably this increase is mediated by tyrosine hydroxylase. The effect of morphine on the activity of this enzyme has been investigated in this study. Groups of rats were treated with a single injection of morphine (60 mg/kg, intraperitoneally) or twice daily (30 mg/kg) for 8 days. Animals were sacrificed by decapitation from 15 minutes to 24 hours postinjection and the midbrain, thalamus, hypothalamus and basal ganglia were dissected freehand on a cold plate and immediately frozen in liquid nitrogen. Tissue tyrosine hydroxylase activity was measured by coupled decarboxylation of dopa formed from 1-^{14}C-tyrosine.[1] Decarboxylation was accomplished using 1-aromatic amino acid decarboxylase prepared from hog kidney, which is highly specific for 1-dopa. The results are shown in Table XXI. There was an approximately 35 percent decrease in thalamus tyrosine

Table XXI. The Effect of Morphine on Tyrosine Hydroxylase Activity

Sacrifice (postinjection)	Activity (fraction of control)			
	Basal ganglia	Thalamus	Hypothalamus	Midbrain
Chronic injections				
15 min	1.03	1.03	1.10	0.96
30 min	1.07	0.66*	1.07	1.03
60 min	0.70*	0.58*	0.84	0.98
4 h	0.97	1.21	0.85	0.95
24 h	1.15	1.06	0.93	0.95
Acute injections				
15 min	1.02	0.98	1.20	1.22
30 min	1.03	0.64*	1.01	1.02
60 min	0.99	1.15	0.80*	1.04
4 h	0.99	0.79	1.06	1.08
24 h	1.04	1.05	0.92	0.98

* Significant by Wilcoxon signed ranks test $p > 0.05$

hydroxylase activity 30 minutes following a single injection of morphine. Repeated injections of the drug resulted in similar decreases in thalamus TH activity at both 30 minutes and 1 hour postinjection. In addition, there was a 20 percent decrease in hypothalamic TH activity 1 hour following a single injection and a 20 percent decrease in basal ganglia activity 1 hour following cessation of the chronic injections. All changes were transient and returned to normal by 4 hours after the last morphine injection.

REFERENCE

1. Waymire, J. C., Bjur, R. and Weiner, N. Assay of tyrosine hydroxylase by coupled decarboxylation of dopa formed from 1-^{14}C-L-tyrosine. Anal. Biochem. 43: 588-600, 1971.

◆◆◆◆◆◆◆◆◆

RELATIONSHIPS OF BRAIN BIOELECTRIC ACTIVITY TO MORPHINE OR ITS ANTAGONISTS

Principal Investigators: *W. L. McFarland and G. N. Catravas*
Collaborator: *H. Teitelbaum, University of Maryland*
Technical Assistance: *W. N. Fry*

The objective of this study is to define patterns of EEG changes in the rat during morphine addiction.

Recording electrodes have been implanted in the cortex, medial thalamus, and caudate nucleus of rats which were then given twice daily injections of morphine (30 mg/kg) for 3-5 days. Relatively consistent changes in the EEG pattern from the three recording sites, i.e., slow waves from cortex and caudate nucleus and higher frequency components in the thalamus have been seen, but the time of onset of these changes, relative to one another, was different from rat to rat. For example, in some rats the effects show up first in the caudate nucleus, in others the cortex shows the initial response. As the rat became behaviorally tolerant (i.e., remained alert after injection) to morphine over a series of days, the EEG also failed to change after injection, remaining apparently normal. At this stage, the behavioral and EEG indices of morphine could be reintroduced by up to four times the usual dose of morphine. When naloxone, a morphine antagonist, was given while the rat was showing these symptoms, the symptoms

disappeared within a few minutes, the rat became active and the EEG returned to a normal pattern. The next step was to produce a lesion in the medial thalamus, since this nucleus has been reported to be a site of action of naloxone. On the day after the lesion was produced the rats showed increased sensitivity to morphine. That is, they were no longer tolerant and showed high amplitude EEG patterns to a single dose of morphine. This effect was not found with lesions elsewhere in the brain. Naloxone reversed the morphine effect despite the fact that the medial thalamus was damaged.

◆◆◆◆◆◆◆◆◆

THE EFFECTS OF OPIATES ON BRAIN CATECHOLAMINES

Principal Investigators: *J. H. Darden and G. N. Catravas*

Endogenous whole brain levels of neurotransmitters (catecholamines) following acute doses of morphine show an initial depletion in the rat as well as other animals. In animals made tolerant to morphine, this depletion is not seen. When depleters of bound catecholamines, such as reserpine, are used on morphine tolerant animals and then compared to reserpine treated controls, a higher level of catecholamines is found in the tolerant animals. This suggests that synaptic vesicles of morphine tolerant rats may be more efficient in catecholamine uptake or less capable of catecholamine transport across vesicle membranes (alteration in release mechanism after excitation).

In our investigation of catecholamine levels following morphine treatment (acute and tolerant), Sprague-Dawley rats were either administered twice daily doses of morphine-HCl (30 mg/kg body weight intraperitoneally) for 7 days to render them tolerant to the drug, or were given a single dose (60 mg/kg body weight) for the acute studies. The animals were sacrificed by decapitation at varying intervals after the last injection, ranging from 15 minutes to 1 hour, along with saline injected controls. Free, which is the nonvesicular fraction, and bound, or vesicular fractions, were separated along with the extrasynaptosomal fractions, using the method of Whittaker.[2] Catecholamine levels (norepinephrine and dopamine) were determined using the method of Weil-Malherbe.[1]

Acute animals. Our preliminary results, illustrated in Table XXII, show an increase in both the extrasynaptosomal and free fractions of norepinephrine during periods ranging from 15 minutes to 1 hour postmorphine injection. This reflects an increase in total norepinephrine for this period even though there was no change in the bound fraction. Data accumulated for dopamine levels in acute animals are limited to

the 1-hour testing period. The extrasynaptosomal fraction of dopamine in treated animals exhibits a significant increase over control levels but there is little or no change in the free and bound fractions.

Table XXII. Norepinephrine and Dopamine Concentrations in the Acute Animal Study

	Norepinephrine			Dopamine
	N = 3 15 min	N = 3 30 min	N = 6 1 h	N = 6 1 h
CS	148	107	129	119
MS	162	140	176	186
CF	31	25	27	25
MF	65	38	32	28
CB	49	22	20	11
MB	29	22	20	3

* C = control; M = morphine treated; S = synaptosomal; F = free; B = bound; and N = number of experiments

Tolerant animals. As seen in Table XXIII, both norepinephrine and dopamine showed an increase in concentrations 1 hour after the last morphine injection. Significant increases were also seen in the free fraction of norepinephrine with no change in free dopamine. Neither of the two demonstrated any differences in the bound fraction.

Table XXIII. Norepinephrine and Dopamine Concentrations in the Tolerant Animal Study

	Norepinephrine (ng/g) 1 hour after last injection	Dopamine (ng/g) 1 hour after last injection
	N = 8	N = 4
CS	106	99
MS	133	116
CF	26	34
MF	53	34
CB	16	5
MB	17	0

* C = control; M = morphine treated; S = synaptosomal; F = free; B = bound; and N = number of experiments

These results indicate that there is a possible alteration in neurotransmitter release from synaptic vesicles as well as structural changes in vesicle membranes resulting in their inability to reuptake the neurotransmitters after excitation.

REFERENCES

1. Weil-Malherbe, H. The chemical estimation of catecholamines and their metabolites in body fluids and tissue extracts. Meth. Biochem. Anal. (Supplement), 1971.

2. Whittaker, V. P. The isolation and characterization of acetylcholine-containing particles from brain. Biochem. J. 72:694-706, 1959.

◆◆◆◆◆◆◆◆◆

MOLECULAR STUDIES OF OPIATE TOLERANCE AND DEPENDENCE IN THE MAMMALIAN BRAIN

Principal Investigators: *G. N. Catravas and C. G. McHale*
Technical Assistance: *O. Z. Williams*

Current literature concerning the effects of opiates on the activity of brain enzymes involved in neurotransmitter metabolism is often contradictory and to a large extent a reflection of species differences, dosage of opiates, and time of sacrifice of the animals following administration of the drug. Furthermore, many of these studies have used entire brains and did not take into consideration the regional distribution of certain neurotransmitters and the role which various areas of the brain may play in the development of tolerance, dependence and withdrawal. In the present study we investigated the changes which chronic administration of morphine induces in the activity of enzymes concerned with the synthesis and degradation of neurotransmitters in discrete areas of the brain of the rat.

Groups of male adult rats were made tolerant to morphine by injecting the drug (30 mg/kg per injection, intraperitoneally) twice daily for 7 days. At the end of the 7th day, one group was sacrificed just before receiving the last injection and was used as base-line controls. The other groups were given the last morphine dose and were sacrificed at various intervals of time ranging from 15 minutes to 24 hours. Experimental and saline injected controls were sacrificed by decapitation and their heads

were instantly frozen in liquid nitrogen. The head was then removed from the liquid nitrogen, partially thawed, and the hippocampus, thalamus, hypothalamus, basal ganglia and cerebral cortex were dissected out. The activities of monoamine oxidase (MAO), acetylcholinesterase (AchE), choline acetyl transferase (CAT) and RNA polymerase were determined.

Results obtained thus far indicate the following: monoamine oxidase activity was found to decrease in all brain regions studied, with lowest values at approximately 30 to 60 minutes after the last morphine injection, and had the tendency to return to normal levels starting with animals which were sacrificed at 6 hours postinjection (Figure 40). An initial increase in the activity of this enzyme was observed in the basal ganglia and perhaps in the hippocampus at approximately 15 minutes after the final morphine injection. Oscillating changes in the activity of AchE above control values were found to occur in all brain areas studied except basal ganglia. In basal ganglia the activity of this enzyme appeared to remain below normal levels (Figure 41). Similar oscillating changes were observed in the activities of the enzymes choline acetyl transferase and RNA polymerase (Figures 42 and 43). Further investigations are being conducted to verify these findings and to obtain statistically meaningful results. Experiments are in progress to determine the effects of single acute doses of morphine on the activities of the above-listed enzymes.

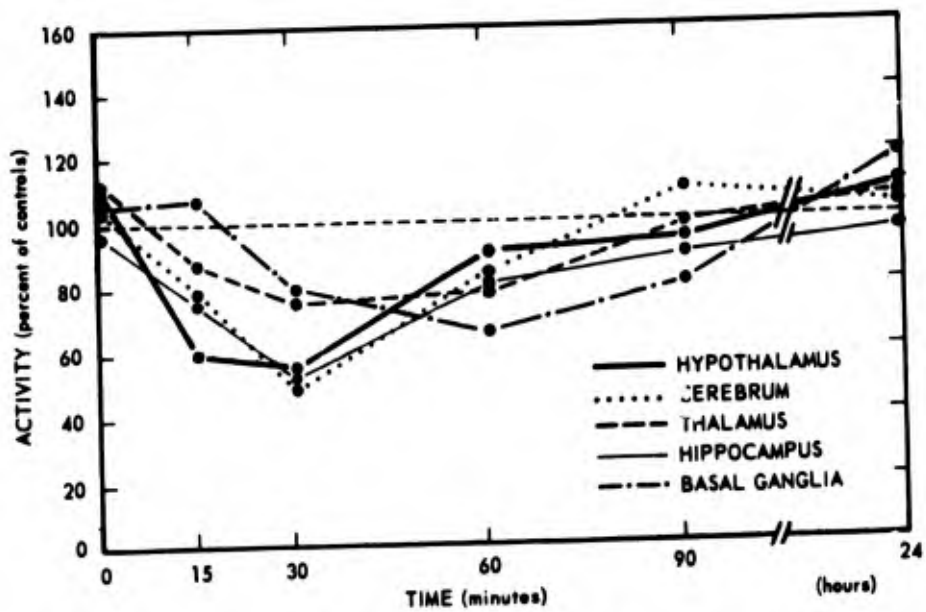

Figure 40. Effect of morphine on activity of monoamine oxidase

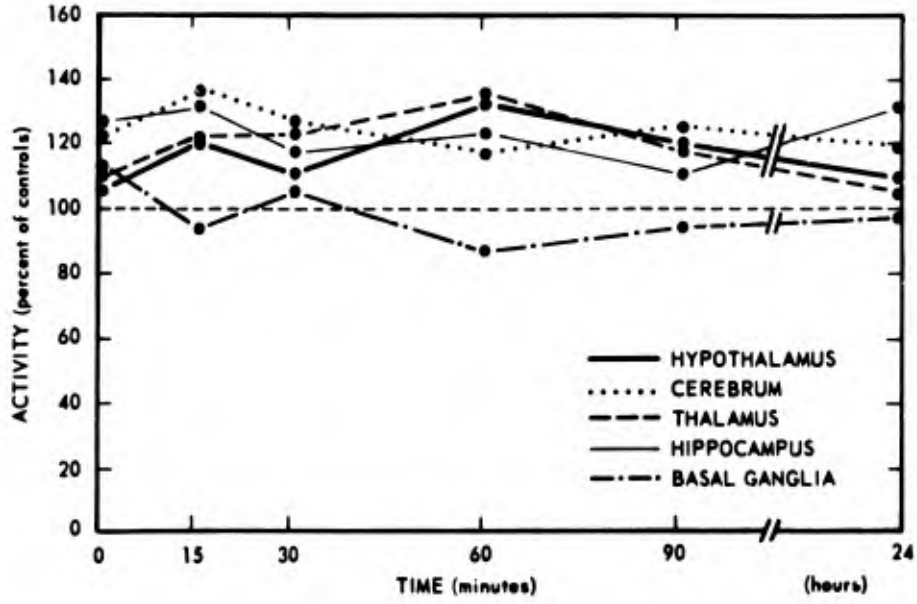

Figure 41 Effect of morphine on activity of acetylcholinesterase

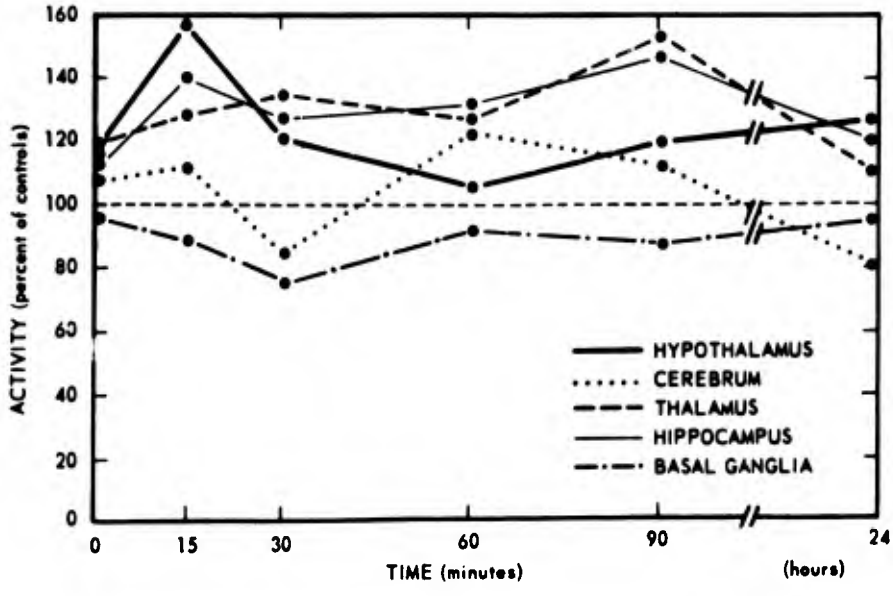

Figure 42. Effect of morphine on activity of choline acetyl transferase

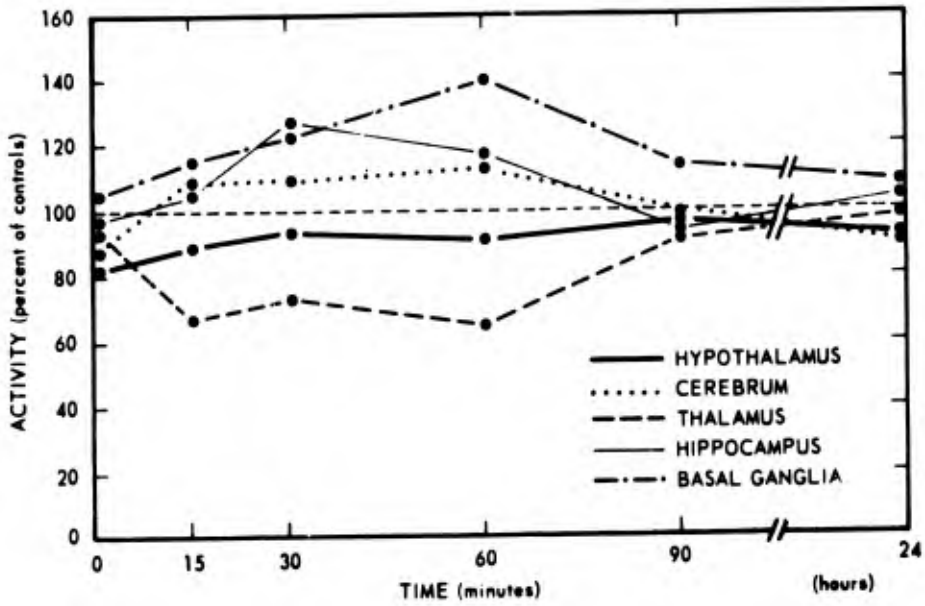

Figure 43. Effect of morphine on activity of RNA polymerase

EFFECTS OF INTRACISTERNAL PHENTOLAMINE ON CEREBRAL VASOSPASM IN THE RHESUS MONKEY

Principal Investigators: *A. N. Martins, A. Kobrine, A. Ramirez, Walter Reed Army Medical Center; T. F. Doyle and J. A. Willis, AFRRI*

Cerebral vasospasm and resulting brain ischemia is an important cause of mortality following subarachnoid hemorrhage. Vasodilators administered either intra-arterially or intravenously have not proven effective therapy. When these drugs are applied topically to the cerebral vessels or when added directly to the cerebral spinal fluid, cerebral vasospasm is often relieved. Phentolamine mesylate has been shown to be an effective spasmolytic when used in this manner. Well tolerated intracisternal doses of phentolamine may be an effective treatment for cerebral vasospasm.

The rhesus monkey is used in this study as the experimental model. Following simulated subarachnoid hemorrhage, regional cerebral blood flow is monitored by a hydrogen washout technique both before and during administration of phentolamine

intracisternally. Regional cerebral blood flow measurement is critical for the successful completion of this research. Since the hydrogen dilution blood flow technique is potentially simple, reliable, and inexpensive, extensive work has been done on the development of this technique.

A system has been developed to linearly measure the concentration of hydrogen in body tissues, using a platinum electrode. The system has been tested both in vitro and in vivo with excellent results. Figure 44 is an example of the system's response to hydrogen concentrations in vitro which approximate those that would be encountered during flow determinations in vivo. A system has been constructed which allows up to eight simultaneous flow measurements in one experimental animal. Problems encountered with electrode stability and maintenance of constant blood PO_2 have been largely solved, and work on the physiology of vasospasm has begun.

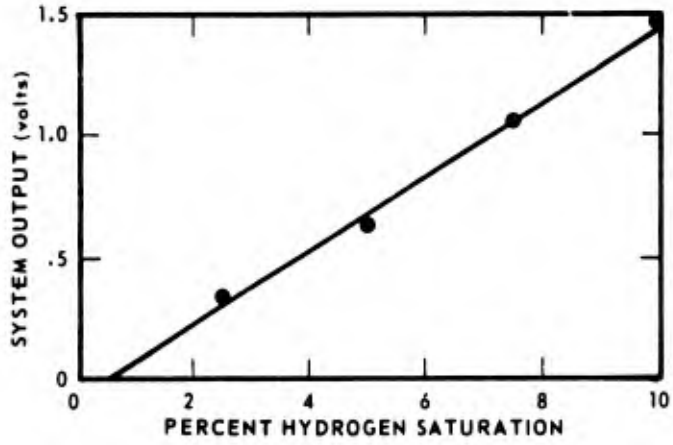

Figure 44. System response to hydrogen saturations from 0 to 10 percent

THE EFFECT OF DEXAMETHASONE ON CEREBROSPINAL FLUID PRODUCTION IN THE RHESUS MONKEY

Principal Investigators: *A. N. Martins, M. Wiese, A. Ramirez, Walter Reed Army Medical Center; and L. S. Solomon, AFRRI*

Several previous investigators have shown that dexamethasone influences the production of cerebrospinal fluid (CSF) in dogs. Spatial compensation can occur as a result of alterations in CSF dynamics, and factors influencing either its production or absorption are clinically significant. Since previous studies have used experimental

animals whose CSF dynamics are quite different from humans, and since several factors known to influence CSF production were not kept constant, the following experiment was designed in an attempt to demonstrate the effect of dexamethasone on CSF production in the subhuman primate.

Ten rhesus monkeys, weighing 3.2 - 4.5 kg, were anesthetized with pentobarbital, intubated, and their respiration was controlled by a volume respirator. Systemic blood pressure, CSF pressure, rectal temperature, and blood gases were monitored throughout the experiment and kept constant. Arterial PCO_2 was maintained at 35 - 45 mm Hg. Maintenance lactated Ringer's solution was given intravenously at 5 cc/kg per hour. The atrium of the left ventricle was cannulated stereotaxically and the cisterna magna was cannulated percutaneously.

Serum albumin tagged with ^{125}I and blue dextran was mixed with mock CSF and buffered to pH 7.35 by bubbling CO_2 into the mixture and then passed through a Millipore filter. Temperature of this mixture was maintained at about 37°C by passing the solution through a heating apparatus. Ventriculocisternal perfusion with the mock CSF solution was then carried out for an initial 2 hours at a rate of 0.184 cc/minute.

CSF from the cisterna magna was collected at 30-minute intervals for 5 hours. Six aliquots were obtained from each 30-minute sample and were placed in separate counting chambers. The remainder of the sample was centrifuged for 5 minutes to separate any small amounts of red blood cells and its concentration determined by spectrophotometric methods.

In the treated animals, 3 hours after perfusion, 0.15 mg/kg of dexamethasone was given intravenously. This dose is comparable to the loading dose used in humans. Ventriculocisternal perfusion was maintained for 4 hours after intravenous dexamethasone was administered to the treated group, and for the same period of time in the control group (untreated). The control group consisted of six rhesus monkeys and the treated group consisted of four rhesus monkeys.

As can be seen from Figure 45, no significant change in CSF production was demonstrated up to 4 hours following administration of dexamethasone, 0.15 mg/kg. intravenously. During the entire experiment, serum PCO_2, pH, PO_2, and temperature were kept constant.

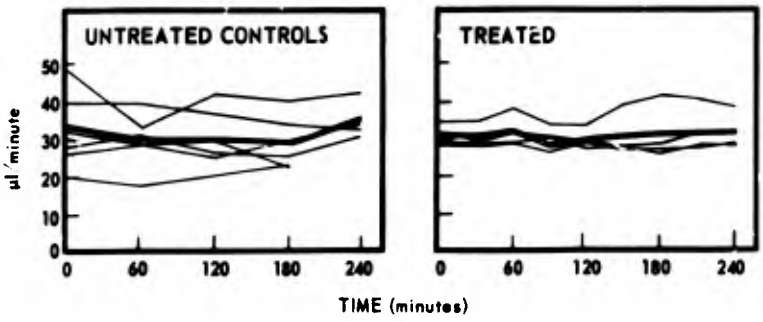

Figure 45.
CSF production rate in monkeys following ventriculocisternal perfusion of dexamethasone

The data obtained in this experiment fail to confirm previous experiments concerning the effect of dexamethasone on CSF production. It is felt that species differences as well as a better controlled experiment probably account for the observed discrepancies.

CELL CULTURE OF NEURONAL TISSUES

Principal Investigator: *W. G. Shain, Jr.*

Understanding of intercellular recognition and interactions within neuronal tissue is of primary importance in elucidating the development and differentiation of the nervous system. Since the nervous system is a highly complex, heterogeneous population of not only neurons but also glial and target cells, it is necessary to study simplified model systems. One such approach is to study intercellular relationships in animals with "simple" nervous systems; i.e., many invertebrate systems. A second approach is to utilize the techniques of cell biology to dissociate and separate individual cells from neuronal tissues. Since neurons and many glia either do not divide or divide at prohibitively slow rates, two techniques have been applied to neuronal tissues to obtain dividing populations of cells. Somatic cell hybridization techniques can be used to manipulate the phenotypic expression of a given cell type by the addition of the genome of a second cell type. In this manner, normal sympathetic neurons which do not undergo cellular division were hybridized with a neuroblastoma cell line in order to produce cells with the propagation characteristics of the latter and the neuronal characteristics of the former. Forty-nine clonal hybrid cell lines have been isolated. One of these lines, X-31, has been characterized. This cell line synthesizes dopa and dopamine and has membrane excitatory properties very similar to the sympathetic parent.

A second approach to obtain dividing populations of cells is to chemically transform cells so that they will continue to divide. The alkylating agent ethyl nitroso urea has been shown by a number of workers to be a powerful carcinogen which in rats affects primarily the central and peripheral nervous systems. This drug has been used transplacentally in late (last trimester) gestation because it is also a powerful teratogen and, if used earlier, results in death or loss of the embryo. The drug has been applied to cell cultures of brain, eyes, and spinal cord from young embryos (approximately halfway through gestation). Since there is considerably more mitotic activity in the CNS at this stage than at later times, a much larger population of neuroblasts

can be challenged by the drug. Cultures of treated cells were allowed to reach confluence and then passaged weekly. At the time of each passage, aliquots of cells were placed in soft agar cultures to select for transformed cells. A number of cells have thus been isolated. When a sufficient number of cell lines have been established, they will be assayed for neuronal and glial characteristics.

IONIC MECHANISMS UNDERLYING NEURONAL THERMOSENSITIVITY

Principal Investigators: *F.-K. Pierau and D. O. Carpenter*
Technical Assistance: *P. J. Torrey*

In invertebrate neurons, spontaneous electrical activity is dependent upon temperature as a result of two independent processes. The first process, activity of an electrogenic sodium pump, increases steeply with temperature and generates a potential across the membrane of these cells which tends to decrease their excitability as temperature is raised. The second process, which results from a greater temperature dependence of the permeability of the membrane to sodium than to potassium, tends to depolarize the neuron and thus increase excitability as temperature is raised. In a variety of invertebrate neurons it has been shown that these two processes interact in different cells and, when one or the other predominates, the neuron is either cold or warm sensitive, depending on which process predominates. In these experiments we attempted to analyze the mechanisms of temperature sensitivity in peripheral afferent fibers from mammalian nerve-skin preparation and to determine whether these two mechanisms responsible for the nonspecific thermosensitivity of invertebrate neurons underlie the thermosensitivity of afferent fibers presumably specialized for perception of temperature.

Experiments have been performed on the nerve fibers innervating the skin of the rat scrotum. This preparation is a particularly good one for the study of temperature sensitive afferent fibers since it contains a high percentage of fibers sensitive only to temperature. Experiments have been done using two procedures, the technique for the dissection of the afferent fibers from the peripheral nerve and preliminary observations have been made from intact animals anesthetized with barbiturates. Temperature of the skin has been changed by perfusing water maintained at different temperatures through a metal plate underlying the scrotal skin. Temperature has been monitored, along with recordings of electrical activity, from small filaments of nerve which contain one or several nerve fiber action potentials. Three types of receptors

have been found, temperature sensitive receptors (including both warm and cold sensitive receptors), mechanoreceptors, and fibers which do not respond either to temperature change or to mechanical stimulus. The response properties to changing local temperature of these three types of afferent fibers have been studied in detail and experiments have been made with a local infiltration of ouabain or saline around the receptive area. Figure 46 illustrates typical responses to a transient temperature change, in this case, from a mechanoreceptive afferent fiber before local saline injection and after local injection of ouabain. These results suggest that for mechanoreceptive afferent fibers ouabain causes a dramatic increase in discharge only at warm temperatures. These results are consistent with a role for an electrogenic sodium pump in maintenance of potential at warm temperatures. Preliminary evidence to date indicates that cold sensitive afferent fibers become more sensitive to warm temperatures after ouabain, suggesting that an electrogenic sodium pump is the basis of the generator potential in these fibers.

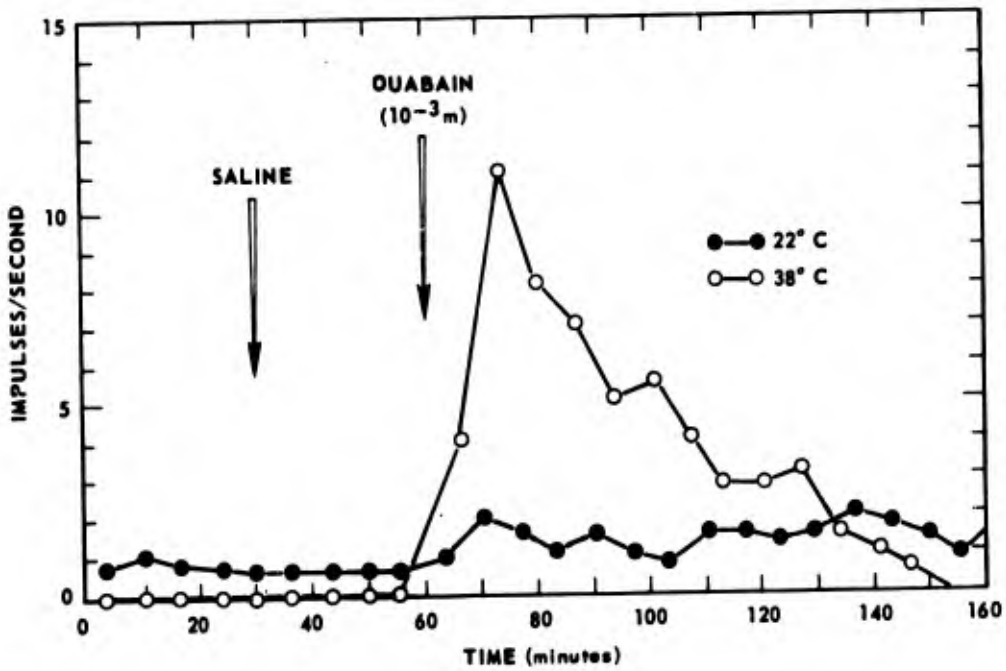

Figure 46. Mechanoreceptive fiber response to temperature change

To examine more rigorously the dependence of the generator potentials in these fibers, we are attempting to isolate nerve and skin from the animal in the chamber where we can control the ionic composition of the medium and add drugs without considering the effects on circulation and other properties of the animal.

NEUROTRANSMITTERS IN THE NERVOUS SYSTEM OF APLYSIA

Principal Investigators: *D. O. Carpenter, G. H. Zeman, P. J. Yarowsky, AFRRI; M. J. Brownstein, J. M. Saavedra and J. Axelrod, National Institutes of Health*

The identification of a chemical substance as being a neurotransmitter in the nervous system of any animal requires that a number of criteria be met. These include that the substance be present in the nervous system, that there be a mechanism of synthesis and a mechanism for inactivation of the transmitter either by degradation or by reuptake. In addition, there must be a demonstration of release of the chemical on nerve cell discharge and a demonstration that this chemical acts on a receptor on the postsynaptic cell to produce a change in permeability of that membrane. The nervous system of Aplysia is a particularly appropriate preparation for the study of the distribution of neurotransmitters because of the very large size of the cell bodies. Not only can one dissect out these large cell bodies and analyze individual neurons for contents of transmitter but these cell bodies are sufficiently large and distinct that they can be identified from preparation to preparation, both for electrophysiological investigations and for investigations of biochemical content. In these experiments we are attempting to examine the electrophysiological properties of identified neurons to transmitters and are using ultramicrotechniques to analyze individual identified neurons for contents of putative neurotransmitters and their synthetic and degradative enzymes.

Preliminary observations on the content of neurotransmitters have been made by surveying the content of whole ganglia peripheral nerves and nonnervous tissue.[1] The putative transmitters measured include serotonin, dopamine, histamine, octopamine, norepinephrine and gamma-aminobutyric acid (GABA). With the exception of norepinephrine, which is not present in measurable quantities in the nervous system of this animal, most of these other putative transmitters are present in concentrations of several micrograms per gram wet weight. By use of ultramicroassay techniques, single cells were examined for these transmitters. Of the approximately 15 large identified cells studied, serotonin, histamine and GABA were found to be present in measurable quantities in most of these cells. The apparent concentrations of these putative transmitters were not identical in all cells. For serotonin, there seemed to be an order of magnitude greater concentration of serotonin in the Retzius' cells of cerebral ganglion than was found in any other cells, even those that are considerably larger. Interestingly, histamine appeared to be present in greatest concentration in smaller cells, suggesting that it possibly might be associated with membrane rather than cytoplasm. However, further experimentation must be done to check this possibility.

The study of the electrophysiological responses of these cells to iontophoretic application of neurotransmitter has been begun to date only with GABA. We have found

that most cells in the ganglia are sensitive to GABA. The majority of cells respond to application of GABA with the hyperpolarizing response, although some identified cells consistently give a depolarizing response. These observations are being expanded and other transmitters are being investigated.

REFERENCE

1. Carpenter, D., Breese, G., Schanberg, S. and Kopin, I. Serotonin and dopamine: distribution and accumulation in Aplysia nervous and non-nervous tissues. Int. J. Neurosci. 2:49-55, 1971.

EFFECT OF IONIZING RADIATION ON SINGLE NEURONS AND SIMPLE NERVE NETWORK IN APLYSIA CALIFORNICA

Principal Investigators: *J. A. Willis and M. L. Wiederhold*
Technical Assistance: *G. L. Gaubatz*

AFRRI has documented changes in central nervous system (CNS) function in a variety of vertebrates following exposure to supralethal doses of ionizing radiation. Attempts to elucidate the basic mechanisms underlying these functional changes have proven difficult due to the complexity of vertebrate nervous systems. To determine whether CNS dysfunction is caused by changes in the important electrical parameters of neurons, this study was carried out in a simple invertebrate nervous system. The abdominal ganglion of the marine mollusc Aplysia californica contains a number of cells which exhibit spontaneous, regular activity. The activity of these pacemaker neurons has been shown to be dependent on both passive ionic conductances in the cell membrane and upon a metabolically driven electrogenic sodium potassium exchange pump. Small changes in any of these parameters due to radiation will produce predictable changes in the pacemaker discharge of the cell.

The initial research on this problem was concerned with learning the Aplysia preparation and further characterizing the effects of the electrogenic sodium pump on the pacemaker discharge. Suitable apparatus for making electrophysiological recordings in high radiation fields, and a special specimen holder, were developed to permit exposure of the Aplysia preparation in the electron linear accelerator (LINAC). A series of experiments are now being carried out in which the Aplysia abdominal ganglion is mounted in front of a collimated LINAC beam and is exposed to 1200-rad

pulses of 20 MeV electrons while making simultaneous recordings of intracellular potential via micropipettes.

The effects of such an irradiation are shown in Figure 47. Following delivery of 40 krads, the cell showed a transient increase in pacemaker activity, followed by a gradual return to base line. The extent of this transient response seems to be dose dependent, as is shown in Figure 48. It is important to note that the doses necessary to elicit gross responses are at least an order of magnitude greater than those required

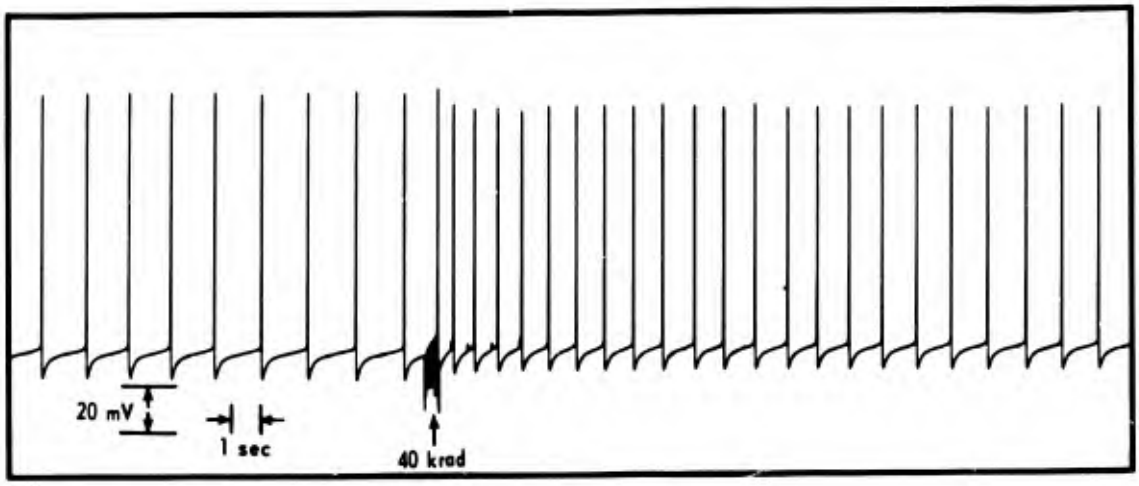

Figure 47. Transient changes following 40 krads 20 MeV LINAC irradiation in cell R6 of Aplysia abdominal ganglion

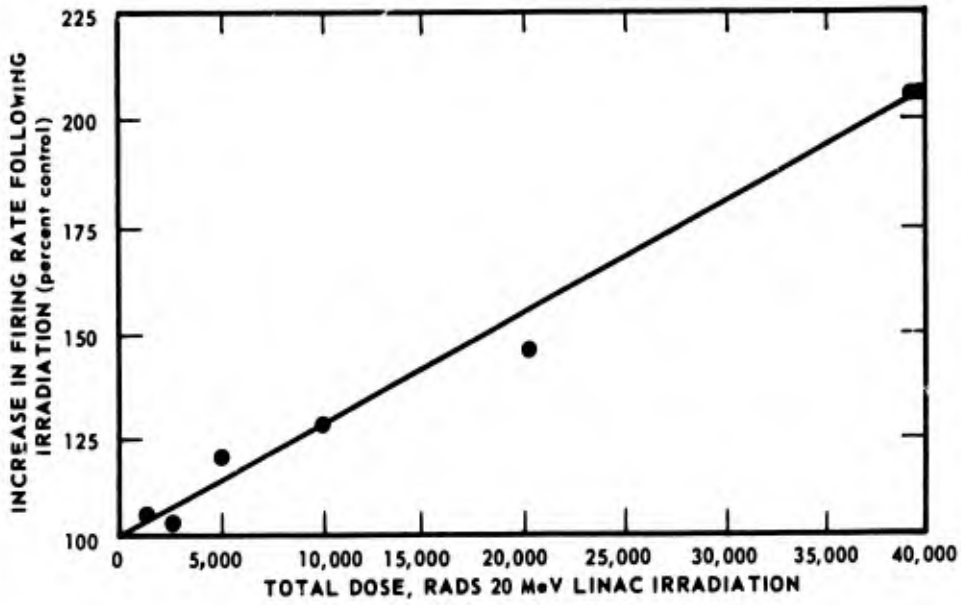

Figure 48. Dose response relationship for transient firing frequency changes following irradiation in cell R6 of Aplysia abdominal ganglion

to elicit changes in CNS function in vertebrates. This is in agreement with the currently held concepts concerning the radioresistance of nervous tissues. Demonstrable changes in pacemaker activity do occur at lower doses and it is reasonable to assume that small changes induced in large neuronal populations could cause a disruption in neuronal integration sufficient to cause behavioral dysfunction.

The transient changes in pacemaker activity following irradiation can be explained as either an increased passive ionic conductance due to physical damage to the plasma membrane leading to depolarization or due to a transient inhibition of the electrogenic sodium pump. Experiments measuring cell input resistance following irradiation and experiments on cells poisoned with a pump inhibitor such as ouabain will check these hypotheses. The effect of radiation on synaptic transmission is being studied.

◆◆◆◆◆◆◆◆◆

NEURORADIOLOGIC STUDIES DURING EXPERIMENTAL HEAD INJURY

Principal Investigators: *S. A. Shatsky and D. E. Evans*
Technical Assistance: *F. E. Miller*

The genesis of anatomic pathologic changes within the brain during blunt trauma is largely unknown. Numerous theories of brain injury have been proposed, including: (1) transmittal of waves of force, (2) vibration of the skull shell, (3) brain translational displacements, (4) skull deformation, (5) pressure gradient formation, (6) sulci rotation, and (7) cavitation. However, there has been little direct physical evidence to validate or refute any of these theories. Most prominently lacking has been the simple description of sequential anatomic changes within the brain that occur during injury.

There have been two major usable approaches to viewing the brain during impact injury, Lucite calvaria studies and flash radiography. Desirable properties of each have been combined in a unique new technique we have developed, flash x-ray cinematography. This has allowed 1000 frame per second cine neuroradiographic studies of the primate brain, during graded experimental impact trauma, to document and quantitate cerebral vascular and ventricular movements and to determine which of these plays a significant role in subsequent pathologic alterations of the brain.

Figure 49 illustrates a deceleration impact sled we have used to simulate nonlethal closed head injuries. It has allowed rigorous monitoring of skull impact load,

triaxial skull accelerations, and cart terminal velocity, as well as allowing absolute stop motion x-ray movies of the brain parenchyma and vasculature during injury.

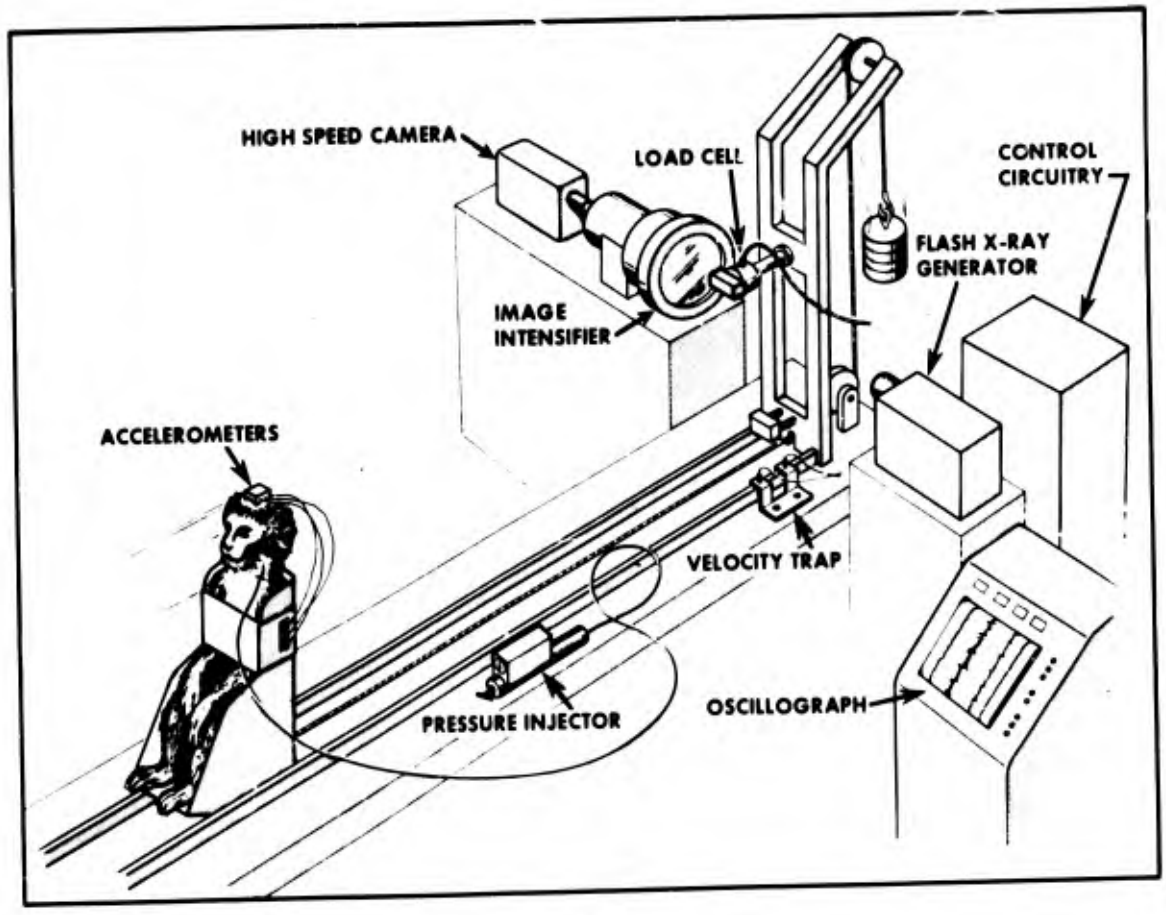

Figure 49. Deceleration impact sled

The most apparent changes within the skull demonstrated during injury are the small vascular displacements in the area adjacent to impact, the transient clearing of blood vessels from the occipital area during the first milliseconds of posterior impacts. This occurred in the absence of gross anatomic changes in the local area. It was also apparent that movements above the tentorium were small at these subconcussive injury levels. Lateral displacements of the anterior cerebral artery were maximally 2-4 mm, and no movements greater than 1.5 mm were documented during occipital impacts.

The most unique finding in these experiments has been the transitory "beaded" or interrupted appearance of the middle cerebral artery and adjacent brain parenchyma during subconcussive lateral impacts. It may represent a compressional fluid wave occurring during impact with consecutive areas of high and low radiographic density,

stopped by the ultrashort (30×10^{-9} sec) flash x-ray pulse, between time zero and the first millisecond postimpact (Figure 50). The cineframes are undergoing holographic enhancement to sharpen these images and allow better interpretation of their meaning.

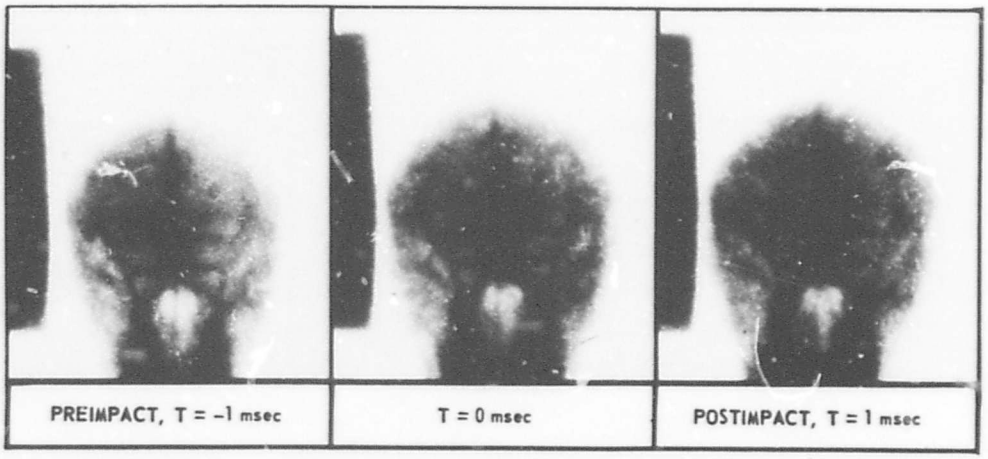

Figure 50. The middle cerebral artery and adjacent brain parenchyma have a "beaded" or interrupted appearance at time of impact. A flash x-ray exposure of 30 nsec was used to stop this motion.

CARDIAC ARRHYTHMIAS AND HEAD INJURY

Principal Investigators: *D. E. Evans and S. A. Shatsky*
Technical Assistance: *F. E. Miller*

Studies on the cardiovascular response of blunt head trauma in the subhuman primate have begun, and at the present time we are collecting data on the changes in blood pressure and cardiac rhythm resulting from graded impacts to the occipital skull. We have observed bradycardia in some animals, tachycardia in others, and some ectopic subatrial beats occurring immediately after impact in lightly anesthetized animals. In more deeply anesthetized primates, no cardiac arrhythmias have occurred following sublethal closed head injury. The major problem to be resolved at the present time is one of appropriate anesthetic agent. We are investigating the use of nitrous oxide and intravenous morphine sulphate to achieve adequate anesthetic effect without depressing the autonomic nervous system.

APLYSIA ACETYLCHOLINE RECEPTORS: BLOCKADE BY AND BINDING OF α-BUNGAROTOXIN

Principal Investigators: *W. G. Shain, Jr., D. O. Carpenter, AFRRI; L. A. Greene, A. J. Sytkowski and Z. Vogel, National Institutes of Health*

The marine mollusc Aplysia has a nervous system containing numerous identifiable giant nerve cells which have proven useful for both electrophysiological and biochemical investigations. Of particular interest is the observation that all of these neurons are sensitive to acetylcholine (ACh). Several snake venom toxins have been shown to block ACh responses in many vertebrate preparations. One of these toxins, the protein α-bungarotoxin (αBT), appears to do so by binding specifically and essentially irreversibly to nicotinic ACh receptors.

We have studied the effects of αBT on the electrophysiological response to ACh of identifiable cells in the nervous system of the Aplysia and the binding of ^{125}I-αBT to a ganglionic preparation.[1,2] Aplysia has three pharmacologically distinct ACh responses and each causes a different conductance change. αBT blocks all three responses of iontophoretically applied ACh. In all cases the inhibition is reversed on washing. Binding of ^{125}I-αBT to the ganglionic preparation is a saturable process. The dissociation constant of binding calculated from rates of association and dissociation of the toxin-receptor complex was 0.8×10^{-9} M. Binding of ^{125}I-αBT was inhibited by unlabeled toxin, ACh agonists and antagonists as well as by eserine, ouabain, and tetraethylammonium but not by the transmitters serotonin and dopamine.

REFERENCES

1. Shain, W., Greene, L. A., Carpenter, D. O., Sytkowski, A. J. and Vogel, Z. Aplysia acetylcholine receptors: blockade by and binding of α-bungarotoxin. Brain Res. (in press).

2. Shain, W., Greene, L. A., Sytkowski, A., Vogel, Z. and Carpenter, D. Acetylcholine (ACh) receptors of Aplysia: effects of α-bungarotoxin (α-BT). Fed. Proc. 32:741 (Abstract 2965), 1973.

STATOCYST RECEPTOR PHYSIOLOGY

Principal Investigator: *M. L. Wiederhold*
Technical Assistance: *P. J. Torrey and P. Y. Okita*

Electrophysiologic studies of the balance organ (statocyst) of the marine mollusc Aplysia are currently in progress. This organ provides a favorable preparation in that it contains relatively large (approximately 10 x 50 x 100 μm) ciliated sensory receptor cells. The receptor cells detect motion, under the influence of gravity, of small concretions (statoconia) within the cyst and serve a function analogous to that of the semicircular canals of vertebrate animals. The fine structure of the statocyst receptive cilia and their associated basal bodies are similar to those of the hair cells in the mammalian inner ear. Thus it is hoped that an understanding of the statocyst receptor cell physiology will give useful insights into the physiology of mammalian hair cells. The Aplysia receptor cells are larger and more accessible than mammalian hair cells, making them much more suitable, with currently available techniques, for intracellular electrophysiologic studies.

We have developed techniques for recording from the statocyst receptor cells with intracellular microelectrodes and observing responses to physiologic stimuli. A tilting preparation table was designed and fabricated which allows us to maintain intracellular recording during tilts of 45 degrees in any direction from the normal vertical. The receptor cells have a resting membrane potential of approximately -45 mV accompanied by base-line fluctuations varying from 2 to 15 mV peak to peak. In the resting state, cell input resistance from 20 to 70 MΩ has been measured. During a gradual tilt which causes the statoconia to deflect cilia of the cell from which recordings are being made, a depolarizing receptor potential of up to 20 mV is observed. This depolarization is accompanied by a decrease of cell input resistance of up to 60 percent. Preliminary calculations indicate that these findings are consistent with deflection of the cilia increasing the conductance of an ionic channel having an equilibrium potential of approximately -20 mV.

A joint project with A. E. McKee of the Naval Medical Research Institute has been initiated to further study the fine structure of the Aplysia statocyst using both transmission and scanning electron microscopy. We have recently developed a technique for observing the cilia on the luminal surface of the receptor cells. Preliminary findings indicate that there are 500-1000 cilia per receptor cell. The statoconia are in intimate contact with the cilia.

STATE OF IONS AND WATER IN LIVING CELLS AND SOLUTIONS

Principal Investigator: *D. O. Carpenter*
Collaborator: *A. F. Bak, National Institutes of Health*

It is generally thought that ions and water in living cells exist in a state similar to that of aqueous solutions where neither is restricted in movement. Evidence for this point of view comes primarily from experiments with the squid giant axon and the demonstration that electrical conductivity, ionic diffusion coefficients and ionic mobility in the axon are similar to free solutions of comparable concentration. We have developed a technique which allows measurement of electrical conductivity from single cells which are too small for the usual direct study of the characteristics of the cytoplasm.[1] This technique utilizes a metal microelectrode, insulated except for the tip, which is subjected to an alternating current at 100 kHz. With suitable electronic components the voltage output recorded between the microelectrode and an external reference electrode is a direct function of the conductivity of the solution at the electrode tip.

Table XXIV presents results of measurements of conductivity of the axoplasm of large axons. In agreement with previous results from other investigators of this classic preparation, the internal conductivity is very similar to that of the external medium. Whereas seawater has a specific resistivity of 25 ohm/cm the average from all of our measurements on the squid giant axons shows specific conductivities of about 35 ohm/cm. The giant axon of Myxicola, a marine animal, has internal resistivity in normal seawater of about 68 ohm/cm, a conductivity almost double that of the giant squid axon.

Table XXIV. Conductivity of Giant Axons

Preparation	Number	Equivalent isotonic salt concentration (percent)	Specific resistivity (ohm/cm)
Seawater		100	25
Loligo opalescens	13	78 (61-88)	32
Loligo pealei	15	65 (49-105)	39
From ganglion			
Stellar axon	5	69 (55-82)	36
Smaller axons	6	55 (55-70)	45
Myxicola			
In normal seawater	6	37 (30-44)	68
In hypertonic seawater (125%)	13	47 (39-60)	53

Table XXV shows the results of conductivities from a variety of invertebrate marine neuron cell bodies. In each case, conductivities are very low and in the case of Anisodoris are as low as 2 percent of the external medium. Table XXVI shows conductivities obtained from a variety of other tissues, including barnacle muscle fibers, frog eggs, and Amphiuma red blood cells. In each case the internal conductivity of these cells is considerably less than that of the external media.

Table XXV. Conductivity of Nerve Cell Bodies

Preparation	Number	Equivalent isotonic salt concentration (percent)	Specific resistivity (ohm/cm)
Seawater		100	25
Aplysia	42	6 (4-7)	434
Navanax	15	4 (2-8)	625
Anisodoris	20	2 (1-3)	1250

Table XXVI. Conductivity of Muscle, Egg and Blood Cells

Preparation	Number	Equivalent isotonic salt concentration (percent)	Specific resistivity (ohm/cm)
Seawater		100	25
Barnacle muscle fibers	16	14 (10-23)	178
Frog Ringer		100	77
Frog oocytes	12	40 (30-50)	190
Amphiuma RBCs	47	22 (11-41)	350

The very low internal conductivity of many of these tissues cannot be explained by the usual view of living cells that the internal medium consists of ions and water in a simple aqueous solution. The low conductivity suggests that macromolecular components of the cell cause a restriction of the ability of ions to carry electrical current. This might result from a binding of ions, a structuring of cell water, or a high microviscosity of the cytoplasm. Further experiments are being performed to attempt to determine the cause of these surprising observations.

REFERENCE

1. Carpenter, D. O., Hovey, M. M. and Bak, A. F. Measurements of intracellular conductivity in Aplysia neurons: evidence for organization of water and ions. Ann. N. Y. Acad. Sci. 204:502-533, 1973.

POTENTIAL HAZARDS OF HIGH AMPLITUDE ELECTROMAGNETIC PULSES TO IMPLANTED CARDIAC PACEMAKERS

Principal Investigators: *G. Brunhart and J. R. Martz*

There are two basically different types of cardiac pacemakers in use: the asynchronous pacemaker which requires no input signal and which has a fixed or adjustable output, and the synchronous pacemaker which senses certain pulses of the heart, such as the atrial P-wave or the QRS complex, and which provides appropriate output signals related to the input it senses. Necessarily, one would expect the possible interference due to electromagnetic fields to depend on the type of pacer in question.

Three categories of interference modes can be distinguished. (1) Catastrophic failure of the pacemaker due to electromagnetic pulse (EMP) induced destruction of circuit components. (2) An extra or arrhythmic output signal induced by an electromagnetic pulse. (3) Momentary cutoff of the output pulse of the pacemaker.

It must be expected that all pacemakers are potentially vulnerable to catastrophic failure. However, since the synchronous type pacemakers are specifically designed to detect electrical activity, they are inherently more vulnerable than the asynchronous type to failure in categories 2 and 3.

Typical burnout levels for modern semiconductors have been found to be in the order of 1-100 μJ. In contrast, the threshold for ventricular fibrillation in normal animals is reported to be two to four orders of magnitude higher. With this in mind, catastrophic failure through transistor burnout is a potential hazard. Four implantable pacers (Medtronic Asynchronous, Medtronic and GE demand, and Cordis atrial triggered) were subjected to up to 10,000 EMP at E peak fields of up to 500 kV/m using various orientations of the pacemakers and the leads. Under these conditions only the Cordis pacemaker failed. The failure could not be repeated after the output transistor was replaced.

Using results reported for pulsed microwave effects on cardiac pacemakers, a conceptual model for interference was devised consisting essentially of three parts, a shielded antenna-receiver, a demodulator, and a small signal tuned amplifier. With the microwave data as a point of departure it was concluded that peak EMP fields of at least 2-3 kV/m would be necessary to cause interference of the categories 2 and 3. Measurements since then conducted at the Air Force Weapons Laboratory, ALECS facility have confirmed these predictions. Further tests are continuing at AFRRI.

There exists another possible hazard to pacemaker wearers in that enough energy could be picked up directly in the leads of the pacer and cause extra beats or even produce ventricular fibrillation. While it is not expected to occur in EMP fields at the present typical pulse rates, this hazard is a real one in pulsed radar beams. The details of this possible hazard are currently under study at AFRRI.

◆◆◆◆◆◆◆◆◆

FREE RADICAL REACTIONS

Principal Investigators: *G. M. Meaburn, J. L. Hosszu and C. M. Cole*

Pulsed radiolysis studies of free radical-induced reactions of DNA. Radiation-induced chemical damage to the DNA component of a living cell is known to be responsible for inhibition of mitosis, impairment of the RNA transcription processes, and modification of the reactions leading to protein synthesis. Free radicals produced by the interaction of ionizing radiation with water react with DNA in a complex manner to destroy its structural integrity. Maintenance of a highly organized macromolecular structure is essential to the biological function of DNA. It is the purpose of this study to investigate more fully the reactions of water-free radicals with the nitrogenous bases of DNA. The conjugated double bond systems of the pyrimidine and purine bases are the light-absorbing (chromophoric) groups responsible for the strong optical absorption of the polynucleotide centered at ~260 nm. A careful examination of the optical properties of DNA in this spectral region, immediately following exposure to a short, high intensity pulse of radiation, has provided new information on the early radiation processes occurring in these systems. Some of the experimental results and the current interpretation of the observations are summarized below.

The methods of kinetic spectroscopy and pulse radiolysis were applied. Dilute solutions (100 mg/liter) of DNA were exposed to single pulses of 40 MeV electrons produced by the AFRRI electron linear accelerator (LINAC). Pulse widths of ~0.5 μsec

were standard throughout the course of the work. Due to the fact that observations were being made in a region where DNA strongly absorbs the analyzing light, special attention was paid to the optical technique used in these experiments. A pulsed xenon arc was employed as the light source, providing an output intensity 10-20 times higher than that from the arc operated in its normal mode. A usable pulse of ~800-μsec duration was obtained. The DNA sample was contained in a small path length optical cell (2 mm) of ultrahigh purity silica. Two high intensity monochromators were ganged in tandem as the wavelength discriminator. This technique eliminated stray light from reaching the photoelectric detectors and considerably increased the accuracy of the experiments. As a direct consequence of the small optical path in the radiation cell, relatively large electron doses were required to produce reasonable optical density changes in the irradiated material. These were of the order of 4.0 - 4.8 krads per pulse.

The first important observation to be made was that, over the time scale studied (800 μsec), no change in optical absorption by native DNA at 260 nm was detected after receiving a single pulse. An increase in absorption had been considered a possibility due to loss of hypochromicity by the radiation-damaged DNA double helix, a process that is known to occur over much longer time scales. A change in the form of a small loss of optical absorption was detectable in these native solutions only after preirradiation to doses >20 krads. The material became increasingly more sensitive to radiation until finally, after receiving ~100 krads, a maximum optical density change per pulse was attained. This effect is shown in Figure 51. Also shown is the behavior of denatured (single stranded) DNA. A very strong decrease in absorption was found following a single pulse and the decrement changed little over a dose range approaching 200 krads. For the examples shown, the solution characteristics were such that the total effect could be reliably assigned to reaction of hydroxyl (OH) free radicals with DNA chromophoric groups.

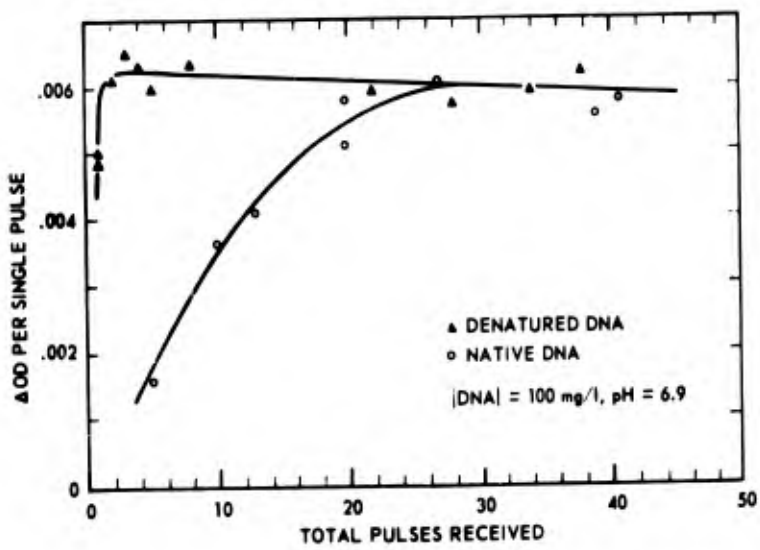

Figure 51. Decrease in optical absorption of irradiated DNA solutions at 260 nm

The reaction leading to loss of absorption, addition of OH to specific double bonds within the bases, has a high specific rate, being complete within ~10 μsec. Measurements of the change have been made for irradiated denatured DNA over an extended spectral range covering much of the permanent absorption band of DNA. The results are shown in Figure 52. The contour of the curve is quite smooth and appears to follow that of the permanent absorption with a maximum value close to 255 nm. The wavelength shift from the 260 nm maximum of the DNA spectrum, if real, may be indicative of a preferred mode of attack by OH on specific bases in the polynucleotide. The kinetics of disappearance of absorption remained unaltered over the entire wavelength range.

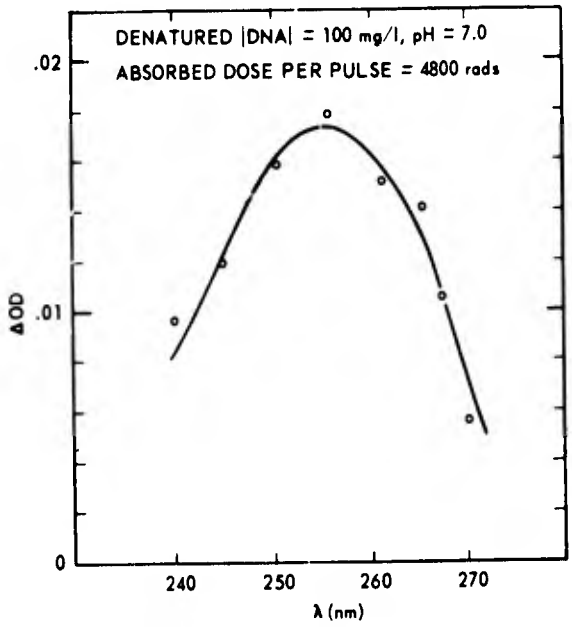

Figure 52. Decrease in optical absorption of DNA after receiving a single electron pulse

The influence of the helical structure of native DNA on the destruction of chromophoric groups is very strong. It appears that some denaturation is necessary before the normally shielded purine and pyrimidine bases become accessible to the diffusing OH radicals. A point of conflict arises, however, in considering the origin of the ultraviolet transient absorption spectra also found in irradiated DNA in its native form. These absorption bands are normally assigned to the formation of adducts of OH with the double bond systems of the bases and imply loss of chromophoric activity. Clearly, this is a question affecting the interpretation of the overall mechanism of radiation-induced damage in DNA to be resolved by further experimental work.

Free radical-induced chain breakage in irradiated solutions of DNA. This phase of the study has been concerned with the difficult problem of assessing the damage to the sugar-phosphate backbone of DNA by ionizing radiation. In dilute aqueous solution,

chain breakage occurs as a result of attack at critical sites in the polynucleotide by diffusing free radicals produced by radiolysis of water. The objective of the investigation is to learn more about the location of these sites and to determine the relative importance of the three major water intermediates, OH, e^-_{aq} and H, in inducing chain breakage.

The extent of chain breakage was quantitatively determined from release of phosphomonoester groups during radiolysis of calf thymus DNA solutions exposed to both ^{60}Co gamma and LINAC electron radiation. The yield of phosphomonoester, G(PME), was measured by enzymatic scission of the remaining ester bond and colorimetric analysis of the resulting phosphate ion (PO_4^{3-}). The investigation so far has been restricted to a single concentration of DNA (100 mg/liter). Phosphate concentrations were determined as a function of absorbed dose over a range of 1-5 krads. Doses were kept as low as practicable in order to minimize the influence of secondary processes, e.g., reactions between long-lived DNA radicals, on the structural stability of the macromolecule. The formation of phosphate ion as a function of dose is illustrated by the linear plots shown in Figure 53.

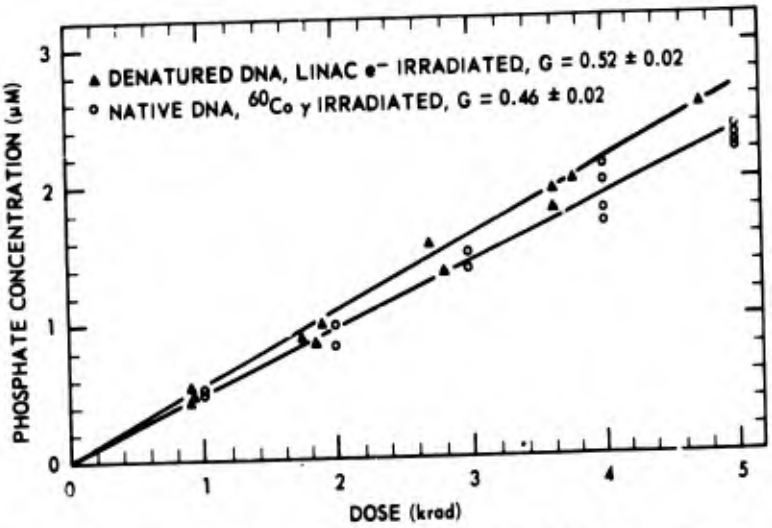

Figure 53. Formation of phosphate ion (PO_4^{3-}) in irradiated DNA solutions following enzyme treatment

The major results and conclusions of this study are summarized below.

A small fraction only of available free radicals reacts to break the polynucleotide backbone. At neutral pH, for example, approximately 8 percent of OH radicals can be accounted for in this way. Reaction with the sugar moiety does not necessarily produce a break. However, product fragments have not been identified, and detailed mechanisms of alternate reaction pathways are not yet available.

The secondary structure plays an important role in determining the extent of chain breakage. In denatured DNA the exposed nitrogenous bases presumably present less

hindered reaction sites to attacking OH radicals and consequently compete more effectively with the phosphodiester bond, thereby reducing the yield of chain breakage to approximately 60 percent of its value in the double helical form of DNA.

Hydrated electrons, e^-_{aq}, are similar in effectiveness to OH radicals in producing breaks in native DNA chains. The reaction mechanism is not yet known, but is believed to involve initial attack of the electrophilic center of the bound phosphate groups. Yields of phosphomonoester are negligible, however, in denatured solutions, again indicating the existence of highly favored reaction sites under such conditions.

ELECTRON LINEAR ACCELERATOR PRODUCTION OF POTASSIUM-43

Principal Investigators: *F. C. Gray, C. M. Cole, G. M. Meaburn and G. Brunhart*

Potassium-43, which has been produced in high flux nuclear reactors and cyclotrons, is an effective agent for myocardial imaging. This study was undertaken to evaluate the production of potassium-43 by the photonuclear reaction $^{44}Ca(\gamma, p)\ ^{43}K$, using the AFRRI electron linear accelerator (LINAC) as the radiation source.[1]

The stable target isotope was purchased as 94 percent enriched $^{44}CaCO_3$ and converted to the oxide to eliminate photoproduction of carbon-11. Samples of ^{44}CaO were sealed in quartz ampules and exposed to high-energy bremsstrahlung radiation produced by passing the LINAC beam through a thick water-cooled tantalum converter.

Chemical separation was performed on an ion-exchange column using a procedure developed at Oak Ridge National Laboratory,[2] modified to utilize a simple pneumatic pressure system to elute the ^{43}K from the column. The eluted ^{43}KCl was taken to dryness, dissolved in normal saline, and filtered. Target material was recovered by elution from the column, as $CaCl_2$, precipitation as the oxalate, and thermal decomposition to CaO.

Production yields of ^{43}K are shown in Table XXVII. The competing (γ, np) reaction produced potassium-42 as an undesirable contaminant. As shown in the table, the ratio of ^{42}K to ^{43}K is satisfactorily reduced by lowering the energy of the electron beam.

Table XXVII. Yields of ^{43}K and ^{42}K for Several Electron Beam Energies

Beam energy (MeV)	Yield (μCi/g ^{44}CaO-hour)		
	^{43}K	^{42}K	Ratio $^{42}K/^{43}K$
30.0	370	23	.062
35.7	770	92	.12
40.4	1100	230	.21
44.5	1500	390	.26

Myocardial scans on beagle dogs were performed using 100-150 μCi per visualization. In the present study, 0.30-g samples of ^{44}CaO were irradiated for each preparation. The yield of ^{43}K may be increased by using larger samples of target material and longer periods of irradiation.

REFERENCES

1. Gray, F. C., Cole, C. M., Meaburn, G. M. and Brunhart, G. Electron linear accelerator production of potassium-43. Bethesda, Maryland, Armed Forces Radiobiology Research Institute Technical Note TN73-15, 1973 (in press). J. Nucl. Med. 14:931-932, 1973 (in press).

2. Poggenburg, J. K. Neutron products at ORNL, pp. 19-22. In: Radioisotope Production Technology Development Meeting, June 2-3, 1970, Oak Ridge, Tennessee, Oak Ridge National Laboratory CONF. 700646, 1970.

◆◆◆◆◆◆◆◆◆

ORGANOMETALLIC DOSIMETERS

Principal Investigators: *G. M. Meaburn, J. L. Hosszu and W. E. Kiker*

The pulse radiolysis investigation of the tetra-alkyl compounds of the Group IV elements, lead, tin, germanium and silicon, is proceeding smoothly. Approximately 40 percent of the experimental program has been completed. At the present rate of progress, the laboratory phase of the investigation will be terminated shortly.

The chemicals are being systematically examined by the methods of kinetic spectroscopy for optical absorptions due to free radicals or ions produced by radiolysis. Some of the results obtained for tetramethyl lead are described here to illustrate the type of observation that is being made on these compounds. The target material, contained in a 4-cm path length cell, was exposed to single 200-nsec pulses of 40 MeV electrons provided by the AFRRI LINAC. The absorbed radiation dose per pulse was ~1 krad. A transient spectrum was observed between 350 nm (the low wavelength cutoff for $Pb(Me)_4$) and 650 nm immediately following a pulse. This is shown in Figure 54. There are two absorbing components in this region, one with a maximum at ~445 nm and a lifetime of ~5 μsec, the other much longer lived (~50 μsec) and centered around 380 nm. The kinetics of disappearance of both absorptions are complex and have not yet been analyzed.

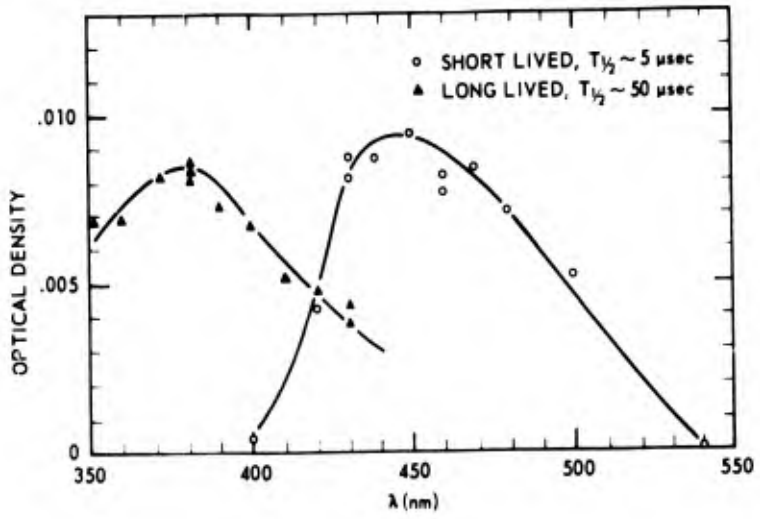

Figure 54. Transient spectrum of irradiated tetramethyl lead

A similar transient spectrum has so far been measured for tetraethyl tin, with the absorption maxima shifted to lower wavelengths. The intensities of the optical bands are also considerably decreased for the tin compound, particularly that of the short-lived component.

STATISTICAL METHODS FOR EEG-BEHAVIORAL STUDIES

Principal Investigator: *S. G. Levin*
Technical Assistance: *E. E. Sereno and J. A. Willis*

Clinicians and researchers face a similar problem in the analysis of EEG records: the reduction of large masses of data to manageable form and the interpretation of the results. To aid in this task, high-speed computers have been used for several years in some research facilities and are finding their way into the more modern hospitals. Using newer analytic techniques, workers have used the EEG to discriminate between normal and dyslexic children, to help locate the focus of epilepsy, to determine central nervous system (CNS) recovery from drugs, and to detect failure in cortical perfusion during cardiac surgery.

The EEG work at the AFRRI was motivated by the desire to understand the mechanism of CNS changes during transient incapacitation following whole-body irradiation. EEG changes were observed, but a more sophisticated method of analysis was required in order to recognize subclinical changes and to locate radiosensitive areas of the brain, hence to determine whether chemical agents could reverse the CNS changes.

Initial efforts followed the conventional spectral (frequency) analysis using the digital computer in place of the analog frequency analyzer. This assisted the researchers in evaluating sections of the EEG but was lacking in many respects; it provided no information about the relation between areas of the brain, many spectra had to be examined for each lead, and data from several leads made the job even more time consuming. No valid methods existed for summarizing data or for making statistical comparisons.

A computer program has been developed that uses the fast Fourier transform algorithm to compute individual power spectra, and moments were utilized to characterize the data.[1] The first moment of the power spectrum provides a measure of the middle of the frequency spectrum and hence permits observation of frequency shifts. The second moment is indicative of the spread of the spectrum, with a small spread associated with a synchronized wave. Total power is also calculated. Seven animals were irradiated and their EEG data were evaluated using these measures. Recent efforts resulted in the development of an overall system for the evaluation of multiple lead EEG's. In addition to the individual power spectra (auto spectra), the power shared by pairs of leads (cross spectra), phase relation between pairs of electrodes and the strength of association between leads (coherency) are all calculated. These quantities are individually plotted on a frequency scale or on a log frequency scale at the option of the researcher. Moments of all auto and cross spectra are computed and plotted in an array. Moments of several epochs can be combined so that different conditions, e.g., preirradiation and postirradiation, can be compared.

EEG epochs from three trained monkeys have been evaluated using this system and preliminary examination of the results is encouraging. When cross spectral results became available, it was evident that the existing electronics, primarily the EEG preamplifiers and amplifiers, were inadequate for the more sensitive analysis. A state of the art amplifier, based on a circuit developed at UCLA, was designed. It consists of a single 3" x 4" printed circuit board containing four integrated circuits which amplifies the 100-μV EEG signal to 2.5 V with noise level orders of magnitude lower than previously possible. The phase shift characteristics are far better than the previous amplifiers, and a set of eight can be mounted on a monkey chair and operated by batteries to keep them isolated from line noise. The 2.5-V signal can be routed directly to the on-line computer interface, which avoids any possible distortion introduced by an analog tape recorder and its electronics, although the data will be simultaneously recorded on tape as insurance. In spite of the reduction of computing time from 15 to 3 minutes per epoch for a single spectrum, phase plot, etc., the total computer time for a series of epochs with several leads can be excessive.

An alternate system includes producing calibrated digitized tapes at AFRRI, a new computer program written for the National Institutes of Health computer permitting analysis of their IBM 360/370 system, and finally the results being printed at the AFRRI.

REFERENCE

1. McFarland, W. L. and Levin, S. G. Effects of pulsed gamma-neutron irradiation on the EEG and behavior of the monkey. Bethesda, Maryland, Armed Forces Radiobiology Research Institute Scientific Report SR72-8, 1972.

◆◆◆◆◆◆◆◆

ELECTRON LINEAR ACCELERATOR (LINAC)

Principal Investigators: *G. Brunhart, J. D. Smarsh, F. C. Gray and V. I. Valencia*
Technical Assistance: *R. E. Severance, R. E. Bates and E. L. Ross*

The following is a summary of the LINAC activities and its utilization in the AFRRI research program. The availability and utilization time are given in Figure 55.

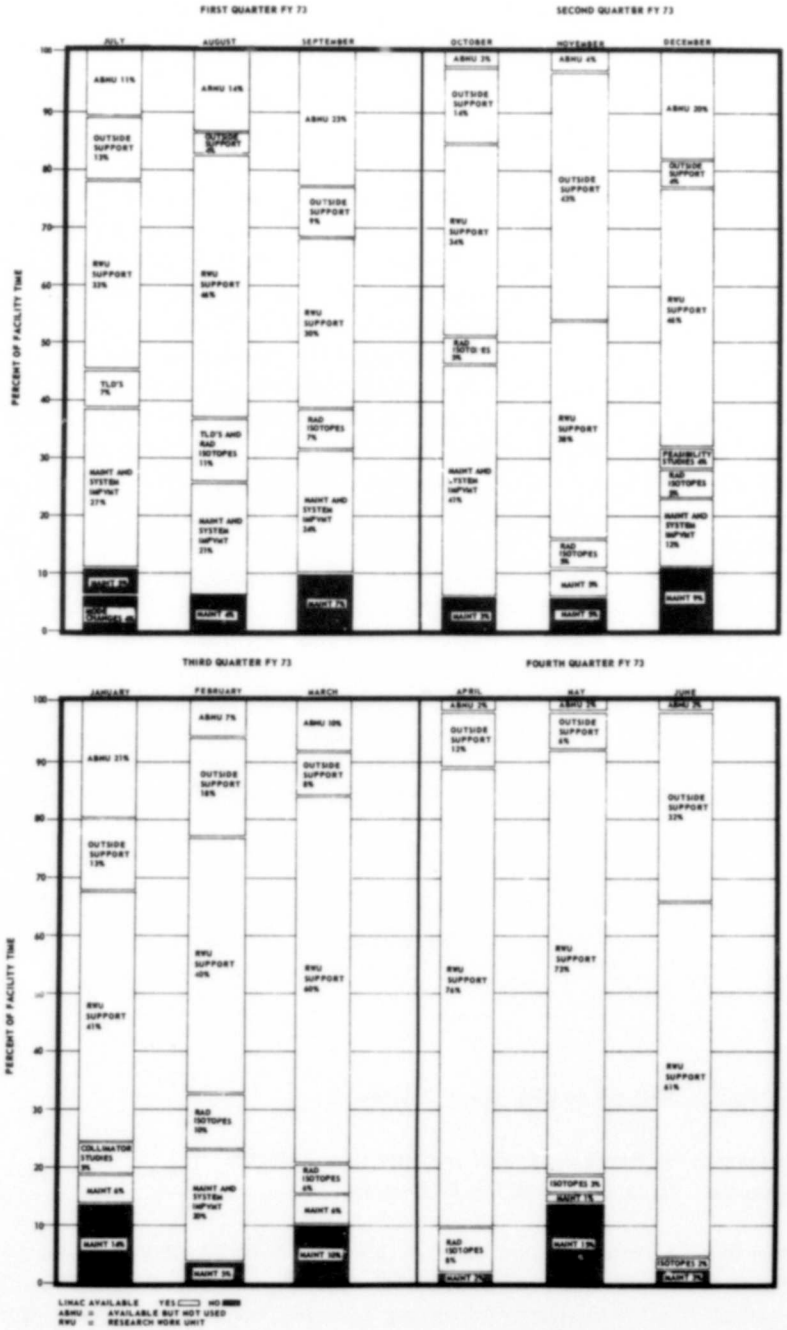

Figure 55. Availability and utilization of LINAC facility time

The LINAC provided irradiation support to scientific experiments. The specimens irradiated included monkeys in a simulated clinical regimen to study the development of radiation-induced myelopathy. Monkeys and miniature swine were irradiated to investigate radiation-induced early transient incapacitation. Miniature swine and rats were irradiated to investigate GABA levels in the brain. Monkeys were irradiated with implanted brain probes to investigate radiation effects on the EEG. Monkeys with implanted brain electrodes were irradiated to study regional cerebral blood flow during and following irradiation. Trained monkeys were irradiated translaterally to the eyes only with the LINAC beam in order to investigate the visual acuity of the animal during and following irradiation. The visceral ganglion of an Aplysia was irradiated utilizing a 4.0-mm diameter collimated LINAC beam to investigate effects on the action potentials. Malaria sporozoites and Venezuelan equine encephalomyelitis virus were irradiated for immunology studies. Various organic materials were irradiated in the course of investigation into the production of artificial membranes. Some of the support provided by the LINAC to AFRRI projects was to the pulse radiolysis study of aqueous solutions of DNA and organometallic compounds. ^{44}Ca, ^{39}K, ^{14}N and other radioisotope precursors were irradiated utilizing the LINAC as a high-energy bremsstrahlung source for the production of ^{43}K, ^{38}K, ^{13}N, respectively, and other radioisotopes with potential clinical applications. Sterilization runs in the megarad range were made for human tissue such as mandibles, heart valves, and crushed bone as well as for rat diet, opium, Silastic, kaolin, and acacia. Air samples and cow liver were irradiated in the high-energy bremsstrahlung beam for purposes of activation analysis. Various electronic components such as transistors and diodes were irradiated at very high dose rates for transient radiation effects on electronics (TREE) investigations. Finally, various types of dosemeters such as ion chambers, Fricke solution, thermoluminescent phosphors, diodes, and variable capacitors were irradiated in dosimetry investigations.

ELECTROMAGNETIC PULSE (EMP) SIMULATOR

Principal Investigators: *G. Brunhart, R. E. Carter and V. I. Valencia*
Technical Assistance: *R. E. Severance and E. L. Ross*

There has been a recent surge of both interest in and concern about possible biological effects of nonionizing electromagnetic radiation. The reasons for this are the widespread use of EMP facilities simulating the electromagnetic environment of nuclear explosions in the atmosphere and at high altitudes, and the development of increasingly powerful microwave generators of higher and higher frequency.

Much work has been done at many laboratories to investigate the hazards of non-ionizing radiation; however, most studies deal with microwaves of relatively high average power levels (and therefore necessarily modest peak field values) and consequently primarily thermal effects. In spite of all the work done there is very little real understanding of the problems involved indicating the complexity of the subject which is frustrated further by the enormous technical difficulties in making meaningful measurements. The questions of measurements of physical quantities, in particular absorbed energy in tissue as related to free-in-air power densities, have become research projects in themselves actively worked on by major laboratories.

AFRRI has acquired an EMP simulator facility to study biological responses to EMP fields under controlled conditions.[1]

In considering EMP effects on a biological system such as an animal, the test subject may be in one of several situations: (1) in contact with or near an extended conductor which acts as an efficient antenna, (2) grounded to earth, or (3) in the field but insulated from ground. The third situation differs from the other two in that no net current flow in or out of the body is possible. Situations (1) and (2) differ essentially in the magnitude of the induced current and the frequency spectrum which will couple into the system. While all three situations can exist, only the third one is being studied initially in the AFRRI simulator.

In the experimental design it was decided to test animals in an environment which was excessive in terms of peak electric field, pulse rise time, and pulse repetition rate in order to amplify any measurable changes. This is particularly important in view of the differences in geometry between man and the animal model (small rodents), and the fact that no prior evidence exists to indicate which parameters of the electromagnetic field would be most important.

The AFRRI EMP system specifications are as follows:

transmission line:	parallel plates, 122 cm wide, 10 m long, 56 cm separation, 95 Ω impedance (with animal load and in shielded room)
power supply:	two ± 150 kV dc supplies
energy storage capacitors:	four 5-nF tubular capacitors, two series banks of two parallel capacitors; total capacitance in banks 5 nF
spark gaps:	triggered, pressurized switch
pulse shape:	double exponential
rise time:	4-5 nsec (10-90 percent)
fall time:	550 nsec (to 1/e of peak)

peak field strength:	10-500 kV/m
pulse repetition rate:	up to 7 pps; single shot
energy per pulse:	160 joules maximum
field power density:	66.3 kW/cm^2 peak (at 500 kV/m)
system line impedance:	95 Ω
spectral content:	double exponential.

A second facility is available at AFRRI which was initially built in-house as a model for tests and design studies. With its present configuration this facility will deliver fields of about 300 kV/m and pulse rise times of about 20 nsec. This system is being used for behavioral studies on rhesus monkeys.

REFERENCE

1. Brunhart, G., Carter, R. E. and Valencia, V. I. AFRRI electromagnetic pulse (EMP) simulator. Bethesda, Maryland, Armed Forces Radiobiology Research Institute Technical Note TN73-14, 1973 (in press).

INDEX TO PRINCIPAL INVESTIGATORS